THE THERMAL AND FLUID SCIENCES CENTER

SMU

RESEARCH REPORT NUMBER 67-2

HEAT TRANSFER ACROSS SURFACES IN CONTACT: STUDIES OF TRANSIENTS IN ONE-DIMENSIONAL COMPOSITE SYSTEMS

GPO PRICE $ _____
CFSTI PRICE(S) $ _____
Hard copy (HC) $3.00
Microfiche (MF) .65
ff 653 July 65

by

Clifford J. Moore, Jr.

Sponsored by

National Aeronautics and Space Administration
Research Grant NsG 711/~~40-007-004~~ 40-007-004

Principal Investigator: Harold A. Blum
Report Period October 1, 1966 to April 1, 1967

March 28, 1967

N67-30861 (ACCESSION NUMBER) 24 (PAGES) CR-84968 (NASA CR OR TMX OR AD NUMBER) 1 (THRU) 33 (CODE) (CATEGORY)
FACILITY FORM 602

SOUTHERN METHODIST UNIVERSITY
INSTITUTE OF TECHNOLOGY
DALLAS, TEXAS, 75222

HEAT TRANSFER ACROSS SURFACES IN CONTACT: STUDIES OF TRANSIENTS IN ONE-DIMENSIONAL COMPOSITE SYSTEMS

A Dissertation Presented to the Faculty

of the

Institute of Technology

of

Southern Methodist University

in

Partial Fulfillment of the Requirements

for the degree of

Doctor of Philosophy

in

Mechanical Engineering

by

CLIFFORD JAMES MOORE, JR.

(B.S.M.E., Southern Methodist University, 1959)

(M.S.A.E., Southern Methodist University, 1964)

March 28, 1967

PRECEDING PAGE BLANK NOT FILMED.

ABSTRACT

Solutions are derived for a class of boundary value problems for the time-dependent temperature distribution in a two layer, composite slab with contact resistance at the interface and contact or convective resistance on the outer boundaries. The results of a parametric computer study using these solutions are presented. This study includes a set of dimensionless correlations of an arbitrarily defined time to approach steady state and a discussion of some transient thermal phenomena which are characteristic of systems of this type.

The applicability of these solutions for the prediction of the transient behavior of real composite systems is evaluated by comparison with experimental results. Experimental data are presented for the transient thermal response of several composite metal systems when subjected to thermal transients which closely approximated the boundary conditions of the theoretical solutions.

Comparisons with the experimental data indicate that the theoretical solutions can be used to predict the transient thermal response of systems to which they are applicable to an accuracy sufficient for most engineering purposes.

TABLE OF CONTENTS

ACKNOWLEDGEMENTS

This work was carried out under contract number NsG-711 for the National Aeronautics and Space Administration, whose sponsorship is gratefully acknowledged.

To my advisor, Dr. Harold A. Blum, under whose direction this work was carried out, I express my sincere appreciation for this guidance and support, and, most of all, for his enthusiasm.

I would like to thank Dr. Jack P. Holman and Dr. Edmund E. Weynand for the many hours of their time given in helpful discussions on several experimental problems. To Dr. Charles W. Tittle, for his valuable assistance in applying his new methods to the theoretical problems, I also express my sincere thanks.

Dr. Kenneth W. Heizer designed all of the electronics for the force control system. For this and for the many hours spent in helping to make an electronic circuit constructed by a mechanical engineer work like an electronic circuit, I offer my grateful appreciation.

I would like to thank Mr. Lenox Carruth, Jr. who,

among many other things, installed the vacuum system and offered many helpful suggestions on the experimental procedures. To my research assistants, Thomas S. Ashley and Robert M. Ashley, both of whom worked on all phases of the experimental program, I express my appreciation for their many contributions. I would also like to thank Mrs. Willa Bates for her many assistances and especially for her work on the bibliography.

To Mr. Harry Atkins of NASA for all of his many efforts in behalf of the project, and to Mr. Erwin Fried of General Electric and Mr. Dan Flynn of the National Bureau of Standards for the information and suggestions they supplied, I express my sincere appreciation.

I would like also to thank Mr. David Williams for carrying out the thermal conductivity measurements. The servo-actuator used in this work was donated by Moog-Servocontrols Inc., their gift is gratefully acknowledged.

Finally, to my wife, Jo for the typing of the manuscript, and, most of all, for the years of patience and understanding I express my heartfelt thanks. To her and my children, Russell and Beth, I dedicate this work.

TABLE OF CONTENTS — CONTINUED

LIST OF TABLES

LIST OF ILLUSTRATIONS

LIST OF ILLUSTRATIONS — CONTINUED

LIST OF ILLUSTRATIONS — CONTINUED

LIST OF SYMBOLS -- CONTINUED

f	Constriction alleviation factor (page 32)	dimensionless
$f_n(x)$	A functional notation (page 77)	dimensionless
G_n	Series coefficients (page 74)	dimensionless
g	Roess's Series (page 35)	dimensionless
gn(x)	A funtional notation	dimensionless
Hn	Series coefficients (page 87)	dimensionless
h	Contact conductance coefficient	$Btu/hr \cdot ft^2 \cdot {}^oF$
k	Thermal conductivity	$Btu/hr \cdot ft. \cdot {}^oF$
L	Total length of regions 1 and 2	ft.
M	Meyer hardness	lb_f/ft^2
M_i, M_2	Numerical moduli (page 90)	dimensionless
N	Total number of contact points	dimensionless
N, N_2, No, N_L	Numerical moduli (page 90)	dimensionless
n	Contact point density	$ft.^{-2}$
P	Pressure	lb_f/ft^2
Q	Heat transfer rate	Btu/hr.
q	Heat flux	$Btu/hr \cdot ft^2$
R	Gas Constant	$ft \cdot lb_f/lb_m - {}^oR$
r	Radius	ft.
S	Steady state constant (page 83)	$Btu/hr \cdot ft^2 \cdot {}^oF$
T	Temperature	^oF or ^oR

LIST OF SYMBOLS

English Letters

A	Area	ft^2
A_1, A_2	Steady state solution constants (page 75)	$ft.^{-1}$
a	Length of region 1	ft.
a	Idealized contact spot radius	ft.
a_1, a_2	Accommodation coefficients	dimensionless
B_n	Series coefficients (page 74)	dimensionless
b	Length of region 2	ft.
b	Idealized contact heat channel radius	ft.
C	Orthogonality factor	dimensionless
C_n	Series coefficients (page 74)	dimensionless
C_v	Constant volume specific heat	
D_n	Series coefficients (page 74)	dimensionless
d	Flatness deviation	ft.
E_{12}	Radiation exchange factor (Page 15)	dimensionless
E_n	Series coefficients (Page 86)	dimensionless
e	Geometric factor (page 29)	dimensionless
F_n	Series coefficients (page 74)	dimensionless

x	Length coordinate.....	ft.

Greek Letters

α	Thermal diffusivity.....	$ft.^2/hr.$
β	Correlation parameter (page 95)...	dimensionless
γ	Specific heat ratio.....	dimensionless
γ_n	Region 1 eigenvalues (page 74)....	$ft.^{-1}$
Δ	Difference operator.....	dimensionless
δ_f	Fluid gap thickness (page 13).....	ft.
δ_n	Region 2 eigenvalues (page 74)....	ft.
ϵ	Contact area ratio (page 30).....	dimensionless
ϵ_1, ϵ_2	Surface emissivities.....	dimensionless
ζ	Elastic conformity modulus (page 38).....	dimensionless
Θ	Time parameter (page 94).....	dimensionless
θ	Time.....	seconds
λ	Mean free molecular path.....	ft.
λ_1, λ_2	Surface roughness wavelengths.....	ft.
μ	Volume average void thickness (page 31).....	ft.
ξ	A constant (page 35).....	dimensionless
ν	A constant (page 29).....	dimensionless
ρ	Density.....	$lb_m/ft.^3$
σ	Stefan-Boltzmann constant.....	$Btu/hr.\text{-}ft.^2\text{-}^oR^4$

τ	Correlation parameter (page 95)...	dimensionless
ϕ	Functional notation (page 38).....	dimensionless
ψ	A constant (page 29).....	dimensionless

Subscripts

1	Region or surface 1
2	Region or surface 2
c	Contact
e	Effective
f	Fluid
g	Gas convection
m	Mean
n	Summation index
r	Radiation
L	At x = L
0	At x = 0

I. INTRODUCTION

Objectives and Scope

It is the primary objective of this writing to present the results of theoretical and experimental investigations made by the writer on one-dimensional composite systems with contact resistances when subjected to thermal transients. These results are believed to be a significant contribution to the fields of heat transfer in composite media and thermal contact resistance. In the remainder of this section some of the basic definitions and ideas associated with the concept of thermal contact resistance are presented to form a background and illustrate the importance of the problem of contact resistance.

In section II the actual mechanism of contact heat transfer is examined and discussed with a view toward understanding what variables influence the phenomenon of contact heat transfer.

In section III the existing literature is examined with a discussion of some of the major works in the field and a categorization of the literature by the type of infor-

mation to be found in the various references.

The derivations of the analytical solutions obtained by the writer for the time-dependent temperature distributions in composite solids with contact resistances are given in section IV. The results of a computer study made with these solutions are also presented and discussed.

Section V contains the descriptions of the equipment and procedures used in obtaining the experimental data. The experimental results are presented in section VI. Conclusions drawn from a comparison of the experimental and theoretical results are presented in section VII. Recommendations for future investigations are also offered in section VII.

Background

The particular area of interest in heat transfer which is concerned with the transfer of heat across surfaces in contact is relatively new. Truly active interest and investigation in this area did not begin until approximately eighteen years ago. Contact resistance studies are basically concerned with the effects on heat transfer rates of the presence of a joint or interface surface of contact between two solid bodies. Although the majority of the back-

ground material in the field is concerned with steady state contact phenomena, it is presented here because of its obvious importance to the study of non-steady contact resistance. In order to introduce the subject it is logical to discuss how the surfaces of solid bodies make contact with each other.

A surface on a solid body which has been formed by a machining process is usually thought of as smooth. There are degrees of "smoothness" for such a surface, depending on the nature of the machining process. To some extent the differences can be qualitatively distinguished by the human senses of sight and touch. However, even though a surface may appear to these senses to be quite smooth, it is known that on a microscopic level the surface is rough. That is, under sufficient magnification, a surface is not smooth but would appear as a series of irregular hills and valleys, much like an aerial view of a mountainous terrain.

All machined surfaces possess some degree of roughness. Consequently, when two such plane[1] surfaces are pressed together they can be in actual contact only at dis-

---

[1]Although most of general remarks apply to all machined surfaces, the present work is concerned only with plane, i.e., nominally flat, surfaces.

crete points. Figure 1 illustrates how the interface between two solids might appear. The two bodies touch only where peaks touch peaks or peaks touch valleys. These contact points are variously called "contacts," "contact spots," and "a-spots," The latter designation was picked up by the early writers from the pioneer work in electrical contacts by Holm [118] [2]. Thus the term a-spot is the most prevalent among writers in the field and it will be used in the present work. The total area of actual contact between two solids is the sum of the areas of the individual a-spots. This total area may be less than 1% of the apparent contact area, and is above 20% only for carefully prepared surfaces [41,43,78].

The fact that the interface contact between two solids occurs only at discrete points gives rise to the heat transfer phenomenon known as "contact resistance." Such an interface, generally referred to as a "contact" or "joint," causes a constriction of the heat flux lines (Figure 1). Thus an additional resistance to heat flow is produced because the heat flow, which is parallel at some distance

---

[2]Numbers in brackets refer to the corresponding references listed in the bibliography.

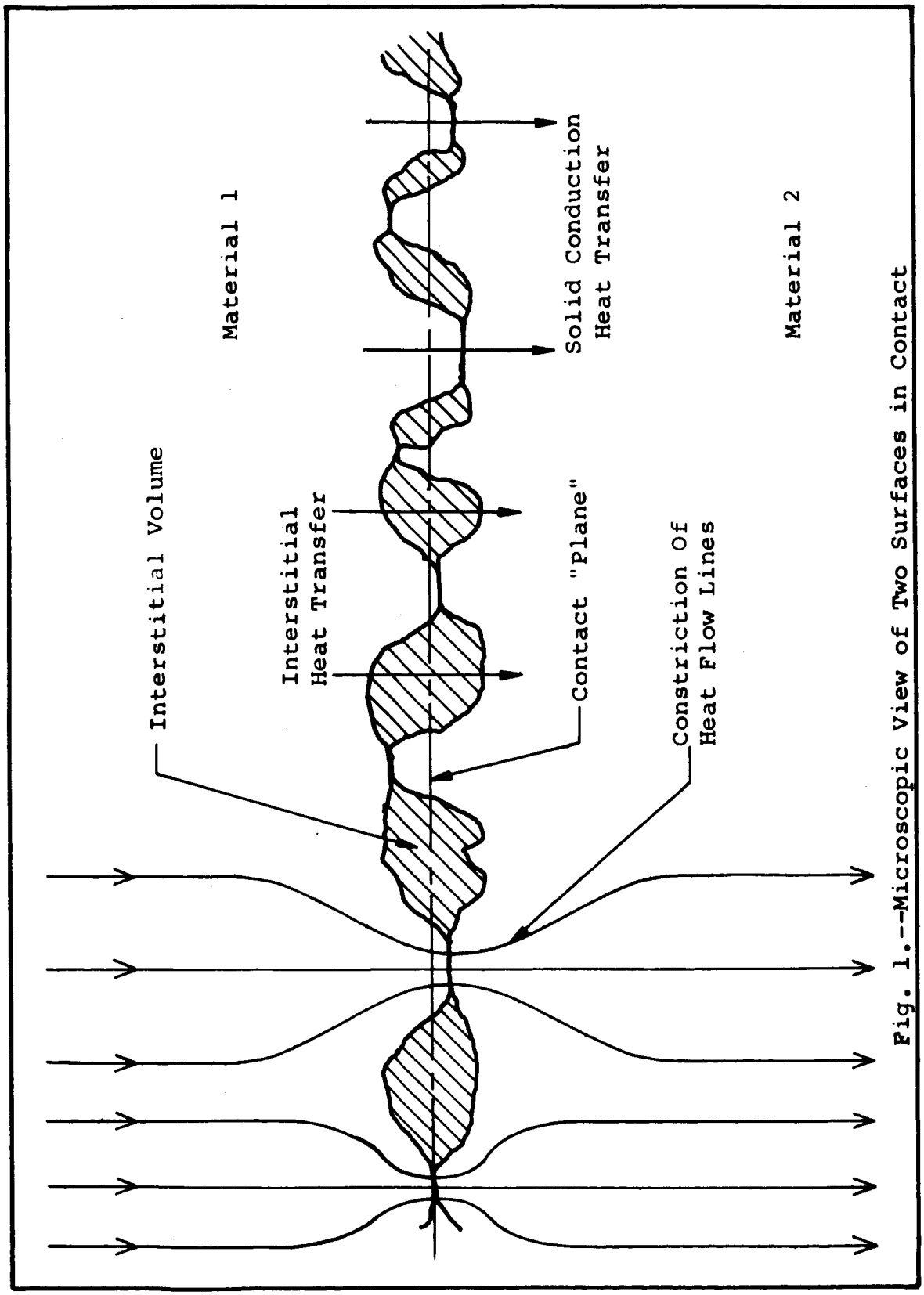

Fig. 1.--Microscopic View of Two Surfaces in Contact

from the interface, must bend to pass through the a-spots. In treating this phenomenon it is a matter of choice as to whether one uses resistance or its reciprocal, the conductance. Most of the authors in this field have chosen to deal with conductance. Therefore, the conductance will be used here (however, the term "resistance" will be used in certain instances because of its intuitive appeal).

Before examining the details of the heat transfer problem of a contact interface it is desirable to give the accepted definition of contact conductance and to comment on it. Contact conductance is defined (analogous to a convection heat transfer film coefficient) as follows:

$$h = \frac{Q_c}{A_c\,(\Delta T)_c} \qquad \text{(Btu/hr-ft}^2\text{-}^\circ\text{F)} \qquad \text{(I-1)}$$

In which Q_c = heat transfer rate across the interface, A_c is the apparent contact area (cross sectional area of solid), and $(\Delta T)_c$ = the apparent temperature drop at the contact. This definition introduces the fiction of an "apparent" temperature drop at the interface. Obviously there is no real discontinuity of the temperature distribution through the solid contacts. There is a continuous distribution of temperature extending through the contact from both solids. However, such a temperature distribution would

be extremely difficult to describe. From Figure 1 it is clear that the distribution would be three-dimensional even if the distribution in main part of the bodies was one-dimensional. For this reason the concept of a contact temperature drop is a convenience. This temperature drop is defined, as shown in Figure 2, as the difference in the temperature obtained by extrapolating the temperature profiles in the two regions to the interface boundary. The description of this definition as fictional is not intended to imply disapproval. On the contrary, it is a practical, working definition. The only caution required here is that if one obtains the temperature profiles experimentally, care must be taken to insure that the measurements are made at a sufficient distance from the contact to insure that the isotherms are essentially parallel planes.

Thus the effect of a contact interface can be thought of either as a discontinuity in the temperature distribution on a macroscopic level, or as a constriction of the heat flow lines on a microscopic level. In either case the important point is that the interface causes an additional resistance to heat transfer. The prediction of this resistance for a given set of conditions, or more commonly, its reciprocal, conductance, is the primary goal of all the the-

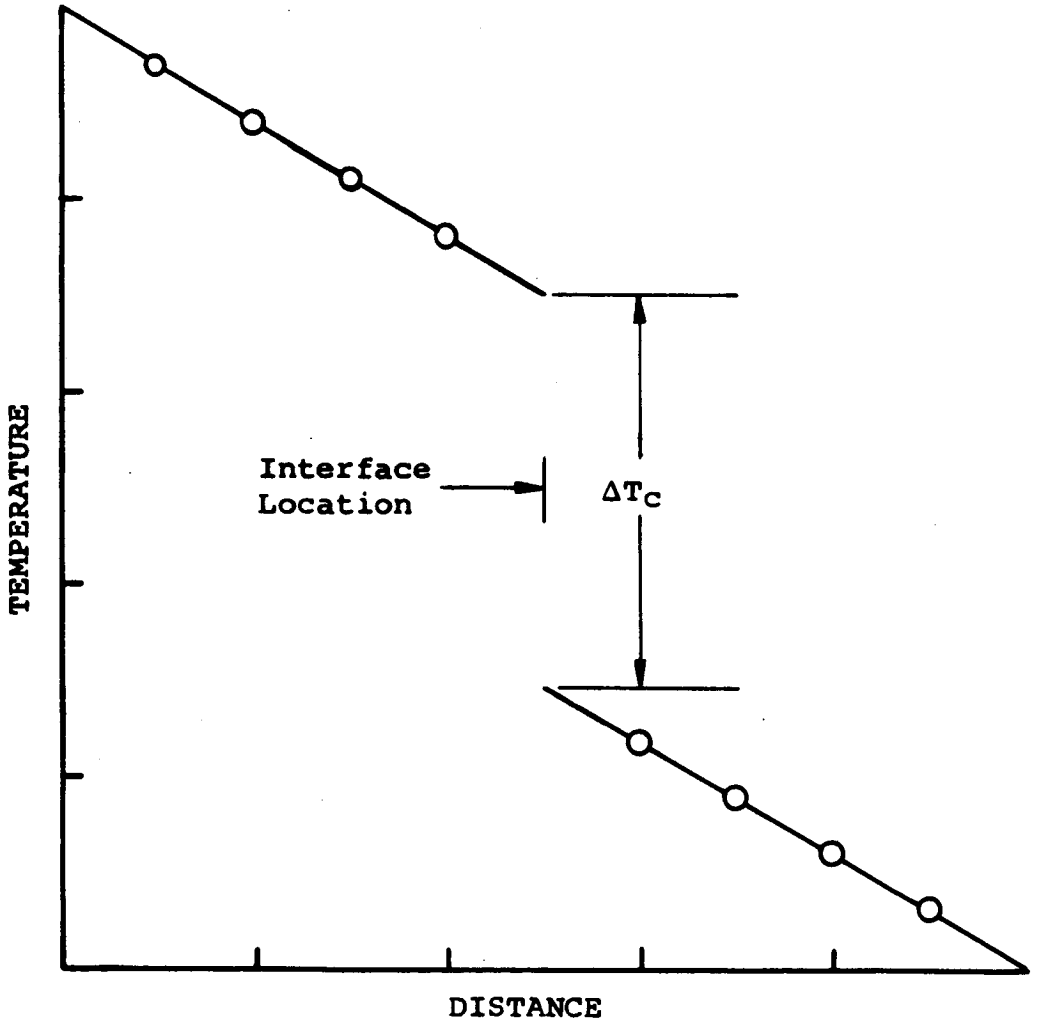

Fig. 2.--Definition of Contact Temperature Drop

oretical and experimental work in this field.

Applications

The study of contact conductance is an important area in the field of heat transfer. Practically all types of equipment and hardware in which the transfer of heat is of importance contain composite structures, or joints, between members or pieces of equipment, etc. Each such joint that does not provide intimate contact, i.e., any joint that is not welded, brazed, etc., produces a contact resistance. The importance of the knowledge of contact phenomena is particularly significant in situations in which the conductance may vary with time or over the range of operating conditions of the equipment. This is especially true if the contact is part of a critical system of heat removal or thermal isolation. A few such applications are: equipment for heat removal and environmental control for electronic components, high temperature heat-treatment equipment, nuclear reactors, high speed aircraft, satellites, and launch and reentry vehicles. The National Aeronautics and Space Administration is currently very interested in contact conductance - as evidenced by their sponsoring of several research projects in this field, including the present work.

Although much work has been done, both theoretically and experimentally, almost all of it has been done for steady-state conditions. These works have produced only a reasonable understanding of steady-state contact conductance. As will be discussed in section III, there is a need for more work to be done in the study of steady-state conductance. On the other hand, very little has been done for non-steady conditions, and it is for this reason that the present work was undertaken.

II. THE MECHANISM OF CONTACT HEAT TRANSFER

The definition of contact conductance was given in Section I in equation (I-1). It was demonstrated by means of Figure 2 how one could calculate the conductance, h_c, from experimental data. However, in order to be able to predict values of h_c for a given situation it is necessary to know what the parameters are that affect it. In other words, a knowledge of the physical mechanism is required. It is the purpose of this section to present a description of the physical mechanism of heat transfer across a contact. Such a presentation must include a description of the conditions under which certain variables exert a considerable influence and when their influence is negligible. Thus there may be some overlap between the conclusions stated here and the discussions in the next section. However, the small amount of repetition is felt to be justified for the sake of presenting an overall picture here.

If there is a flow of heat between two solid bodies in contact the mechanism by which the heat flux traverses the contact plane is, in general, very complex. As illustrated in Figure 1, heat may be transferred across an interface

in the following ways.

1) solid-to-solid conduction heat transfer through the contact points.

2) conduction heat transfer through the interstitial gas (if a gas is present).

3) solid-to-solid radiation heat transfer between the portions of the surface that do not touch, i.e., through the interstitial volume.

4) convection heat transfer through the interstitial gas.

Although the above heat transfer modes are somewhat interdependent, for the purposes of analysis they will be assumed to be independent. Such a simplification of conditions always creates some doubt about conclusions drawn on this basis. However, as will be shown, the resulting conclusions indicate that the differences in the amounts of heat transferred by the different modes are orders of magnitude apart. Thus, the conclusions are believed to be justified since it would be difficult to imagine that the simplification of the model would produce distortions of this size. With the assumption of independence the total conductance, h, of the contact interface can be assumed to be the sum of the four individual conductances:

$$h = h_s + h_f + h_r + h_g \qquad \text{(II-1)}$$

where the subscripts refer to solid, fluid, radiative, and convective conductances, respectively.

Figure 3 is an idealized representation of a contact interface which will be used to analyze the importance of the various contact heat transfer modes.

Interstitial Convection

It will be assumed that the contact points are widely spaced, i.e., the size of the contact spots (their radii) is small compared to the distance between them, see Figure 3. It is also assumed that the gap thickness, δ_f, is small compared to the distance between contact spots. With these assumptions the convection analysis can be based on two large parallel flat plates separated by a distance δ_f (the effective fluid gap thickness). Three different cases of orientation could arise: 1) gap horizontal with the upper plate at a higher temperature; 2) gap horizontal with the lower plate at a higher temperature; and 3) gap vertical. For the first case no convection will occur[245, p. 272]. For the second and third cases, experimental work has shown that no convection occurs unless the Grashof number (based

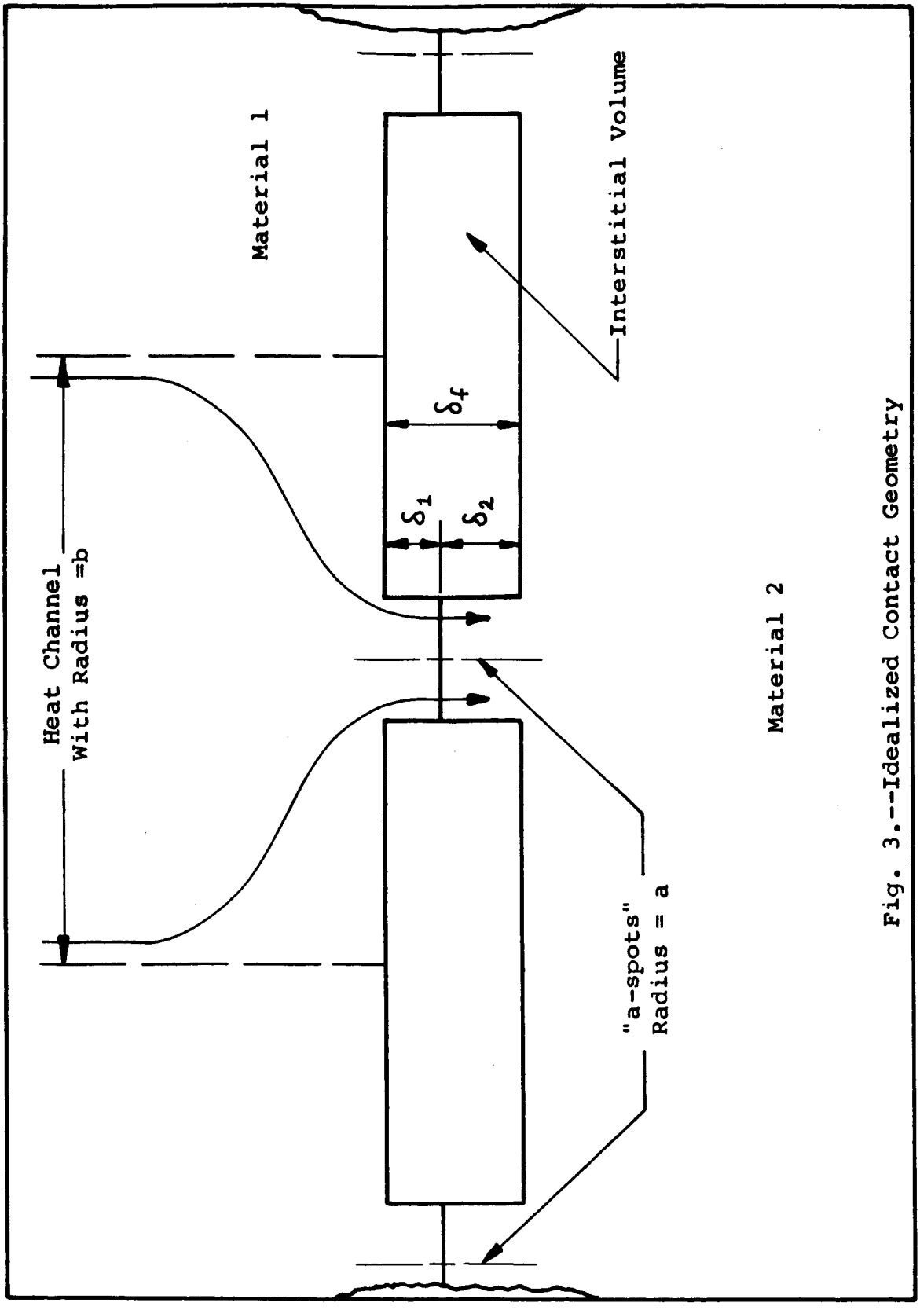

Fig. 3.--Idealized Contact Geometry

on gap thickness) is greater than 1700 and 2000, respectively [245, p. 272-3]. In the type of engineering surfaces normally encountered the Grashof number (based on δ_f and properties at the mean interface temperature) ranges from 10^{-3} to 10^{-1}. Therefore the convective heat transfer for any realistic contact problem is safely ignored.

Gap Radiation

With the same assumptions made above, the radiative heat transfer analysis can also be based on large parallel flat plates. For such a configuration the radiative heat transfer rate per unit area is given by Jakob [246, p. 3] as

$$q_{1-2} = E_{12}\,\sigma\,(T_1^4 - T_2^4) \qquad \text{(II-2)}$$

where σ is the Stefan-Boltzmann constant, T_1 and T_2 are the respective surface absolute temperatures, and ϵ_1 and ϵ_2 are the emissivities of the surfaces. If the assumption of gray surfaces is made the interchange factor is given by

$$E_{12} = \frac{1}{1/\epsilon_1 + 1/\epsilon_2 - 1} \qquad \text{(II-3)}$$

Using (II-2) and the conductance definition the following relation for radiative conductance results

$$h_r = \frac{E_{12}\,\sigma\,(T_1^4 - T_2^4)}{(T_1 - T_2)} \qquad \text{(II-4)}$$

or,

$$h_r = E_{12}\,\sigma\,(T_1^3 + T_1^2 T_2 + T_1 T_2^2 + T_2^3) \qquad \text{(II-5)}$$

If the assumption is made that the temperature difference $(T_1 - T_2)$ is small compared to the mean temperature $(T_m = \frac{T_1 + T_2}{2})$, then (II-5) becomes

$$h_r \cong 4 E_{12}\,\sigma\,T_m^3 \qquad \text{(II-6)}$$

For most thermal contacts the above assumptions are reasonable. It can be seen from (II-6) that the contact conductance would depend strongly on the mean interface temperature if radiation were a considerable portion of the total heat transfer. Experimental work has shown that this dependence does not occur [24,27,47,140]. There is some dependence on T_m, but the extent to which it appears indicates that it is primarily the result of the dependence of the solid and fluid conduction modes. Using (II-6) and experimental results for the total conductance, Fenech and Rohsenow [84] have found that for mean contact temperatures below 1100°F the radiative heat transfer amounts to less than 1% of the total. Similarly, Clausing [58] has stated the radiation accounted for less than 2% in the worst conditions of his experimental work. Therefore except in the presence

of very high temperatures or very poor conductors the contribution of gap radiation to contact heat transfer is negligible. In the present experiments the gap radiation conductance coefficient was estimated from (II-6) to be about 0.2 Btu/hr.-ft.^{2}-^{o}F. Comparing this with lowest value of the total conductance coefficient measured, 29 Btu/hr.-ft.^{2}-^{o}F, shows that it is less than 1%.

Thus, in the remainder of this work, the terms h_g and h_r in equation (II-1) are assumed to be negligibly small. The total conductance will be written unsubscripted and the solid and fluid components will be subscripted with "s" and "f" respectively, i.e.,

h = total contact conductance = $h_s + h_f$

Gas Conduction

Utilizing the same assumptions about the gap size and spacing as were used above, the interstitial fluid conductance can be written as the reciprocal of the fluid resistance,

$$h_f = \frac{1}{R_f} = \frac{1}{\delta_f / k_f} = \frac{k_f}{\delta_f} \qquad \text{(II-7)}$$

where δ_f is the "effective" gas thickness and k_f is the fluid thermal conductivity. The prevailing theories and practices regarding the evaluation of δ_f are presented in

the next section. It suffices here to say the δ_f is small and it is related to the surface roughness. By means of equation (II-6) it can be seen that because δ_f is small, h_f can be quite large even though k_f is typically small for most gases and some liquids. In some cases even with air in the interstices the fluid conductance may account for a major portion of the heat transfer. For example, Barzelay, et al [24,25] report total conductances as low as 250 Btu/hr.-ft.^{2}-^{o}F for a stainless steel contact with a surface roughness of 120 microinch at a mean interface temperature of 200^{o}F (for low contact pressures where solid conduction is small). For such a case k_f is approximately .0181 Btu/hr.-ft.- F [245] and δ_f is approximately 3.0 x 10^{-4}ft. With the values equation (II-7) gives

$$h_f = \frac{0.0181}{3 \times 10^{-4}} \cong 60 \quad BTU/hr\text{-}ft^2\text{-}^oF$$

This would indicate that for this case the fluid conductance accounts for approximately 25% of the total heat transfer. Cases have been reported where the fluid conductance accounts for over half the total [41], and even as high as 98% [137]. Equation (II-7) also brings out another important point: that one can accomplish a reduction in contact resistance by putting a fluid with high thermal conductivity in

the interstices.

For most gases with the pressures normally encountered the dependence of thermal conductivity on pressure is small. However at low pressures where the mean free path of the gas molecules is of the order of, or greater than, the gap thickness this no longer holds. Since thermal contacts in a vacuum are of considerable importance, especially in the present work, the influence of low pressures on the gas conductivity will be discussed here.

Again referring to Figure 3, the analysis will be based on two large flat parallel plates. For this configuration the following equation for the heat transfer rate per unit area is given by Kennard [247 p. 317],

$$q_f = \frac{a_1 a_2}{a_1 + a_2 - a_1 a_2} \rho \left(\frac{RT}{2\pi}\right)^{\frac{1}{2}} \left(c_v + \frac{R}{2}\right)(T_1 - T_2) \qquad \text{(II-8)}$$

In which a_1 and a_2 are the accommodation coefficients of the two surfaces, ρ , R and c_v are gas density, gas constant, and constant-volume specific heat, respectively. It is convenient to define an "effective" accommodation coefficient as follows,

$$a_e = \frac{a_1 a_2}{a_1 + a_2 - a_1 a_2}$$

Equation (II-8) can be put into the form in which it customarily appears by using the above definition and the follow-

ing thermodynamic relations:

$$\rho = \frac{P}{RT} \quad , \quad C_v = \frac{R}{\gamma - 1}$$

Where γ is the ratio of specific heats. Thus (II-8) becomes

$$q_f = a_e P' \left(\frac{\gamma+1}{\gamma-1}\right)\left(\frac{R}{8\pi T'}\right)^{\frac{1}{2}} (T_1 - T_2)$$

with the definition of h_f this becomes

$$h_f = a_e P' \left(\frac{\gamma+1}{\gamma-1}\right)\left(\frac{R}{8\pi T'}\right)^{\frac{1}{2}} \qquad \text{(II-9)}$$

The prime notation was introduced to account for accommodation effects. The T' is the mean of T_1' and T_2' which are respectively, the temperatures corresponding to the mean speeds of the molecules leaving the respective surfaces. The p' is the pressure of a gas which has the density of the gas in the gap but which is maxwellian and at a temperature T'. The T' can be calculated from the actual plate temperatures and the accommodation coefficients. It is sufficient for present purposes to realize that if a_1 and a_2 do not differ greatly, T' will be close to the mean of T_1 and T_2 (if $a_1 = a_2$, T is exactly T_m). Thus for most commonly encountered contacts p' and T' may be taken as p and T_m. With these statements and equation (II-9) it is readily seen that the free molecule fluid conductance is inversely pro-

portional to the square root of the mean temperature and directly proportional to the pressure. The significant point about (II-9) is that the conductance is independent of the gap thickness. It should be emphasized that this conclusion only holds for the conditions of the derivation of (II-8), namely, free molecular motion. The usual criterion for free-molecular motion is that the Knudsen number, λ/δ_f, be greater that 10, where λ is the mean free molecular path. In most of the published contact conductance investigations the maximum value of δ_f is less than .002 inches. Using the above criterion and this δ_f one finds that equation (II-9) is valid for mean free paths greater than .02 inches, or, in terms of pressure, for pressures less than 100 microns of H_g. The most common values of δ_f that are usually encountered are less than the above and thus the assumption of free molecular flow is valid for lower mean free paths, i.e., for higher pressures. In the present experimental work the largest δ_f was calculated to be less than .0002 inches.

It has been shown how one could calculate the value of the fluid conductance for the conditions of normal pressures and very low pressures. The former requires the determination of the effective gap thickness, which is usually

not a simple task, whereas the latter requires a knowledge of the mean gap pressure and temperature, the gas properties γ and R, and the accommodation coefficients. For a situation in between these extremes it would be very difficult to evaluate gas conductivity analytically. Fortunately, however, the conditions of interest are usually either atmospheric or high vacuum conditions.

Solid Conduction

For most cases of practical importance the solid conduction mode accounts for the largest part of the total contact heat transfer. Exceptions have been noted in the previous paragraphs. Because solid conductance is the predominant mode, especially in a vacuum, it has received a great deal of attention.

In the absence of oxide films or other surface contamination this mode of contact heat transfer can be treated as simple conduction. The additional resistance to the flow of heat is caused by the fact that the heat flux lines must converge to pass through the areas of solid-solid contact. This constriction of heat flow lines has led to the use of the term "constriction resistance" or "constriction conductance". The analysis of the solid conduction contribution

may be carried out in several ways. In the following paragraphs four separate methods of calculating the solid conductance term are presented. These four represent the major contributions thus far published. Though there have been other works published, they are only adaptations or modifications of the ones presented below.

There are some differences and some similarities between the four approaches which should be emphasized here. For this purpose it is necessary to understand the two kinds of surface irregularities which can exist on a solid surface. All surfaces possess a certain roughness. A surface may also have waviness. Surface waviness is the macroscopic "non-flatness" of a surface as opposed to surface roughness which is microscopic. Figure 4 is a sketch which shows how these surface characteristics might appear. Obviously the heat flowing across a contact formed by bringing together two surfaces which have both roughness and waviness could suffer two types of constriction. The heat flow lines would have to converge first to the "macroscopic contact areas" which exist because of the waviness. Then, within these areas, they would have to converge again to pass through the microscopic contact spots. Thus the terms "macroscopic constriction resistance" and "microscopic constriction resistance"

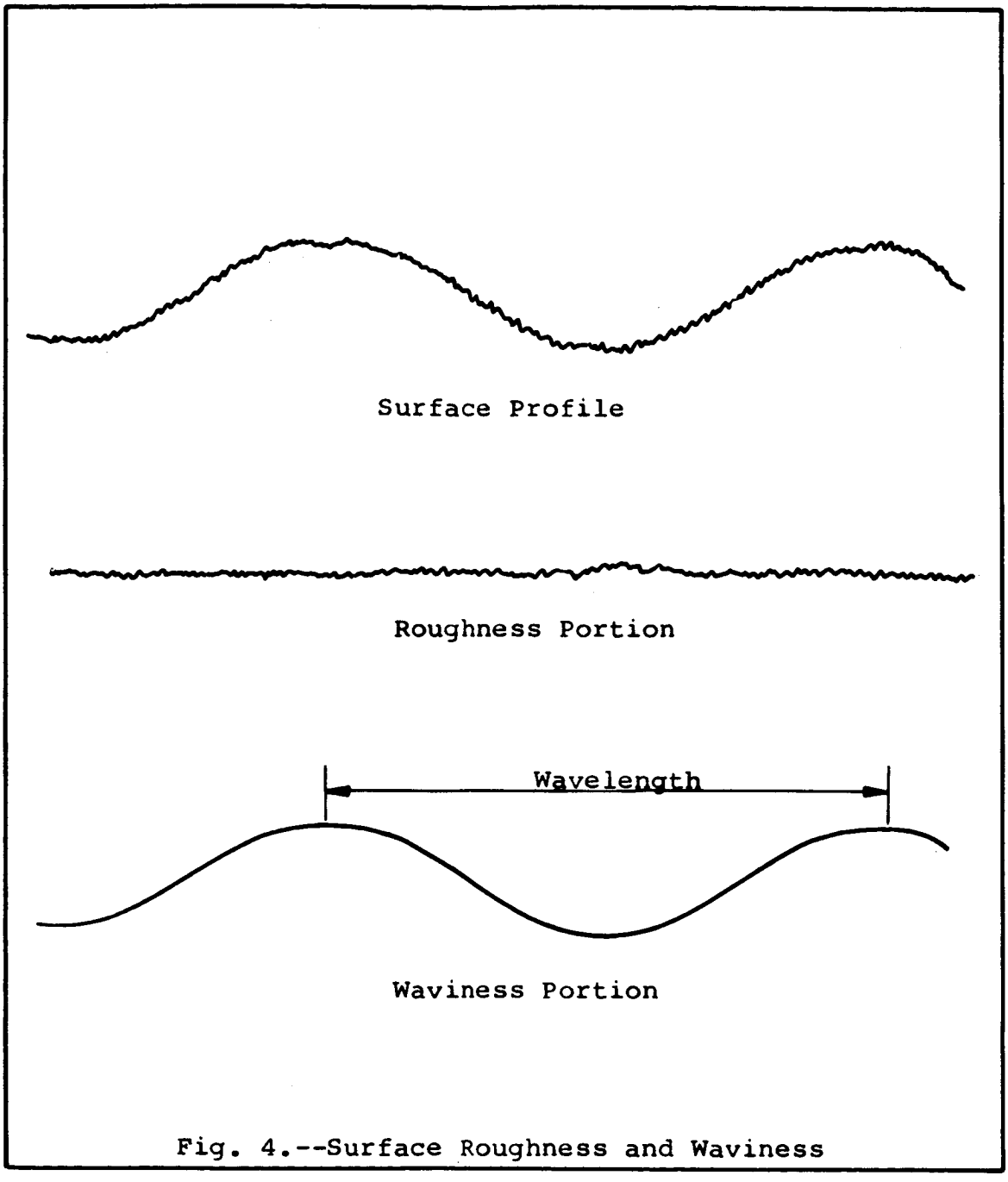

Fig. 4.--Surface Roughness and Waviness

have come into use. The basic difference between the four approaches to be discussed lies in the assumptions made regarding which of these two constriction resistances is predominant. The first three of the four approaches which are discussed below are similar in that they assume that the microscopic resistance dominates the contact resistance. They differ however in that the first two start with an attempt to solve for the temperature distribution in the immediate vicinity of the contact, whereas the third uses a simpler approach. Two of three do employ the concept of waviness in some way, whereas the other assumes that the microscopic contact spots are distributed uniformly over a non-wavy surface. The fourth method assumes that the macroscopic constriction resistance dominates. All four methods are discussed individually below. A brief discussion of the significance of their basic assumptions and the limits of their applicability is presented at the conclusion of this section.

The Approach of Cetinkale and Fishenden:

Cetinkale (Veziroglu) and Fishenden [55] made a theoretical analysis of thermal contact conductance using a model as depicted in Figure 3. In this model there are N such contact spots over the entire surface. The heat flow at a large

distance from the contact interface is assumed to be parallel and uniform throughout the solid. Figure 5 is a sketch, to a more realistic scale, of the idealized contact element showing approximately how the isotherms and heat flow lines should appear. Also shown is the "dividing flow line" which separates the heat flow through solid spot from that which flows through fluid gap. The isothermal surfaces in the vicinity of the solid spot were assumed to be ellipsoids of revolution and the flow lines are then hyperbolas. An expression for an elemental resistance was written in terms of the two parameters which occur in the equations of the ellipses and hyperbolas. The expression was integrated to yield an equation for the contact resistance in which only one parameter remains to be eliminated. The authors deduced the value of the remaining parameter from the results of relaxation solutions for a series of cases which covered a representative range of quantities a/b and $bk_f/\delta_f k_m$. After some further manipulation the following expression for the solid contact conductance is obtained.

$$h_s = \frac{\left(\frac{a}{b}\right) k_m}{b \tan^{-1}\left\{\frac{b}{a}\sqrt{1-\frac{k_f}{h_s \delta_f}} - 1\right\}} \qquad \text{(II-10)}$$

It can be seen that the resulting expression is a transcendental equation for h_s and thus must be solved by some tri-

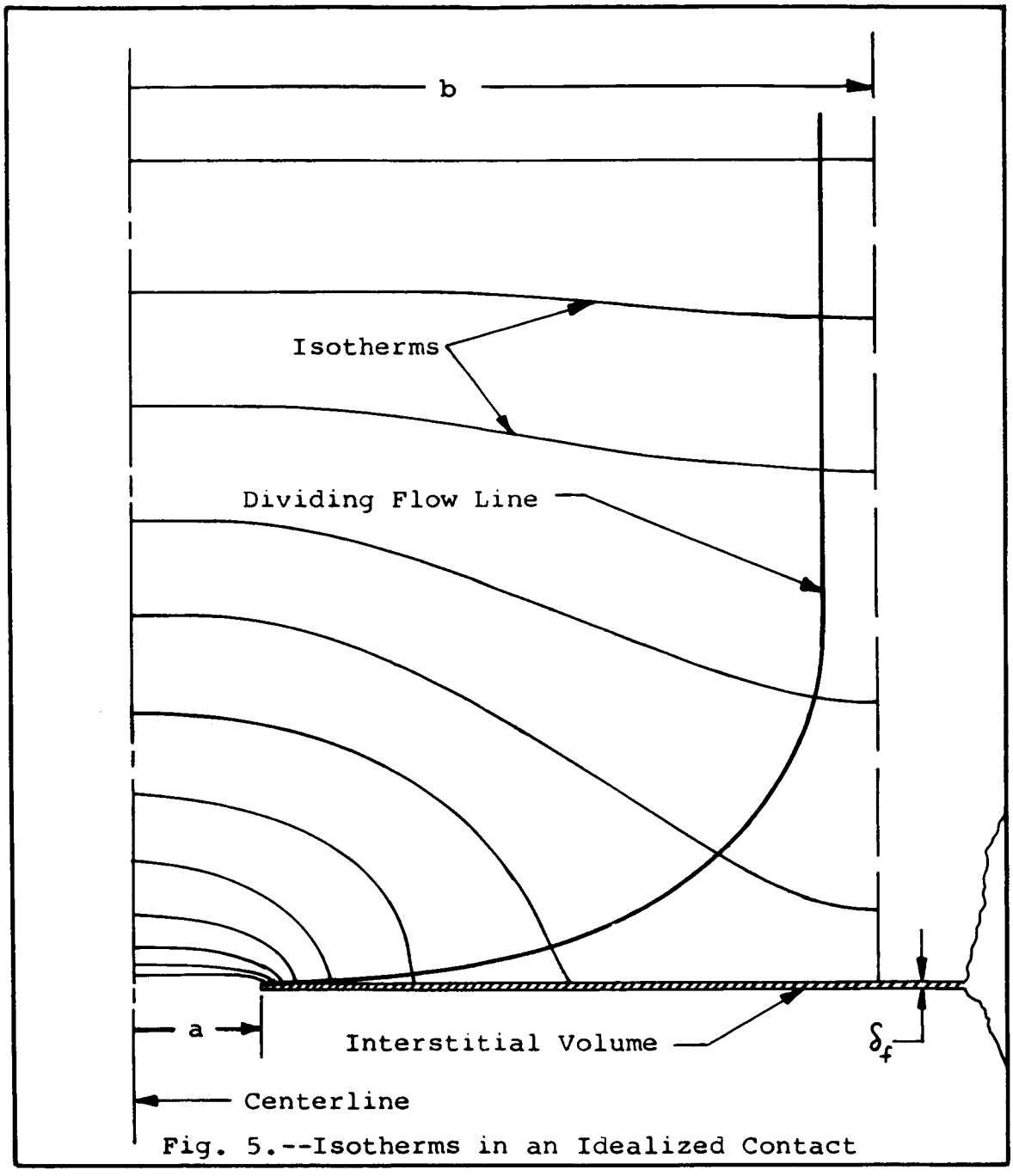

Fig. 5.--Isotherms in an Idealized Contact

al and error procedure. Of the parameters which appear in equation (II-10), k_m (harmonic mean of k_1 and k_2) should be known for a given set of materials. For cases in which radiation can be neglected and the fluid is either a gas at higher pressures or a liquid, the effective conductivity of the gap is simply the fluid thermal conductivity. Otherwise the quantity k_f / δ_f, which is h_f, can be calculated by combining the results of the previous sections of the present work. Cetinkale (Veziroglu) and Fishenden call the ratio a/b the "constriction number." They assume that when pressure is applied to the contact, the softer of the two contact metals flows plastically until the average a-spot pressure is equal to the Meyer hardness. Thus, since

$$\frac{a}{b} = \sqrt{\frac{N\pi a^2}{N\pi b^2}} = \sqrt{\frac{A}{A_c}} = \frac{\text{Apparent Contact Area}}{\text{Actual Contact Area}} \qquad \text{(II-11)}$$

and since

$$pA = MA_c = \text{total applied load}$$

the constriction number can be calculated from

$$\frac{a}{b} = \sqrt{\frac{P}{M}} \qquad \text{(II-12)}$$

For those cases where δ_f is needed separately, the authors suggest that

$$\delta_f = e \cdot (\beta_1 + \beta_2) \qquad \text{(II-13)}$$

Where e is a geometric factor depending on the shape of the surface irregularities and β_1 and β_2 are the respective arithmetic mean heights of the surface roughnesses. The authors noted that for ground surfaces, δ_f is almost constant. Finally, the heat channel radius, b, must be found from the relation

$$b = \psi \cdot (\lambda_1 + \lambda_2) \cdot \left(\frac{a}{b}\right)^{\nu} \qquad \text{(II-14)}$$

Where λ_1 and λ_2 are the wavelengths of roughnesses of the two surfaces. The quantities ψ and ν are constants which must be experimentally determined using heat transfer results. Experimental results obtained by these authors for ground surfaces were: 0.61, 0.0048, and - 5/3 for e, ψ and ν respectively.

The Approach of Fenech and Rohsenow:

Although the work of Fenech and Rohsenow [85] came later than the other two which remain to be discussed, it is presented here because of the similarity of approach to the paper described above.

Fenech and Rohsenow [85], using the contact model depicted in Figure 3, obtained solutions for the temperature distribution in the metals in region of the contact. How-

ever, since the exact boundary conditions are extremely complex, the solutions were found for a set of approximate or average boundary conditions. The resulting expression for the total contact conductance, i.e., the sum of the fluid and solid conduction terms is,

$$h = \frac{k_f}{\delta_f}\left[\frac{(1-\epsilon^2)\left(\frac{4.26\sqrt{\pi}\frac{\delta_1}{\epsilon}+1}{k_1} + \frac{4.26\sqrt{\pi}\frac{\delta_2}{\epsilon}+1}{k_2}\right) + 1.1\epsilon f(\epsilon)\left(\frac{1}{k_1}+\frac{1}{k_2}\right)}{(1-\epsilon^2)\left[1-\frac{k_f}{\delta_f}\left(\frac{\delta_1}{k_1}+\frac{\delta_2}{k_2}\right)\right]\left[\frac{4.26\sqrt{\pi}\frac{\delta_1}{\epsilon}+1}{k_1} + \frac{4.26\sqrt{\pi}\frac{\delta_2}{\epsilon}+1}{k_2}\right]}\right] + 4.26\epsilon\sqrt{\pi} \qquad \text{(II-15)}$$

In which the quantities not previously defined are $n = N/A$ = the number of contact spots per unit apparent area, $\epsilon = \sqrt{\frac{A_c}{A}}$ = the square-root of the ratio of the real to apparent contact areas, and the function $f(\epsilon)$ is a transcendental function. The value of $f(\epsilon)$ is plotted in the paper, however, the authors point out that for most practical situations $\epsilon < 0.1$ and that in this range $f \approx 1.0$. In equation (II-15) it is noted that h is the sum of two fractions. The first fraction, shown by the square brackets in the numerator, represents the gap heat flow, and the second fraction represents the solid metallic conduction. In order to use equation (II-15) three remaining quantities must be evaluated, namely, δ_f, M and ϵ. The authors develop the following approximate expression, valid for small ϵ, for the average fluid gap thicknesses.

$$\delta_i = \frac{\mu_i}{1 - \frac{k_f}{k_i}} \quad , i = 1,2 \qquad k_f \neq k_i \qquad \text{(II-16)}$$

Where the two μ_i are the volume average void thicknesses of the two surfaces. The parameters μ_1, μ_2, η and ϵ may be determined from surface profile measurements obtained with a profilometer. For each surface it is necessary to obtain two profiles taken perpendicular to one another. If the two surfaces are not randomly rough the orientation of the two profile readings on the two surfaces should correspond to the orientation they will have when contact is made. The recorded profiles are reproduced on transparent sheets, and all measurements are made visually and/or graphically by superpositioning the corresponding profiles. The volume average void thickness is determined with the aid of a planimeter. An actual count is made to determine n. Actual contact area, A_c, is measured directly, thus ϵ can be calculated. The profiles are shifted laterally a small amount and the processes repeated. Averaging the results thus obtained gives better values for the measured quantities. Test results and comparison with the above approach are discussed in the next section.

The Approach of Laming:

The same basic contact model as is shown in Figure 3 was employed by Laming [143] in his simplified approach to predicting solid conductance. Laming assumed, as did Cetinkale (Veziroglu) and Fishenden, that when a contact is loaded the softer metal yields plastically until the local pressure borne by an a-spot is equal to the Meyer hardness value, M, of the material.

Thus from the simple force balance,

$$PA = MA_c = M(N\pi a^2)$$

a relation for the spot radius, a, can be found.

$$a = \left(\frac{1}{n\pi}\frac{P}{M}\right)^{\frac{1}{2}} \qquad \text{(II-17)}$$

In equation (II-17), n is the a-spot density, or number of contacts per unit apparent area (N/A). Laming then used the work of Holm [118] who showed that the ideal constriction conductance of a single a-spot is $2ak_m$, i.e., for a single a-spot which is infinitesimally small compared to the heat channel feeding it and is adjacent to a non-conducting gap. Next, the author assumes that this relation can be modified to apply to a single finite size a-spot by use of a "constriction alleviation factor," f, in the following way.

$$\text{single-spot conductance} = \frac{2ak_m}{1-f}$$

The term (1-f), which is dimensionless, is actually the first two terms of a series derived by Roess [184]. However, the series is a power series in (a/b) having only odd terms, and, as Laming points out for most practical cases only the first two terms are needed. Thus, from Roess's work f has the approximate value 1.41 (a/b), see equation (II-22). In order to evaluate n, Laming assumes that the waviness of each surface consists of parallel ridges (such as would result from using a shaper) of wavelengths λ_1 and λ_2, and that the angle of intersection between the ridge lines of the two surfaces when they are brought together is α. Then the conductance is given by

$$h_s = \frac{2k_m}{1-f}\left(\frac{\sin\alpha}{\pi\lambda_1\lambda_2}\cdot\frac{P}{M}\right)^{\frac{1}{2}} \qquad \text{(II-18)}$$

For the fluid gap conductance Laming used k_f / δ_f, where δ_f is the effective fluid gap thickness, and its value must be determined from experimental data. In his work Laming found the value of δ_f to be equal to two-thirds of the volume average gap thickness, which can be found from surface profile records. His method involved determining the zero load conductance, by extrapolation, for tests of the same set of surfaces with fluids having different thermal conductivities. Only the parameter (a/b) remains to be found. By

forming the ratio of solid conduction heat flow to total heat flow, Laming shows that the ratio (a/b) is given by

$$\frac{a}{b} = \left(\frac{P}{M}\frac{h}{h_s}\right)^{\frac{1}{2}}$$

Thus the final form of the total contact conductance is

$$h = \frac{k_f}{\delta_f} + \frac{2k_m}{1-f}\left(\frac{\sin\alpha}{\pi\lambda_1\lambda_2}\cdot\frac{P}{M}\right)^{\frac{1}{2}} \qquad \text{(II-19)}$$

where h_s is given by equation (II-18), and the f appearing there is given by

$$f = 1.41\left[\frac{P}{M}\left(1+\frac{k_f}{\delta_f h_s}\right)\right]^{\frac{1}{2}} \qquad \text{(II-20)}$$

From which it can be seen that an iterative process is required to find h since the equation for f contains h_s. Laming points out that f is small and convergence is rapid for most practical cases. Therefore, using Laming's simplified approach, one needs only to have the Meyer hardness (approximately 3 times the compressive yield strength if unavailable) and surface profiles which give both roughness and waviness, in addition to the thermal properties, to be able to predict contact conductance.

The Approach of Clausing and Chao:

Clausing and Chao [58] made analyses of both the microscopic and macroscopic constriction conductances. For the

microscopic constriction conductance analysis they employed the model shown in Figure 3 and used the work of Holm [118] and Roess [184], as Laming [143] did, to arrive at the following relation for h_s.

$$h_s = \frac{2a k_m n}{g(a/b)} \qquad \text{(II-21)}$$

In which all terms have been previously defined except g (a/b), which is Roess's series:

$$g(a/b) = 1 - 1.40925\,(a/b) + 0.29591\,(a/b)^3 + \cdots \qquad \text{(II-22)}$$

The authors assume, following Holm [118], that the a-spots do not deform completely plastically. They argue that the asperity deformation is partially elastic. To account for this they assumed that the average pressure borne by an a-spot is only a fraction of the microhardness, M. That is,

$$P = \frac{F}{n\pi a^2} = \xi M \,, \qquad (0 < \xi < 1) \qquad \text{(II-23)}$$

Finally, the authors assume that an average value of $\xi = 0.3$ and a value of unity for g(a/b) are representative for most contacts. With these assumptions equations (II-21) and (II-23) give

$$h_s \cong \frac{2P k_m}{aM} \qquad \text{(II-24)}$$

Holm [118] demonstrated experimental justification for the assumption of equation (II-23), however, he recommended a value of $\xi = 0.5$. The lower value assumed by Clausing and Chao is hard to justify.

For their analysis of the macroscopic constriction resistance Clausing and Chao employ basically the same model as shown in Figure 3, except that here the contacting region radius is called a_L and the heat channel radius is called b_L (L for large). The contacting portion (radius a_L) consists of a large number of contact spots (each with a radius a) and there are no contacts outside the radius a_L. Figure 6 shows the geometry employed in the case of a single macroscopic contact. Again employing the work of Holm and Roess the authors arrive at the following relation for the solid conductance:

$$h_s = \frac{2k_m(a_L/b_L)}{\pi b_L g(a_L/b_L)} \qquad \text{(II-25)}$$

For this macroscopic problem the authors assume that the contact region area is controlled by elastic deformation of the contact members. They assume that the flatness deviations of the surfaces may be simulated by spherical caps of radii r_1 and r_2, as shown in Figure 6. The heights, d_1 and d_2, of the unloaded caps are called the "equivalent

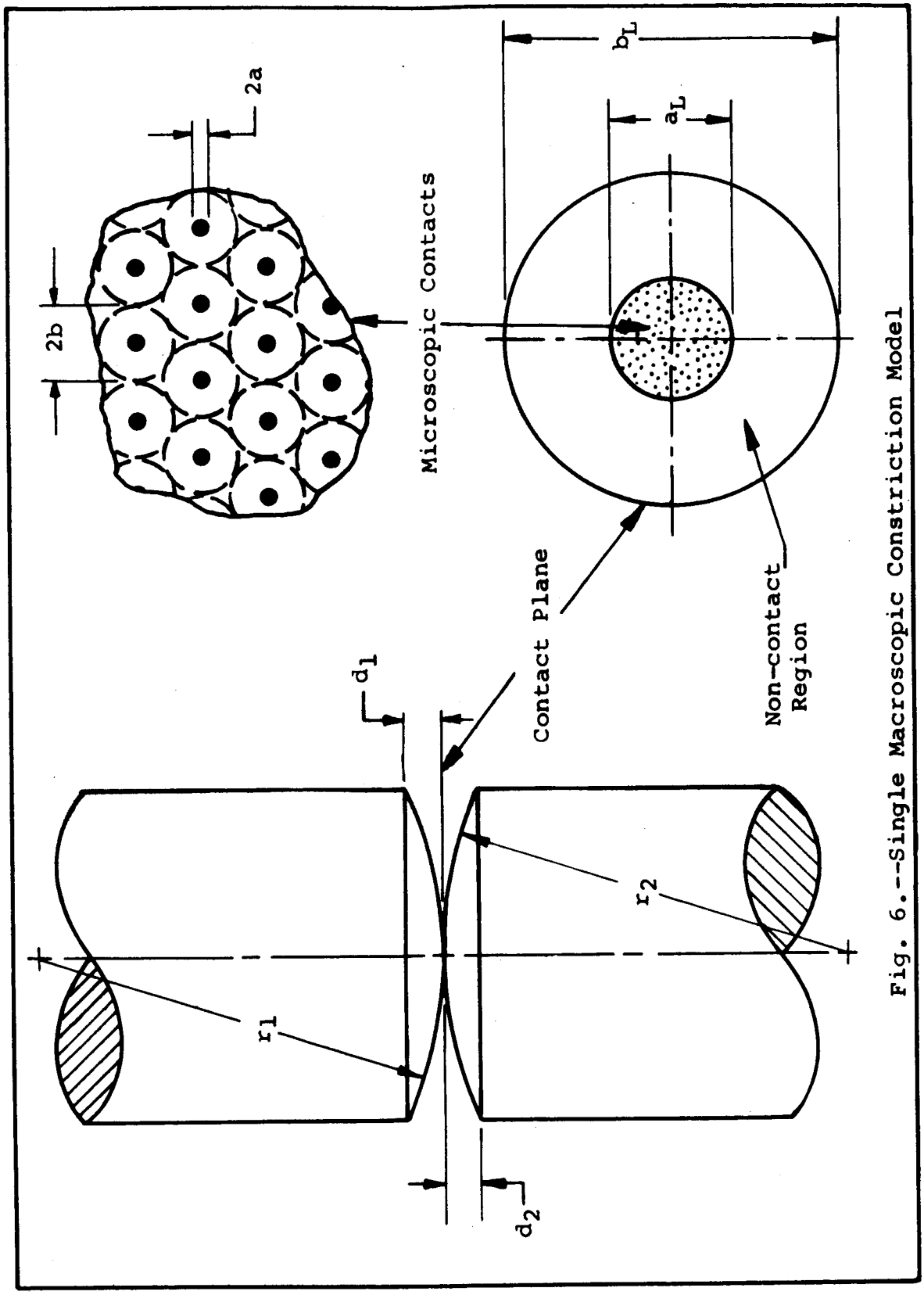

Fig. 6.--Single Macroscopic Constriction Model

flatness deviations" of the respective surfaces. To obtain the load-area relationship for this model the authors use the well known elastic deformation work of Hertz [116]. This results in the following relationship for (a_L/bL):

$$\frac{a_L}{b_L} = 1.285\left[\left(\frac{P}{E_m}\right)\frac{b_L}{(d_1+d_2)}\right]^{\frac{1}{3}}, \qquad (a_L/b_L < 0.65) \quad \text{(II-26)}$$

In which E_m is the harmonic mean of the two moduli of elasticity, E_1 and E_2. The dimensionless quantity in brackets in equation (II-26) is called the "elastic conformity modulus" and given the symbol, ζ. Thus, substituting (II-26) into (II-25) gives

$$\frac{h_s b_L}{k_m} = \frac{2.57[\zeta]^{\frac{1}{3}}}{\pi g(1.285\zeta^{\frac{1}{3}})} = \phi(\zeta) \quad \text{(II-27)}$$

It should be noted that b_L was a known quantity in the work of Clausing and Chao, since their test specimens were made to approximate the model shown in Figure 6. For any practical contact surface b_L would be difficult to evaluate. The present writer assumes that b_L could possibly be estimated from surface waviness. The authors compare the magnitudes of the microscopic and macroscopic constriction resistances by calculating values of the ratio of equations (II-27) and (II-24) for some "representative" surfaces and pressures. From these calculations they conclude that for

many surfaces the macroscopic constriction resistance is dominant by approximately 2 orders of magnitude. The results of a comparison of their theory and experiments is discussed in section III.

Summary on Solid Conduction Mode

An evaluation of the relative merits of using any of the above four methods hinges on three things (1) type of surface; (2) type of data available; (3) accuracy desired.

For reasonably flat, rough surfaces the method of Cetinkale (Veziroglu) and Fishenden, Fenech and Rohsenow, and Laming are all applicable. Of these three Laming's approach is the simplest and requires the least amount of data and effort. The method of Fenech and Rohsenow requires much more work in evaluating some of the parameters but gives more accurate results. The Cetinkale (Veziroglu) and Fishenden approach probably lies somewhere between the other two in accuracy and has the disadvantage of requiring some experimental heat transfer results, unless the average values of the parameters which they report are used. Clausing and Chao [58, pa. 59] state that ".....it is doubtful that their models [models which consider only microscopic constriction]

can be valid." However, the above three approaches have met with reasonable success in predicting contact conductance of surfaces for which they are applicable.

For smooth surfaces in which there is considerable large scale waviness there is no doubt that the emphasis of Clausing and Chao on the macroscopic constriction is applicable. Their experimental results for cylindrical specimens with spherical ends agrees well with their theory. However, there is no indication of how their method could be applied to practical surfaces. For surfaces which fall in between the "rough-flat" and "smooth-wavy" categories no theory has yet been published.

III. LITERATURE SURVEY

The purpose of this section is to provide a survey of the current status of the contact conductance literature. It was the decision of the writer not to present the standard type of review of this literature. Instead, it is hoped, that a more useful document would result from a presentation based on the following outline: 1) reviews of some of the major works in the field and some of the highlights of past research, and; 2) a tabulated review, categorized by the type of information to be found in the various references.

Discussion

Most of the earliest published works concerning contact resistance were written by people who were interested in measuring thermal conductivity. In the course of their experiments these investigators were aware of the temperature discontinuities caused by contact resistance at the interfaces. For the most part these early writers were concerned with attempts to eliminate the contact resistance.

The earliest work found by the present writer that

deals with thermal contact resistance was published by Northrup [171] in 1913. Northrup's paper is an exposition of the analogy between the flow of heat and the flow of electricity, which leads up to a proposal of an apparatus for measuring thermal conductivity or thermal contact resistance. The method is based on comparing the temperature drop across a fixed length of a standard material to the temperature drop across the same length which consists partly of the standard material and partly of an unknown material or a contact resistance. The results are expressed as an equivalent length of the standard material. Northrup reports the contact resistance of a single copper-copper interface as being equivalent to 31.2 cm of copper at a load of 1.6 kg on the 3.8 cm diameter rods. Although Northrup's method left a lot to be desired —— one could not find thermal conductivity accurately unless the contact resistance was eliminated —— his idea of expressing thermal contact resistance as an equivalent length of some material was to become standard practice for a while.

In 1919 Taylor [217] was interested in measuring thermal conductivities of some insulating materials for electric motors. Taylor, by experiment, realized the shortcomings of Northrup's relative method and modified the apparatus to

eliminate the problems. The method used by Taylor is a comparative method in which the temperature drop in each part of the apparatus is measured separately. It is basically the method which has been used by almost all thermal contact resistance investigators since then, including the present work. Taylor, does not report any values of contact resistance but, does report that the addition of such substances as glycerin, vaseline, glue and shellac reduced the contact temperature drop to a negligible amount in the cases of low heat flux.

At the Bureau of Standards, in 1922, Van Dusen [225] developed the basic apparatus one further step to include a spring for controlling the pressure of contact between two or more thermal conductivity specimens in series. Van Dusen was concerned with measuring thermal conductivities of metals and very thin slices of poor conductors. Thus his interest in contact resistance was in finding ways to eliminate it, and he reports that wetting the surfaces with water or light mineral oil effectively eliminated the problems. He states that for his standard specimens (brass) with surfaces ground fairly flat, actually, convex with a radius of curvature of 30 meters, the dry contact resistance was equivalent to 1 - 1.5 cm of brass at contact pres-

sures of 1 - 5 kg/cm^2. He also reports that when the surfaces were lapped together with water or dilute glycerin the contact resistance was reduced to the equivalent of less than 0.5 mm of brass. Although the data are scant it is interesting to note that Van Dusen was aware that surface finish was also important to contact conductance.

Jacobs and Starr [127] , in 1939, published the first work in which the sole purpose was to investigate thermal contact resistance. It is also, oddly enough, the first work for contacts in a vacuum environment. They were interested in obtaining data for designing a mechanically operated thermal switch for use in low temperature research. Their data, which were obtained for gold, silver, and copper surfaces polished to approximately optical flatness, were reported as curves of contact conductance versus contact pressure. In their apparatus the contact pressure was varied by controlling the pressure in a bellows which was external to the vacuum system. Measurements were made at room temperature (25°C) and at - 195°C and for contact pressures from zero to 2.5 kg/cm^2. The most interesting result of this work was that they observed a linear variation of contact conductance versus contact pressure for copper, but for silver and gold the variation was approximately with contact

pressure to the 1/3 power. Jacobs and Starr were obviously aware of the primary variables affecting contact resistance, however, they failed to report any actual, measured surface conditions or vacuum pressure.

In 1948, Fishenden and Kepinski [86] published a short note in which they reported the contact resistance of an interface formed by bringing together the two surfaces of a round steel rod which had been cut through with a saw. The contact resistance is given as being equivalent to approximately a 0.001 inch thick layer of air when the rods were replaced together in the orientation in which they were sawed, and a .002 inch thick air gap when the two pieces were rotated 30^{o} about the axis of the rods. No information is given about the steel composition, surface roughness or contact pressure. Although the work was called a "preliminary note" by its authors the present writer has been unable to find any subsequent published work to follow up the original note.

The years 1948-49 represent the beginning of the significant work in contact resistance. Interest in the subject began to increase, and the caliber of the work began to improve at that time.

Brunot and Buckland [47] experimentally investigated

the contact resistance for two types of steel contacts. Results are given for 2-inch square laminated steel blocks (with heat flow parallel to the lamination planes) for tests in which the lamination planes of the two blocks were parallel and perpendicular but in direct contact, and for tests in which thin shims of aluminum, steel or cement was placed in the contact. Results are also presented for two 2-inch square cold-rolled steel blocks with surface roughnesses of 4 to 1000 microinches (rms). Contact pressures in the first case ranged from 25 to 200 psi and in the second case the range was from near zero to 300 psi. For the laminated blocks the authors found that the parallel laminations resulted in higher resistances than the perpendicular laminations. It was also observed that the addition of the thin shims served to reduce the contact resistance — with aluminum foil giving the greatest reduction. For the solid steel blocks it was found that the smoother the surface finish the lower the contact resistance, and that the variation of contact resistance with pressure is greater for the rougher surface finishes.

Weills and Ryder [233] presented the most complete set of data that had been published at that time. They presented contact conductance results for dry (air in the interface)

and oil-filled interfaces between surfaces of various roughnesses of aluminum, steel, and bronze. Test blocks were 3 inch diameter bars 3 inches long. Heat flow was measured independently and thus allowed the thermal conductivities of the specimens to be measured. The contact conductance results show the effects of mean joint temperature, contact pressure and surface finish. The effect of plating the steel surface with copper was also studied. Complete information about the test samples, including chemical composition and mechanical properties, and test conditions are given. From their results the authors found that the thermal conductance of a dry joint increases with contact pressure, linearly for steel, and exponentially for aluminum and bronze, and that the thermal contact conductance increased with decreasing surface roughness for both dry and oil-filled contacts. At low contact pressures the thermal contact resistance was decreased by a factor of 2 with the addition of oil in the interface. They also reported that the contact conductance increases slightly with mean interface temperature, the increase being greater for smoother surfaces. Weills and Ryder are also apparently the first to report a hysteresis-like variation in the contact conductance versus contact pressure relation when the contact pressure is de-

creased following an increase. The decreasing pressure conductances were found to be higher than those measured at the same pressure when reached by an increase in pressure.

The effects of contact pressure, mean interface temperature and surface roughness of a series of steel-steel joints were investigated by Kouwenhoven and Potter [140]. In this paper thermal contact resistance was measured for a contact formed between two specimens of mild steel, one specimen in every test having a surface roughness of 3 microinches (rms) while the second specimen surface roughness was varied over the range of 3 to 3320 microinches (rms). Tests were made for several combinations of roughness with contact pressure variations from 195 to 3000 psi while keeping the mean joint temperature fairly constant (170 - 197°F). A similar set of tests were made for a contact mean joint temperature of 600°F. The former set of tests was made with air in the joint, the latter set was done with Argon to prevent corrosion. Two other sets of contact resistance data were obtained for several combinations of surface roughness by varying the heat flux so that the mean joint temperature was varied from 350 to 700°F while keeping the contact pressure constant at 195 psi in one case and 1575 psi in the other. The authors concluded that the thermal contact re-

sistance decreases exponentially with contact pressure,with the rate of decrease being greater for rougher surfaces. For very smooth surfaces they found that the contact resistance was essentially independent of pressure. Both of these conclusions are in qualitative agreement with other investigators [24,47,233]. They concluded that the contact resistance at a constant contact pressure is substantially independent of contact temperature (over the range investigated). However, their data contradict this in several cases in which the variation was about the same as that found by others. The authors also have an interesting comparison between a theoretical contact area ratio and the actual thermal resistance ratio for changes in contact pressure in the case of some specimens with ruled roughness. For the simple theoretical model the ruled ridges are assumed to be 45^{o} isosceles trapezoids in profile. The comparison for a 3 microinch surface was very good, but for the rougher surfaces the thermal resistance ratio decreased more rapidly (with increasing contact pressure) than the contact area ratio.

One of the more significant theoretical works in the field was published in 1951 by Cetinkale (Veziroglu) and Fishenden [55]. The details of their approach were discussed previously in section II. The authors presented a drawing

of the test apparatus but do not present their test data. They mention only the ranges of the test parameters and indicate that agreement between theory and experiment was good.

Barzelay, et al [24 - 29] published a series of NACA reports on their investigations of thermal contact conductance. Their results,too numerous to detail here, covered both cut-bar apparatus measurements and conventional skin-stringer type aircraft joints. Materials tested were aluminum (7075-T6 and 2024-T4) and 416 stainless steel. A large range of surface roughness and contact pressure was studied. The effects of mean joint temperature and the addition of thin foils to the interface were studied. Complete test conditions and results are reported. The most interesting results of these references are the following. They are apparently the first to observe that surface roughness is not always dominant in controlling contact conductance but that flatness deviation (waviness) sometimes predominates. It was also noted that in some of the skin-stringer tests the warping of the members due to thermal expansion produced some adverse effects on the contact heat transfer.

An equally important "first" reported by Barzelay, et al [25] was the difference observed in contact conductance for dissimilar metal joints when the direction of heat flow

was reversed. They found that the contact conductance for an interface in which heat flowed from an aluminum specimen to a stainless steel specimen was several times higher than when the heat flow direction was reversed, other test conditions being the same.

Barzelay and Holloway [26,27] are the first published work to study the effects of an interface on thermal transients. They made tests on a number of riveted aluminum stringer-skin combinations in which they measured the temperature at several points on a T-shaped stringer riveted to a flat skin. The skin was subjected to a constant radiant heat flux to simulate aerodynamic heating. It was found that the interface resistance had a significant delaying effect on the time-temperature history of a given point on the stringer. There was considerable scatter in the conductance data which they attributed to the warping effects.

Further work on the directional effect in dissimilar metals was carried out by Rogers [187]. In Rogers' experimental apparatus the direction of heat flow was changed without separating the test specimens. Tests were carried out with aluminum and steel specimens at a constant contact pressure of 122 psi. Results showed that for the same aluminum

steel joint (in air) the contact conductance was about 20% higher when heat flowed from the aluminum to the steel than when the heat flow was reversed. When these specimens were tested in a vacuum the difference was approximately 100% due to the low conductance in the vacuum. Other combinations tested were chromel-alumel and copper-steel. The former showed no clearly defined directional effect, the latter only a slight effect. Rogers suggested that the directional effect might be associated with the mechanism of conduction at the points of metallic contact.

Williams [236], in a comment on Rogers' paper, suggested that the directional effect was a result of surface oxidation. Williams states that the difference in lateral (parallel to contact plane) thermal expansion could literally "scour" the oxide layer off the aluminum surface. In response to Rogers' paper, Moon and Keeler [167] applied the theory of solid state heat conduction. They showed that the effect could be qualitatively explained by demonstrating that the electronic conduction contribution was directional. They stated that accurate quantitative-analysis was impossible due to lack of data on the work functions of metals. However, Ashby [5] claims that Moon and Keeler made an error in their analysis and that such an effect is not demonstrated

by the corrected calculations. It is clear that at this time the directional effect in dissimilar metal contacts is not well understood. Results of research which is presently in progress at several institutions may serve to clarify this phenomenon.

In the design of nuclear reactors contact resistance can be an important consideration. Several papers have been written which are concerned with the contact resistance of materials and/or configurations which are applicable to reactor design. One of the first of these was published by Boeschoten and Van Der Held [141] in which surfaces of aluminum-aluminum, aluminum-steel and aluminum-uranium were studied. One of their purposes was to determine the gas and solid conduction contributions separately. This was accomplished by running tests at constant contact pressure and mean interface temperature while varying the ambient gas and gas pressures. The conductance curves for three gases, air, helium and hydrogen, were extrapolated to zero gas pressure, thus giving the value of the solid-solid conductance. From a simplified analysis they calculated the average a-spot radius to be approximately 30 microns. This value was found to be relatively independent of materials and contact pressure for the range of their test conditions.

Wheeler [235] wrote a survey paper in which he examined some of the published vacuum conductance data. He concluded that most of the existing (unclassified) work could not be extrapolated with sufficient accuracy to the higher heat flux levels characteristic of nuclear reactors. In a later work [234] Wheeler presented some data for materials and heat flux levels typical of nuclear reactors. He also tried a different approach to conductance data correlation which consisted of plotting contact conductance versus the ratio of apparent contact pressure to the yield strength of the softer contact material. His results showed considerable scatter. He also attempted to find the effective gap thickness by conducting tests on the same joint in a vacuum and with different gases. The results were highly doubtful since the gap thicknesses calculated were on the order of 2 to 10 times the total surface roughness heights. It seems likely that these results may indicate the presence of large scale flatness deviations of which Wheeler was unaware.

Skipper and Wootton [203] studied the contact conductance of uranium-Magnox and uranium-aluminum joints. In addition to the effects of mean temperature and gas pressure they also reported data on the effects of very thick oxide films. For gas-cooled reactor applications Sanderson [188]

also investigated the contact conductance between uranium and Magnox surfaces. Data are reported for the effects of contact pressure, interface temperature, ambient gas pressure and surface finish. The reduction of contact conductance by oxide and nitride surface layers is also reported.

One of the first attempts to make a general correlation of thermal contact conductance data was made by Graff [103]. He plotted the data of several investigators in the form of two dimensionless groups: $hp/k\rho$ versus p/B. The former group is the product of conductance and contact pressure divided by the product of the thermal conductivity and the density of the metal. The latter group is the ratio of contact pressure to Brinell hardness number. These dimensionless groups did not correlate the data. Graff suggested the reason for this was the lack of a roughness parameter.

Most contact conductance data published were obtained with cylindrical specimens with axial heat flow. The work of Barzelay [24-29] on "practical" joints has already been mentioned. Aron and Colombo [13] report some data on a single, bolted type aircraft joint. One of the first experimental works using flat plate specimens was published by Fried and Costello [96]. They measured thermal contact conductance for 5 x 5 x 1/8 inch thick plates of aluminum and

magnesium. Contact pressures ranged from 2 to 35 psi; a range the authors felt representative of bare space vehicle joints. They found that smoother surface finishes gave higher conductances, but that flatness deviations could have significant effects on the conductance for smooth and rough surface finishes. The authors also reported that the addition of soft shim materials, such as aluminum and lead foils and thin, copper wire-mesh cloth, could improve the conductance by as much as a factor of 2 - 4 times the value for a bare joint. Of these three, lead foil gave the largest increase. Fried, in a later paper [94], found that the addition of a silicone grease could greatly increase the contact conductance.

Jansson [128] also investigated interstitial filler materials for contact conductance improvement. He found that for the materials and conditions tested, indium foil gave the largest improvement. Other materials tested were, in order of descending improvement, epoxy cement, lead, aluminum and gold foils. Indium foil was also found to give better conductance improvement than lead, and aluminum foils by Koh and John [139]. From the results of this study they concluded that foil softness was more significant than the thermal conductivity of the foil. They also demonstrated

experimentally that there is an optimum foil thickness for a given joint.

Further work on thin plates was done by Stubstad [206,207]. He measured the contact conductance for a joint between two 3 x 3 x 1/8 inch plates in a vacuum at very low contact pressures, i.e., 2 to 20 psi. Materials tested were aluminum, copper and stainless steel. He observed that the contact conductances was an order of magnitude higher at atmospheric pressure than in a vacuum of 10^{-5} mm Hg, which demonstrates the large gas conduction contribution at low contact pressures. It was also observed that test repetition with different sample orientations produced large variations in the contact conductance.

In 1961, Laming [143] presented a simplified analytical approach to the prediction of contact conductance. The details of his approach were presented in section II. He reported test data for steel-brass, steel-aluminum, brass-aluminum and brass-brass contacts with air, water and glycerol in the joints. Agreement of his test data with his theoretical equations was poor at low contact pressures (20 psi) and improved somewhat with higher contact pressures. However, he found that if a load dependent value of the Meyer hardness was assumed, all his test results correlated

with the theory very well. The load dependent microhardness hypothesis results in high hardness values at low loads. Although there is some evidence to support this hypothesis, Laming [143, p. 75] states that the only claim made for it is ".....its value in correlating the heat transfer data." However, his assumptions have at least been partially justified by the recent results of Williams [238]. Williams ran tests on mild steel and nickel specimens and controlled the number of contacts spots by using ridged surfaces of various ridge frequencies. His test results showed that the effective hardness of the nickel specimens increased by a factor of 5 when the average spot load was reduced from 1000 lbf to 0.1 lbf. Similar results for mild steel were also reported.

Laming's simple theory (i.e., without load dependent hardness) predicts that the solid conductance should vary as contact pressure to the one-half power. His test results show that the variation is nearer the two-thirds power. However, Fried [94] found, using his own data for aluminum and magnesium, that the contact conductance in a vacuum (therefore only solid conductance) varied very nearly as the one-half power of contact pressure. This may suggest that Laming's discrepancies arose from his method of estimating the fluid conduction contribution.

Fenech and Rohsenhow [85] presented a thorough analytical treatment of contact conductance, the details of which have already been discussed. To test their theory they obtained contact conductance data for an armco iron-aluminum joint with maximum roughnesses of 150 microinches (rms). Contact pressures ranged from 92 to 2625 psi. Agreement between measured results and theory was very good. They also tested several "idealized" contacts. These consisted of stainless steel specimens with a machined pyramid surface against an optically flat surface, and an iron pyramid surface against and an optically flat-topped pyramid surface of aluminum. Plots of measured and theoretical contact conductance versus mean joint temperature for contact pressures of 92 to 6226 psi show good agreement for these surfaces, the agreement being better for the stainless steel specimens. Another set of tests are reported for some solid cylinders with a neck machined in them to simulate a single conduction channel and a-spot (see Figure 3). Results are plotted for three sizes of neck, i.e., three values of the ratio of spot radius to heat channel radius ($^{a}/_{b}$). Curves of conductance versus mean contact temperature for air, water and mercury in the gap show reasonable agreement between theory and experiment.

Henry [115] compared the test data of Adamantiades [4] with the theoretical prediction method of Fenech and Rohsenow. The experimental results were for stainless steel surfaces which had been ground to a "mirror finish" and subsequently blasted with small glass spheres to achieve random roughness. Plots of measured and theoretical contact conductance versus contact pressure for three mean temperatures were presented. Agreement was very good.

The above comparisons show that for test conditions which meet the assumptions of the theoretical analysis the agreement with experiment is good. However, to date, the theory has not been compared with "everyday" engineering surfaces, mostly due to lack of sufficient test information. Thus there is still some question of its general applicability. The only real disadvantage to the approach of Fenech and Rohsenow [85] is the very involved graphical procedure that is required to determine the necessary surface parameters. Others at Massachusetts Institute of Technology have been working on methods of simplifying the work required to obtain these parameters. The results of these efforts are summarized by Henry [115].

Clausing and Chao [58] presented a theoretical analysis which assumes that macroscopic heat flow constrictions

caused by the flatness deviations of a surface dominate the metal contact resistance. This is opposed to the analyses of others [55,85,143] which assumed only microscopic constrictions due to uniformly distributed microscopic contact spots. Clausing and Chao conducted experiments on cylindrical specimens whose contact surfaces were spherical caps. These specimens matched their theoretical model, which is shown in Figure 6. Materials tested were aluminum, stainless steel, and brass. Contact pressures varied from about 10 to almost 1000 psi. Agreement between theory and experiment was very good for all reported data. It should be noted that the test specimen and theoretical model have only one macroscopic contact. Most real surfaces of practical importance would have several such contact areas. The authors do not suggest how the theory could be applied to a practical surface. The real value of their approach, and their experimental verification, is that it does account for macroscopic effects, which are known to be important under some conditions. However, as is true for the other theoretical approaches, further work remains to be done before the contact conductance of general engineering surface can be predicted.

In addition to the work of Barzelay [25], which has

already been mentioned, the only other published experimental work on thermal transient effects on contact conductance is the recent paper by Schauer and Giedt [190]. The authors derived theoretical equations and devised an experimental method for determining the contact conductance between two thin plates during transient heat transfer. The method is based on the heating of one of the plates with a capacitor-bank discharge and recording the temperatures of the contact surfaces as they come to thermal equilibrium. Tests were performed on aluminum-stainless steel and stainless steel-ceramic interfaces. The heating time was approximately 100 microseconds and the temperature data were recorded by an oscilloscope for about 160 milliseconds. The metal specimens were 0.032 inch thick and the ceramic specimen was 0.302 inch thick. These test results showed that the contact conductance of the aluminum-stainless specimens increased sharply with time, whereas the opposite was true for the stainless steel-ceramic specimens. The method of calculation assumes that no heat is transferred during the short capacitor discharge time, that all the heating occurs in the plate of lowest electrical resistivity and that an instantaneous temperature rise was produced. The first two of these assumptions seem to have been satisfied by the ex-

periment. However, due to the fact that the thermocouples were embedded in epoxy cement there was an indicated transient rise in the temperature difference. This made it necessary to extrapolate to time zero to get the initial temperature difference, and also ruled out experimental verification of a doubtful boundary condition. This together with possible errors in thermocouple location make the results highly doubtful. Even if the results are valid they indicate that the conductance approached a steady value very rapidly (say 100 milliseconds) and therefore the indicated transients would be of no significance in most practical situations. The method also has the strict limitation of being applicable only to very thin pairs of dissimilar solids due to the method of heating.

One other work on transient conductance effects deserves mention here. Aaron and Blum [2] performed a theoretical analysis of the effects of varying the ambient gas pressure on the contact conductance and temperature distribution in two contacting cylinders. They predicted the existence of a threshold pressure above which the contact conductance would be independent of pressure. They also demonstrated that for most practical joints the gas pressure within the contact voids would respond very rapidly to ambient

pressure changes. Some results of the present work which appear to be at least a partial experimental verification of these predictions will be discussed in section VI.

Summary

A glance at the above brief review shows that the phenomenon of thermal contact resistance is far from being completely understood. Although a great deal of experimental data have been obtained, empirical correlations of them have been unsuccessful. Theories have been presented, and test data on well prepared samples of particular configurations have agreed well with the theories. Yet, no means is presently available for the accurate prediction of the thermal contact conductance of a general engineering interface. The failure of past work is due mainly to the fact that no statistically meaningful means of characterizing the contact between two surfaces is yet available. The validity of the statement that the past work is truly a failure is supported by the fact that the National Aeronautics and Space Administration has recently awarded a contract to E. Fried of General Electric to measure, individually, the contact conductance of over 100 separate practical joints for the Apollo spacecraft.

Tabulated Review

The brief reviews presented above obviously do not represent more than a fraction of the total number of thermal contact resistance references. However, they do represent, in the writers opinion, a good sampling of the literature, both from the standpoint of historical development and the standpoint of indicating the important effects that have been observed. An interested reader can refer to the tabulated review below to obtain more information about any of the particular aspects of contact resistance.

There are 244 references listed in the Bibliography section which pertain to thermal contact resistance or a closely related topic. No claim of completeness is made. However, it is believed that at least a majority of the subject references are included in this list. The results of the review are presented in Tables 1,2 and 3. The headings used in the three tables are discussed individually below. Two points concerning the tables, which the writer wishes to emphasize are:

1. The categories were chosen which seemed to be the most useful based on the writer's own experience.
2. The writer was unable to obtain copies of some of the references listed in the Bibliography. There-

TABLE 1. EXPERIMENTAL RESULTS FOR CONTACTS IN THE PRESENCE OF CONDUCTING FLUIDS	
IN AIR	4,14,15,16,24,25,26,27,28,29,32,34,36,40,41,47,55,61,74,85,86, 89,110,114,130,139,140,143,152,160,161,162,163,164,173,182,185, 188,194,195,196,203,206,207,225,233,234
IN OTHER GASES	40,41,74,85,140,161,162,182,188,195,196,203,234
WITH A LIQUID OR GREASE IN THE INTERFACE	41,55,85,97,143,217,225,233
WITH FOILS, SHIMS OR POWDERS IN THE INTERFACE	6,15,16,24,25,34,40,47,74,85,89,139,160,161,162,163,164,188, 203,209,225,233,234
EFFECTS OF SURFACE ROUGHNESS	15,24,25,36,41,47,55,61,74,85,89,110,114,130,139,140,143,152, 160,161,162,163,164,173,182,185,196,225,233,234
EFFECTS OF CONTACT PRESSURE	14,15,25,34,36,41,47,55,61,74,85,89,110,114,130,139,140,143, 152,160,161,162,163,164,173,182,188,194,195,196,203,206,207, 224,233,234
BOLTED OR RIVETED	11,16,26,27,28,29,60,68,89,90,208,210,216
DISSIMILAR METALS	4,14,15,24,25,40,41,48,55,61,74,85,89,130,143,152,164,173,179, 182,185,190,203,234,235,236,237
EFFECTS OF MEAN TEMPERATURE	16,24,25,26,27,48,85,89,114,130,139,140,152,161,162,182,185, 188,195,196,203,233,234

TABLE 2. EXPERIMENTAL RESULTS FOR CONTACTS AT LOW AMBIENT GAS PRESSURES	
IN AIR	10,13,14,15,19,23,32,33,37,41,58,59,64,74,80,81,87,89,91.92, 94,96,97,127,135,153,159,161,162,163,173,182,185,188,195,196, 203,206,207,234,238,242,243
IN OTHER GASES	32,41,74,182,196,203,234
WITH A LIQUID OR GREASE IN THE INTERFACE	37,40,58,64,92,94,97
WITH FOILS, SHIMS OR POWDERS IN THE INTERFACE	15,32,40,64,89,92,96,97,159,188,234
EFFECTS OF SURFACE ROUGHNESS	15,19,37,41,58,59,64,74,87,89,91,92,94,96,97,135,153,173,182, 185,188,196,234,238,242,243
EFFECTS OF CONTACT PRESSURE	13,14,15,19,32,37,41,58,59,64,74,87,89,91,92,94,96,97,127 135,153,159,173,182,196,203,206,207,234,238,242,243
DISSIMILAR METALS	14,15,32,37,41,59,89,92,97,135,173,182,185,203,234,235,236, 237
BOLTED OR RIVETED STRUCTURES	10,13,80,81,89,204
EFFECTS OF MEAN TEMPERATURE	23,32,33,37,58,64,89,159,182,185,234

TABLE 3.
SPECIAL TOPICS AND TOPICS CLOSELY RELATED TO THERMAL CONTACTS

THEORETICAL TREATMENT OF CONTACT CONDUCTANCE	31,57,58,59,77,83,85,114,138,143,167,184,197,199,242
TRANSIENT CONTACT CONDUCTANCE DATA OR THEORY	2,26,34,39,46,60,127,190,231
COMPOSITE SOLID TEMPERATURE DISTRIBUTIONS	8,21,39,66,69,90,108,122,134,148,156,157,168,174,184,189, 192,198,205,211,222,224,227,228,229
METAL SURFACE CHARACTERISTICS	12,30,43,44,51,53,57,65,72,78,79,85,88,91,104,105,111,113, 115,116,118,126,136,140,149,150,154,155,169,178,193,215, 221,230,238
EFFECTS OF CONTACTS ON THERMAL STRESSES	22,28,45,50,100,106,146,175,201,240
CONTACTS AT LOW TEMPERATURES	9,23,32,33,56,159,170,218,220,244
NUCLEAR REACTOR APPLICATIONS	3,17,40,48,67,70,71,161,162,166,172,183,187,191,203
SURVEYS AND REVIEWS	7,18,19,35,76,89,91,94,101,103,123,124,125,138,180,202,213, 219,235,239

fore some references do not appear in any of the tables. Only those references which were reviewed by the writer are included in the tables, with a few exceptions where the title clearly indicated one of the special or related topics.

Discussion of Reference Tables

Those references which contain experimental results for contacts in the presence of a conducting fluid are listed in Table 1. References which contain data on the specific subheadings are listed next to each subheading. The numbers in all the tables refer to the corresponding entries in the Bibliography. The subheading topics are self explanatory.

Table 2 contains those references which present experimental results for contacts at low ambient pressures. Most of these are, of course, for air vacuum. Subheading topics are the same as for Table 1. If a reader is interested in a combination of topics, e.g. bolted and riveted joints with interface fillers, it is a simple process to check both subheadings and find the common entries.

Table 3 contains references pertaining to special or related topics. The first subheading contains those refer-

ences which have anything that might be considered a theoretical approach to contact resistance. References that allude in any way to thermal transients in the presence of thermal contacts are in the second subheading. The third subheading is a list of references which contain theoretical analyses of the temperature distribution in composite solids of various shapes and with various boundary conditions. Almost all of these assume perfect thermal contact between regions, but are included here as a closely related special topic. The remaining related topic subheadings are self explanatory.

As mentioned above, no claim of completeness is made for the entries in the tables. However, checking those references listed under any specific heading should provide a very good start.

IV. THEORETICAL STUDIES

A general description of the class of boundary value problems for which solutions are obtained in this work is presented first. This is followed by an outline of the derivations and the solutions obtained. The method of obtaining the numerical solutions for the same problems is discussed briefly. Some remarks concerning the accuracy of the results obtained, including a comparison of the analytical and numerical results are given. A presentation and discussion of the results obtained from a parametric computer study using the solutions concludes this section.

The Boundary Value Problem

The problem of interest here is that of obtaining the space-time temperature distribution in a composite solid medium consisting of two regions separated from each other by an interface which has a resistance to heat flow.

Figure 7 depicts the geometry employed and some of the necessary nomenclature. Both regions are assumed one-dimensional and homogeneous within themselves, each with a constant thermal conductivity and thermal diffusivity. However,

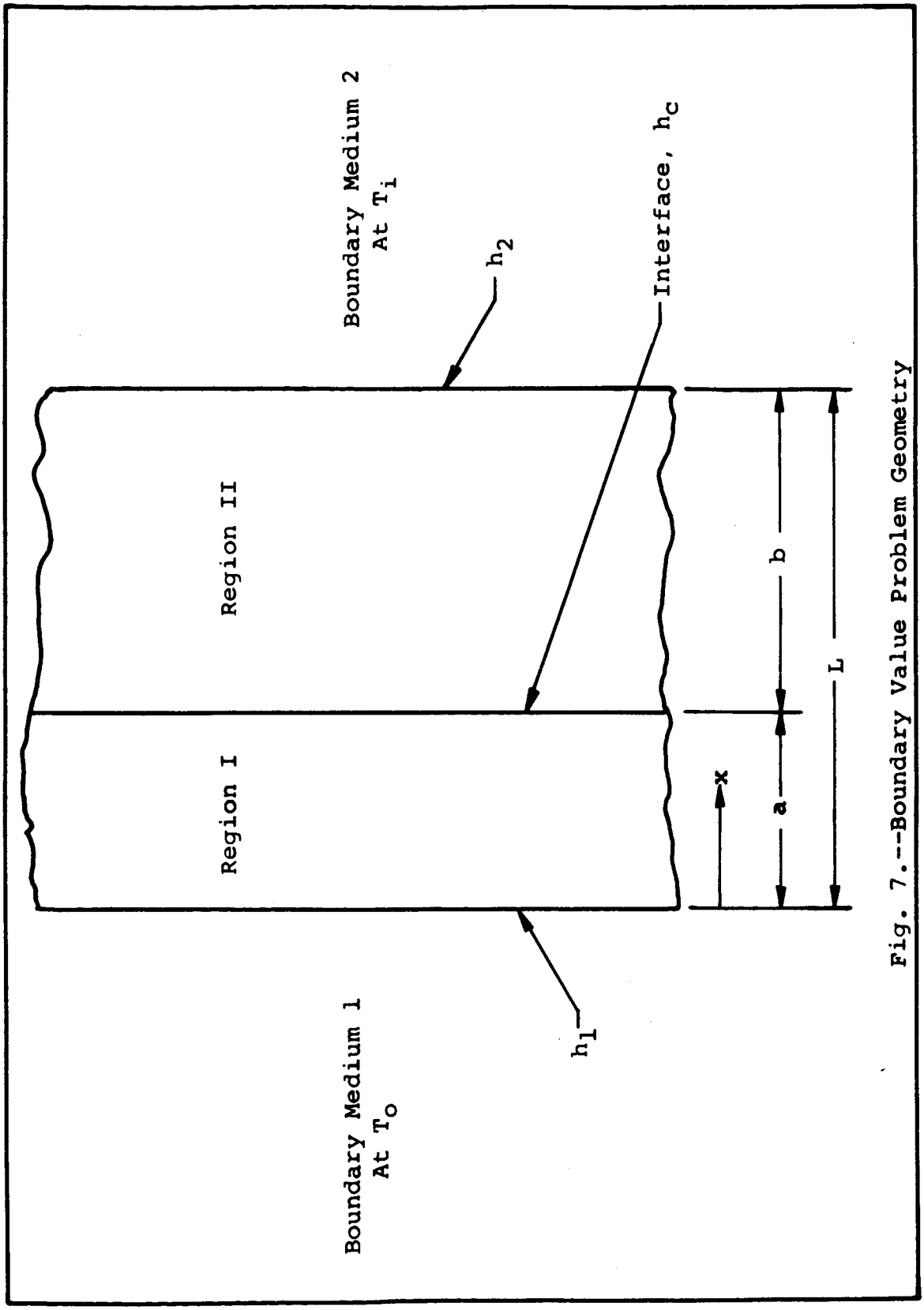

Fig. 7.--Boundary Value Problem Geometry

there is a discontinuity in these thermal properties across the interface which necessitates separate solutions for the two distributions, as indicated in Figure 6 [248]. Both solutions must obey the one-dimensional Fourier equation. Thus for the distribution we have,

$$\frac{\partial^2 t_1}{\partial x^2} = \frac{1}{\alpha_1}\frac{\partial t_1}{\partial \theta} \qquad 0 \le x \le a$$

$$\frac{\partial^2 t_2}{\partial x^2} = \frac{1}{\alpha_2}\frac{\partial t_2}{\partial \theta} \qquad a \le x \le L \qquad \text{(IV-1)}$$

Applicable boundary conditions are as follows. Initially both regions are assumed to have time-independent temperature distributions. To complete the problem description it is necessary to specify the changes that occur at time $\theta = 0$ at any of the three physical boundaries and the other conditions imposed. For the present work the conditions at the outer boundaries ($x = 0$ and $x = L$) may be of the temperature or gradient type and the interface boundary will be of the gradient type. The detailed conditions employed in the separate cases studied are developed below.

Case A.

Initially both regions are at a uniform temperature, t_i. At $\theta = 0$ the temperature at $x = 0$ is suddenly raised to a value t_o and held constant. The temperature at $x = L$

is held at its initial value and the contact resistance at the interface is held constant. Symbolically, these conditions are as follows:

$$t_1(x,0) = t_i \tag{IV-2}$$

$$t_2(x,0) = t_i \tag{IV-3}$$

at the ends

$$t_1(0,\theta) = t_o \qquad \theta > 0 \tag{IV-4}$$

$$t_2(L,\theta) = t_i \qquad \theta > 0 \tag{IV-5}$$

at the interface

$$k_1\left(\frac{\partial t_1}{\partial x}\right) = k_2\left(\frac{\partial t_2}{\partial x}\right) \qquad x = a,\ \theta > 0 \tag{IV-6}$$

$$k_1\left(\frac{\partial t_1}{\partial x}\right) = h_c\,(t_2 - t_1) \qquad x = a,\ \theta > 0 \tag{IV-7}$$

$$\frac{\partial}{\partial \theta}\left(k_1 \frac{\partial t_1}{\partial x}\right) = \frac{\partial}{\partial \theta}\left(k_2 \frac{\partial t_2}{\partial x}\right) \qquad x = a,\ \theta > 0 \tag{IV-8}$$

The solution obtained from equation (IV-1) by the standard technique of separation of variables in product form is well known. With the proper choice of sign on the separation constants the solutions for the two regions are:

Region (I)

$$\frac{t_1(x,\theta) - t_i}{t_o - t_i} = 1 - A_1 x + \sum_n B_n \left[C_n \cos \gamma_n x + \sin \gamma_n x\right] e^{-\gamma_n^2 \alpha_1 \theta} \tag{IV-9}$$

Region (II)

$$\frac{t_2(x,\theta) - t_i}{t_o - t_i} = A_2(L - x) + \sum_n B_n \left[F_n \sin \delta_n x + G_n \cos \delta_n x\right] e^{-\delta_n^2 \alpha_2 \theta} \tag{IV-10}$$

These solutions have been written as the sum of steady state and transient parts to take advantage of the fact that the steady state solutions are simply linear functions of x. For the transient portions the summations have already been indicated in anticipation of the requirements of expanding the initial boundary condition in a Fourier series. The constants A_1 and A_2 are the well known steady state temperature slopes, and can be written as,

$$A_1 = \frac{1}{a + \frac{k_1}{h_c} + b\frac{k_1}{k_2}} \qquad \text{(IV-11)}$$

$$A_2 = \frac{1}{a\frac{k_2}{k_1} + \frac{k_2}{h_c} + b} \qquad \text{(IV-12)}$$

The solution of the problem is completed by determining the unknown coefficients B_n, C_n, F_n, and G_n, and the eigenvalues γ_n and δ_n. It is noted that the form of coefficients was chosen in anticipation of simplifying the calculations.

Application of the boundary condition (IV-4) leads to the following

$$0 = \sum_n B_n [C_n (1) + 0]$$

Therefore, $C_n = 0$.

Upon applying (IV-5) it is seen that

$$0 = \sum_n B_n [F_n \sin \delta_n L + G_n \cos \delta_n L]$$

or, $$G_n = -F_n \tan \delta_n L \qquad \text{(IV-13)}$$

Boundary condition (IV-8) is simply a statement of the assumption that there is no heat storage in the infinitesimal thickness of the interface. Its application yields

$$\gamma_n^2 \alpha_1 = \delta_n^2 \alpha_2$$

or, $$\delta_n = \gamma_n (\alpha_1/\alpha_2)^{\frac{1}{2}} \qquad \text{(IV-14)}$$

Next, (IV-6) is applied and results in

$$k_1 \sum_n B_n \gamma_n \cos \gamma_n a = k_2 \sum_n B_n \delta_n [F_n \cos \delta_n a + G_n \sin \delta_n a]$$

Substituting (IV-13) and (IV-14) into the above equation and applying some trigonometric identities gives

$$F_n = \frac{\frac{k_1}{k_2}\left(\frac{\alpha_1}{\alpha_2}\right)^{\frac{1}{2}} \cos \gamma_n a \cos \delta_n L}{\cos \delta_n b} \qquad \text{(IV-15)}$$

The application of (IV-7) yields

$$k_1 \sum_n B_n \gamma_n \cos \gamma_n a =$$
$$h_c \left[\sum_n B_n (F_n \sin \delta_n a + G_n \cos \delta_n a) - \sum_n B_n \sin \gamma_n a\right]$$

Substituting (IV-13), (IV-14) and (IV-15) into the above, together with some algebraic and trigonometric simplification, gives the following

$$-\gamma_n = \frac{h_c}{k_2}\sqrt{\frac{\alpha_2}{\alpha_1}} \tan\left(\gamma_n b \sqrt{\frac{\alpha_1}{\alpha_2}}\right) + \frac{h_c}{k_1} \tan(\gamma_n a) \qquad \text{(IV-16)}$$

Equation (IV-16) is the eigenvalue equation from which the region I eigenvalues, γ_n, may be found. Once

found, these values give the region II eigenvalues, δ_n, by means of equation (IV-14). The coefficients F_n and G_n are then determined by equations (IV-15) and (IV-13).

Only the primary series coefficients B_n remain to be found to complete the solution. It is well known that their values are determined by satisfying the so-called initial condition, i.e., the time boundary condition. However, ordinary Fourier series expansion is inadequate here because the solution eigensets, namely,

$$\begin{aligned} f_n(x) &= \sin \gamma_n x \qquad 0 \le x \le a \\ f_n(x) &= F_n \sin \delta_n x + G_n \cos \delta_n x \qquad a \le x \le L \end{aligned} \tag{IV-17}$$

are not orthogonal over the full x-interval (0, L). However, Tittle has shown [222] that these functions are "quasi-orthogonal" and that an orthogonal set $g_n(x)$ can be constructed from a linear combination of the $f_n(x)$. These orthogonal functions, $g_n(x)$, can then be used for the expansion of the boundary function to determine the coefficients B_n. Proof of this theorem, called the "theorem of quasi-orthogonality," is given by Tittle [222]. Briefly, the procedure is as follows.

The set $g_n(x)$ is given by

$$\begin{aligned} g_n(x) &= \sin \gamma_n x \qquad 0 \le x \le a \\ g_n(x) &= C[F_n \sin \delta_n x + G_n \cos \delta_n x] \qquad a \le x \le L \end{aligned} \tag{IV-18}$$

In the above, the term C, is the "orthogonality factor." Application of the theorem results in

$$B_n = \frac{\int_0^a (1+A_1 x)\sin\gamma_n x\,dx + C^2\int_a^L A_2(x-L)[F_n\sin\delta_n x + G_n\cos\delta_n x]\,dx}{\int_0^a [\sin\gamma_n x]^2 dx + C^2\int_a^L [F_n\sin\delta_n x + G_n\cos\delta_n x]^2 dx} \qquad \text{(IV-19)}$$

The orthogonality factor, C, is determined from the orthogonality condition, which is,

$$\int_0^L w(x)\, g_m(x)\, g_n(x)\,dx = 0 \qquad m \neq n \qquad \text{(IV-20)}$$

The weighting function, W (x), appropriate to the coordinate system for this case is unity. Substitution of equation (IV-18) into equation (IV-20) gives

$$0 = \int_0^a \sin\gamma_m x \sin\gamma_n x\,dx + C^2\int_a^L [F_m\sin\delta_m x + G_m\cos\delta_m x]\cdot [F_n\sin\delta_n x + G_n\cos\delta_n x]\,dx \qquad \text{(IV-21)}$$

From this it can be seen that, alternatively, C^2 could be thought of as a discontinuous weighting function for the original functions $f_n(x)$. In a later and more general unpublished paper [253] Tittle has given this interpretation. Regardless of interpretation equation (IV-21) will determine the value of C. However, Tittle has shown that the value of C is independent of boundary conditions and is the same for this class of problems, namely

$$C = \left(\frac{\alpha_1 k_2}{\alpha_2 k_1}\right)^{\frac{1}{2}} \qquad \text{(IV-22)}$$

The writer has verified equation (IV-22) by carrying out the integration of (IV-21). With the value of C given by equation (IV-22) the integration of equation (IV-19) can be evaluated.

The resulting form for the B_n is

$$B_n = -\frac{2}{D_n}$$

where D_n is given by

$$D_n = \gamma_n a - \frac{\sin 2\gamma_n a}{2} + \frac{k_1}{k_2}\sqrt{\frac{\alpha_2}{\alpha_1}}\left(\frac{\cos\gamma_n a}{\cos\delta_n b}\right)^2\left(\delta_n b - \frac{\sin 2\delta_n b}{2}\right) \qquad \text{(IV-23)}$$

Assembling the results gives the final form of solution for the distributions, which are,

Region I

$$T_1(X,\theta) = 1 - A_1 X - \sum_{n=1}^{\infty} \frac{2\sin\gamma_n X\, e^{-\gamma_n^2 \alpha_1 \theta}}{D_n} \qquad \text{(IV-24)}$$

Region II

$$T_2(X,\theta) = A_2(L-X) - \sum_{n=1}^{\infty} \frac{2[F_n \sin\delta_n X + G_n \cos\delta_n X]\, e^{-\delta_n^2 \alpha_2 \theta}}{D_n} \qquad \text{(IV-25)}$$

Wherein all quantities have been previously defined except the following

$$T_1(X,\theta) = \frac{t_1(X,\theta) - t_i}{t_o - t_i}, \quad T_2(X,\theta) = \frac{t_2(X,\theta) - t_i}{t_o - t_i} \qquad \text{(IV-26)}$$

Equations (IV-24) and (IV-25) have been used to generate theoretical data for some representative systems.

This data will be presented later in this section.

Case B.

Initially a steady-state temperature distribution is established through the system. At time $\theta = 0$ the contact conductance is suddenly changed to a new constant value, h_c', while the outer boundary temperatures are kept constant at t_o and t_i. Symbolically these boundary conditions are,

$$T_1(x,\theta) = 1 - A_1' x \qquad 0 \le x \le a \qquad \text{(IV-27)}$$

$$T_2(x,\theta) = A_2'(L-x) \qquad a \le x \le L \qquad \text{(IV-28)}$$

$$T_1(0,\theta) = 1 \qquad \theta > 0 \qquad \text{(IV-29)}$$

$$T_2(L,\theta) = 0 \qquad \theta > 0 \qquad \text{(IV-30)}$$

$$k_1\left(\frac{\partial T_1}{\partial x}\right) = k_2\left(\frac{\partial T_2}{\partial x}\right) \qquad x=a,\ \theta>0 \qquad \text{(IV-31)}$$

$$k_1\left(\frac{\partial T_1}{\partial x}\right) = h_c'(T_2 - T_1) \qquad x=a,\ \theta>0 \qquad \text{(IV-32)}$$

Boundary condition (IV-8) is also applicable. The method of solution is identical to that of the previous case and is not repeated here. Except for the numerator of the B_n coefficients, the solution form is identical. These solutions are,

Region I

$$T_1(X,\theta) = 1 - A_1' X + \sum_{n=1}^{\infty} \frac{2 k_1 A_1' \left(\frac{1}{h_c'} - \frac{1}{h_c}\right) \cos\gamma_n a \sin\gamma_n x \, e^{-\gamma_n^2 X_1 \theta}}{D_n} \quad \text{(IV-33)}$$

Region II

$$T_2(X,\theta) = A_2'(L - X) + \sum_{n=1}^{\infty} \frac{2 k_1 A_1' \left(\frac{1}{h_c'} - \frac{1}{h_c}\right) \cos\gamma_n a \left[F_n \sin\delta_n x + G_n \cos\delta_n x\right] e^{-\delta_n^2 X_2 \theta}}{D_n} \quad \text{(IV-34)}$$

Wherein F_n and G_n are the same as in equations (IV-15) and (IV-13). The eigenvalue equations are the same as equations (IV-16) and (IV-14) except that in (IV-16) h_c is replaced with h_c'. Similarly, the slopes A_1' and A_2' are given by equations (IV-11) and (IV-12) after replacing h_c with h_c'.

Case C.

In this problem, as in case A, the initial temperature, t_i, is uniform throughout the system. However in this case there are also heat transfer resistances at the outer boundaries characterized by the conductance coefficients h_1 and h_2. The interface contact conductance coefficient, h_c, is still present, thus giving gradient type boundary conditions at all three physical boundaries. It should be noted that even though these solutions were developed for the purpose of comparison with experimental results

for contact conductances at all three boundaries, they are equally applicable to the situation of convective fluid heat transfer at the outer boundaries with contact resistance in the interface. The forms of the boundary condition equations, for the two phenomena are identical, and the only difference involved is the name given to h_1 and h_2.

At time $\theta = 0$, the $x = 0$ boundary is exposed to a medium at temperature t_o through the conductance coefficient h_1, while the $x = L$ boundary is kept in contact with a medium at temperature t_i through the conductance coefficient h_2. The contact conductance coefficient is kept constant at h_c. In symbolic form these conditions are,

$$T_1(x,0) = 0 \qquad 0 \le x \le a \qquad \text{(IV-35)}$$

$$T_2(x,0) = 0 \qquad a \le x \le L \qquad \text{(IV-36)}$$

$$k_1\left(\frac{\partial T_1}{\partial x}\right) = h_1[T_1 - I] \qquad x=0\,,\ \theta>0 \qquad \text{(IV-37)}$$

$$k_2\left(\frac{\partial T_2}{\partial x}\right) = h_2[T_2 - 0] \qquad x=L\,,\ \theta>0 \qquad \text{(IV-38)}$$

$$k_1\left(\frac{\partial T_1}{\partial x}\right) = k_2\left(\frac{\partial T_2}{\partial x}\right) \qquad x=a\,,\ \theta>0 \qquad \text{(IV-39)}$$

$$k_1\left(\frac{\partial T_1}{\partial x}\right) = h_c[T_2 - T_1] \qquad x=a\,,\ \theta>0 \qquad \text{(IV-40)}$$

Equation (IV-8) is also applicable here and it is ob-

vious that the same relation between the eigenvalues, i.e., equation (IV-14), again occurs.

As in case A the solutions may be written as a sum of steady-state and transient portions. The steady-state solutions are well known and similar to those of case A. As before, the transient solutions resulting from the separation of variables in equation (IV-1) are written in a form which reduces the work required in obtaining the series coefficients.

Region (I)

$$T_1 = K_1(x) + \sum_n B_n \left[C_n \cos\gamma_n x + \sin\gamma_n x \right] e^{-\gamma_n^2 \alpha_1 \theta} \qquad \text{(IV-41)}$$

Region (II)

$$T_2 = K_2(x) + \sum_n B_n \left[F_n \sin\delta_n x + G_n \cos\delta_n x \right] e^{-\delta_n^2 \alpha_2 \theta}$$

Here the steady state solutions are given by,

$$K_1(x) = 1 - S\left(\frac{1}{h_1} + \frac{x}{k_1}\right)$$

$$K_2(x) = S\left(\frac{L-x}{k_2} + \frac{1}{h_2}\right) \qquad \text{(IV-42)}$$

wherein

$$S = \frac{1}{\frac{1}{h_1} + \frac{a}{k_a} + \frac{1}{h_c} + \frac{b}{k_2} + \frac{1}{h_2}} \qquad \text{(IV-43)}$$

Application of boundary condition (IV-37) gives

$$C_n = \frac{k_1 \gamma_n}{h_1} \qquad \text{(IV-44)}$$

It is noted that as h_1 becomes large, C_n approaches zero

and thus agrees in the limit of an indefinitely large h_1 with case A.

Next equation (IV-38) is applied and results in

$$G_n = F_n\left[\frac{N_n + \tan \delta_n L}{N_n \tan \delta_n L - 1}\right] \qquad \text{(IV-45)}$$

where

$$N_n = \frac{k_2 \delta_n}{h_2} \qquad \text{(IV-46)}$$

As above, it can be seen that as h_2 becomes very large, N_n approaches zero and the relation between G_n and F_n reduces to that of case A, as shown in equation (IV-13).

Application of the first interface boundary condition, equation (IV-40), together with equations (IV-45) and (IV-14) gives

$$F_n = -\frac{k_1}{k_2}\sqrt{\frac{\alpha_2}{\alpha_1}}\,\frac{[C_n \sin \gamma_n a - \cos \gamma_n a][N_n \sin \delta_n L - \cos \delta_n L]}{N_n \sin \delta_n b - \cos \delta_n b} \qquad \text{(IV-47)}$$

Examination of equation (IV-47) shows that it also agrees with the limiting case.

The eigenvalue equation results from the application of the second interface boundary condition. However, if the resulting equation is written out so that it involves only γ_n and the physical constants it is extremely involved. Since the results could never be used to any appreciable ex-

tent without the aid of a digital computer it is simpler to leave the equation in terms of γ_n and the grouped constants. This result is

$$\gamma_n = \frac{h_c}{k_1}\left[\frac{C_n + \tan\gamma_n a}{C_n \tan\gamma_n a - 1}\right] + \frac{h_c}{k_2}\sqrt{\frac{\alpha_2}{\alpha_1}}\left[\frac{N_n + \tan(\gamma_n b\sqrt{\frac{\alpha_1}{\alpha_2}})}{N_n \tan(\gamma_n b\sqrt{\frac{\alpha_1}{\alpha_2}}) - 1}\right] \qquad \text{(IV-48)}$$

Inspection of equation (IV-48) shows that it, too, reduces in the limit to the corresponding equation for case A. Only the series coefficients B_n are needed to complete the solution. The method of obtaining the B_n is exactly as before and the orthogonality factors, or discontinuous weighing functions, are the same. The resulting equation for B_n is slightly more complicated than before since two of the integrals, see equation (IV-19), contain an additional term due to the fact that the C_n is not zero. Several handwritten pages are required for the integration and simplification, thus only the result is given here.

Region (I)

$$T_1(x,\theta) = 1 - S\left(\frac{1}{h_1} + \frac{x}{k_1}\right) - \sum_{n=1}^{\infty} \frac{2[C_n \cos\gamma_n x + \sin\gamma_n x]}{E_n} \cdot e^{-\gamma_n^2 \alpha_1 \theta} \qquad \text{(IV-49)}$$

Region (II)

$$T_2(x,\theta) = S\left(\frac{L-x}{k_2} + \frac{1}{h_2}\right) - \sum_{n=1}^{\infty} \frac{2[F_n \sin\delta_n x + G_n \cos\delta_n x]}{E_n} e^{-\delta_n^2 \alpha_2 \theta}$$

where E_n is given by

$$E_n = (C_n^2+1)\gamma_n a + (C_n^2-1)\sin\gamma_n a\cos\gamma_n a + 2C_n\sin^2\gamma_n a + \frac{k_1}{k_2}\sqrt{\frac{\alpha_2}{\alpha_1}}\left[\frac{\cos\gamma_n a - C_n\sin\gamma_n a}{\cos\delta_n b - N_n\sin\delta_n b}\right]^2\left[(N_n^2+1)\delta_n b + (N_n^2-1)\sin\delta_n b\cos\delta_n b + 2N_n\sin^2\delta_n b\right] \quad \text{(IV-50)}$$

This completes the solution for case C.

Case D.

In this problem the initial temperature distribution is linear, i.e., steady state heat flow. At time $\theta = 0$ the conductance coefficients are changed from h_1, h_c and h_2 to new constant values h_1', h_c' and h_2', while the outer boundary medium temperatures, t_o and t_i, are kept constant.

The solution of this problem is identical to that of case C except for the numerator of the series coefficients B_n. For this reason the steps of the solution will not be repeated here. The resulting temperature distributions are,

Region I

$$T_1(x,\theta) = 1 - S'\left(\frac{1}{h_1'} + \frac{x}{k_1}\right) - \sum_{n=1}^{\infty}\frac{H_n[C_n\cos\gamma_n x + \sin\gamma_n x]}{E_n}e^{-\gamma_n^2\alpha_1\theta} \quad \text{(IV-51)}$$

Region II

$$T_2(x,\theta) = S'\left(\frac{L-x}{k_2} + \frac{1}{h_2'}\right) - \sum_{n=1}^{\infty}\frac{H_n[F_n\sin\delta_n x + G_n\cos\delta_n x]}{E_n}e^{-\delta_n^2\alpha_2\theta}$$

The eigenvalues γ_n are determined from equation (IV-48) by replacing h_1, h_c, h_2 with h_1', h_c', h_2'. For the other terms equations (IV-44) through (IV-47) and (IV-50) may be used with the appropriate values of γ_n. The equation for S' is just like equation (IV-43) except that h_1', h_c', h_2' should be substituted for h_1, h_c, h_2. The numerator term H_n is given by

$$H_n = 2S'\left\{\left[\cos\gamma_n a - C_n \sin\gamma_n a\right]\left[\left(\frac{1}{h_c}-\frac{1}{h_c'}\right)+\frac{\left(\frac{1}{h_2}-\frac{1}{h_2'}\right)}{N_n \sin\delta_n b - \cos\delta_n b}\right]-\left(\frac{1}{h_1}-\frac{1}{h_1'}\right)\right\} \quad \text{(IV-52)}$$

It should be noted here that a solution for the problem of case A has been previously found by Seide [192]. However, since Tittle's generalized orthogonality work [222] was not available, the solution of [192] was obtained by taking separate origins for the space coordinates of the two slabs and by judiciously choosing certain muliplying factors. The validity of Seide's solution is not doubted, but his procedure is not as straightforward as that used here, and the resulting solution is slightly more complicated. Thus only the form of the present solution for case A is original since a prior solution of the problem exists. The solutions of cases B through D, for the more complex boundary conditions, are believed to be original contributions since no solutions of these problems were found in the lit-

erature. Actually only the solutions of cases C and D need be considered, since, as previously mentioned, cases A and B are special cases of C and D, respectively.

Numerical Solutions

To provide a check against possible errors in the analytical solutions, a finite difference numerical solution technique was used to generate solutions for the same problems. The nodal equations necessary for the numerical solution may be derived either by applying finite differences to Fourier's equation and the boundary conditions, or by writing a simple heat balance for each node used in the solution. Both of these methods are well known and will not be repeated here. A sketch representative of the one dimensional system for heat transfer purposes is shown in Figure 8. The following are the nodal equations which were used for the digital computer solutions.

Region I

For the x = 0 boundary node:

$$T_{1(1)}^{\theta+\Delta\theta} = \frac{2M_1}{N_o} T_o + 2M_1 T_{1(2)}^{\theta} + \left[1 - \frac{2M_1}{N_o} - 2M_1\right] T_{1(1)}^{\theta} \qquad \text{(IV-53)}$$

For the interior nodes:

$$T_{1(n)}^{\theta+\Delta\theta} = M_1\left[T_{1(n-1)}^{\theta} + T_{1(n+1)}^{\theta}\right] + \left[1 - 2M_1\right] T_{1(n)}^{\theta} \qquad (1 < n < n_a) \qquad \text{(IV-54)}$$

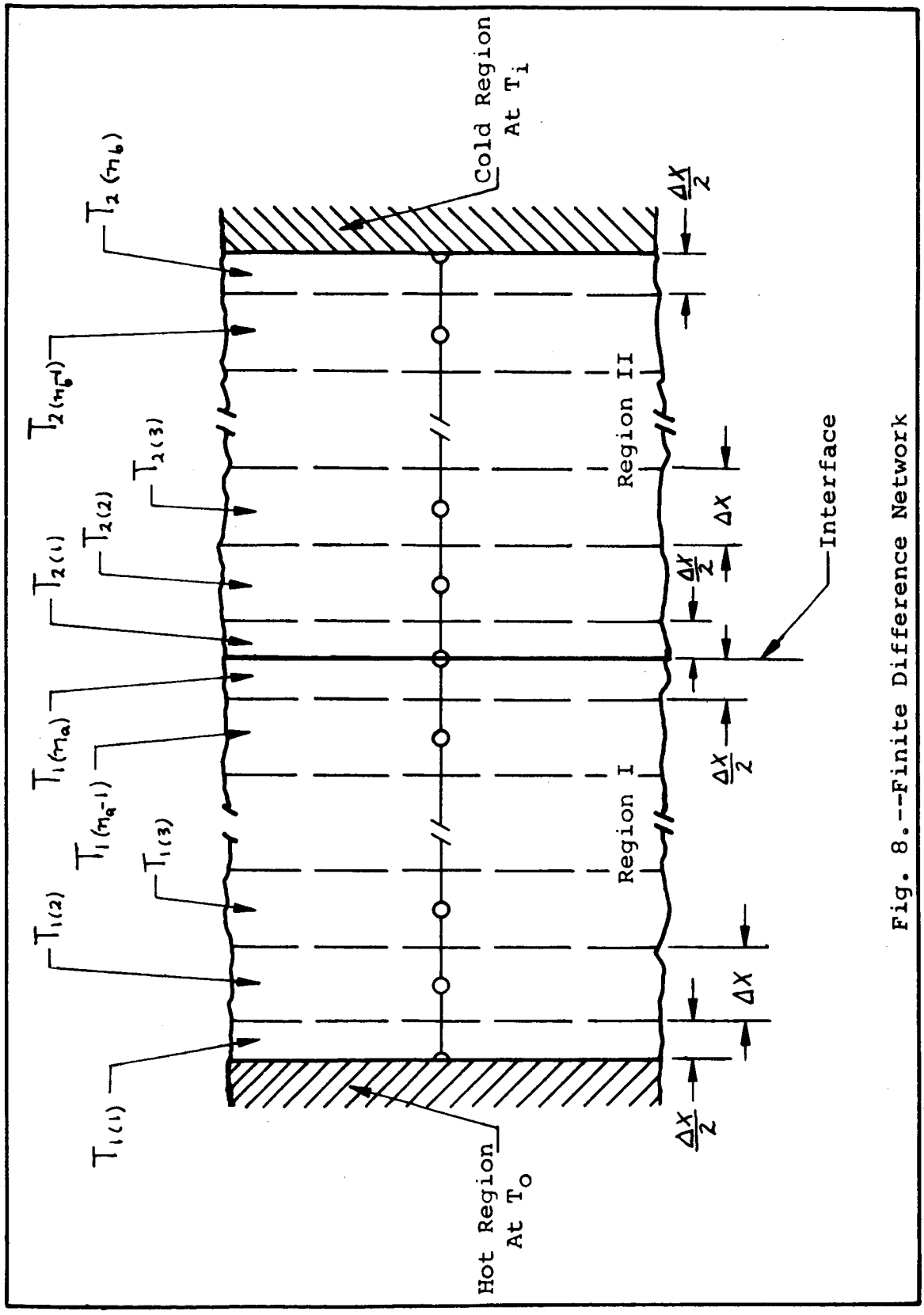

Fig. 8.--Finite Difference Network

For the contact boundary node:

$$T_{1(n_a)}^{\theta+\Delta\theta} = 2M_1 T_{1(n_a-1)}^{\theta} + 2\frac{M_1}{N_1} T_{2(1)}^{\theta} + \left[1-2M_1-2\frac{M_1}{N_1}\right] T_{1(n_a)}^{\theta} \qquad \text{(IV-55)}$$

Region II

For the contact boundary node:

$$T_{2(1)}^{\theta+\Delta\theta} = 2M_2 T_{2(2)}^{\theta} + 2\frac{M_2}{N_2} T_{1(n_a)}^{\theta} + \left[1-2M_2-2\frac{M_2}{N_2}\right] T_{2(1)}^{\theta} \qquad \text{(IV-56)}$$

For the interior nodes:

$$T_{2(n)}^{\theta+\Delta\theta} = M_2\left[T_{2(n-1)}^{\theta} + T_{2(n+1)}^{\theta}\right] + \left[1-2M_2\right] T_{2(n)}^{\theta} \qquad (1 < n < n_b) \qquad \text{(IV-57)}$$

For the x = L boundary node:

$$T_{2(n_b)}^{\theta+\Delta\theta} = 2\frac{M_2}{N_L} T_i + 2M_2 T_{2(n_b-1)}^{\theta} + \left[1-2\frac{M_2}{N_2}-2M_2\right] T_{2(n_b)}^{\theta} \qquad \text{(IV-58)}$$

where

$$M_1 = \frac{\alpha_1 \Delta\theta}{(\Delta X)^2} \quad , \quad M_2 = \frac{\alpha_2 \Delta\theta}{(\Delta X)^2}$$

$$N_1 = \frac{k_1}{h_c \Delta X} \quad , \quad N_2 = \frac{k_2}{h_c \Delta X} \qquad \text{(IV-59)}$$

$$N_o = \frac{k_1}{h_1 \Delta X} \quad , \quad N_L = \frac{k_2}{h_2 \Delta X}$$

For those cases where there is no contact resistance at the outer boundaries, equations (IV-53) and (IV-54) are not required. The equations for the outer boundary nodes would then be the same as for the interior nodes in the respective regions.

In order to insure stable solutions it is necessary

that the coefficients of the last temperature in each of the equations (IV-53) through (IV-58) be positive. It was found that length increments of 0.1 inch and time increments of 0.01 second achieved this stability in every case studied.

Comparison of The Numerical and Analytical Solution

The above nodal equations and the preceding analytical solutions were programmed for use on a digital computer. For a number of cases, which represented the extremes in terms of thermal properties and hot and cold region lengths, both solutions were used for identical problems. The computer results were obtained in the normalized form indicated in the analytical solutions, i.e.,

$$\frac{t(x,\theta) - t_i}{t_o - t_i}$$

In this form the "temperature" (actually it is a reduced temperature ratio) at any location, x, and any time, θ, is a number less than 1 and greater than zero. For the runs of the identical problems the results of both solutions were printed out for all the nodal locations (i.e., every 0.1 in.) and for times from 1.0 second to the steady state time. For reasons explained below the "steady state time" was taken to be the time at which the temperature drop across the slowest reacting portion of the system reached 99.0% of its steady

state value. These results were printed out by the computer to five decimal places. The results of the analytical and numerical solutions were always identical to the number of significant figures stated. Thus any difference between the results of the two solutions was less than one part in 10^5. Since this accuracy was quite sufficient, no further checks were made to determine more exactly what the difference may have been. It should be emphasized that the solutions were checked in this way for the complete range of variables used in study.

After the above-mentioned accuracy checks were made only the analytical solutions were used to generate the data for the study. The reason for this is that the analytical method requires less computer time. The nature of the present study was such that the desired output from the solutions was the "time to approach steady state" as defined above. With the numerical solution of this time dependent problem it is necessary to iterate the solution from time zero up to the steady state time for all the nodal points. In the present study, in which the desired times ranged from approximately 15 to several hundred seconds, such a process requires many iterations. On the other hand, the analytical solutions are "point" solutions. This means that it is pos-

sible to calculate the solution at any location and at any time. Advantage is taken of this fact on the computer by: (1) calculating the temperatures only at the desired locations, i.e., at the boundaries and (2) by taking large time steps at first and then smaller steps to determine the steady state time. In the present study the savings in computer time was considerable.

It should be noted, however, that the numerical solutions served the very useful purpose of providing a check on the analytical solutions. Also, if it were desired to vary the thermal properties or boundary conditions continuously, then the limitations of the analytical approach would necessitate the use of a numerical solution.

Results of Computer Study

The original purpose of the computer study was to furnish information for the design of experiments. These gedanken experiments provided data which aided in the selection of metals to be tested, and which helped in the planning of experiments with regards to test duration. It is for this reason that the 99% criterion was chosen. It should be pointed out here that all the results presented below are for a situation corresponding to analytical solu-

tion cases A and B above. That is, for no contact resistance at the outer boundaries. At the time this work was done it was thought that the boundary conditions of the experimental work could be made to approach this situation. However, it later proved impossible to achieve these conditions experimentally. Thus for the comparisons between theory and experiment which are presented in section VI the analytical solutions of cases C and D were used.

During the course of the early computer study, made for experiment planning, interest grew in two ideas brought out by the study. The first of these was the possibility of making a general correlation on the time to reach steady state. Such a correlation would be of some practical importance. The second was a phenomenon which was found to occur in certain instances and which eventually came to be called the "overshoot phenomenon."

Because of time limitations most of the effort in this study was concentrated on the time to reach steady state correlation. The results of this correlation study are shown in Figures 9 through 13. All those figures are plots of a dimensionless time

$$\Theta = \theta\left[\frac{\alpha_1}{a^2} + \frac{\alpha_2}{b^2}\right] \qquad \text{(IV-60)}$$

versus a "thermal time-constant ratio"

$$\tau = \frac{b}{a}\sqrt{\frac{\alpha_1}{\alpha_2}} \qquad \text{(IV-61)}$$

for various values of an "inverse Biot number"

$$\beta = \frac{k_1}{h_c a} \qquad \text{(IV-62)}$$

The correlations show, as reflected by the above quantities, the effects of geometry, material and contact conductances.

Figure 9 represents all cases where the materials in both regions are the same. In the data used to plot the curves of Figure 9 the total length (a + b) ranged from 0.5 to 8.0 inches, the length ratio ($^b/_a$) ranged from approximately 0.1 to 10, and the metals ranged from stainless steel to pure aluminum. The latter gives a range of thermal conductivity of 10 to 117 Btu/hr.-ft.-^oF, and a range of thermal diffusivity of 0.15 to 3.33 $ft.^2/hr.$ Contact conductances were in the range 25 to 4000 Btu/hr.-ft.-^oF. For these cases the β parameter is simply the length ratio ($^b/_a$). The overall significance of this figure is that it makes it possible to estimate how long it would take a composite system to reach steady state after being subjected to a sudden temperature change on one side. It should be noted

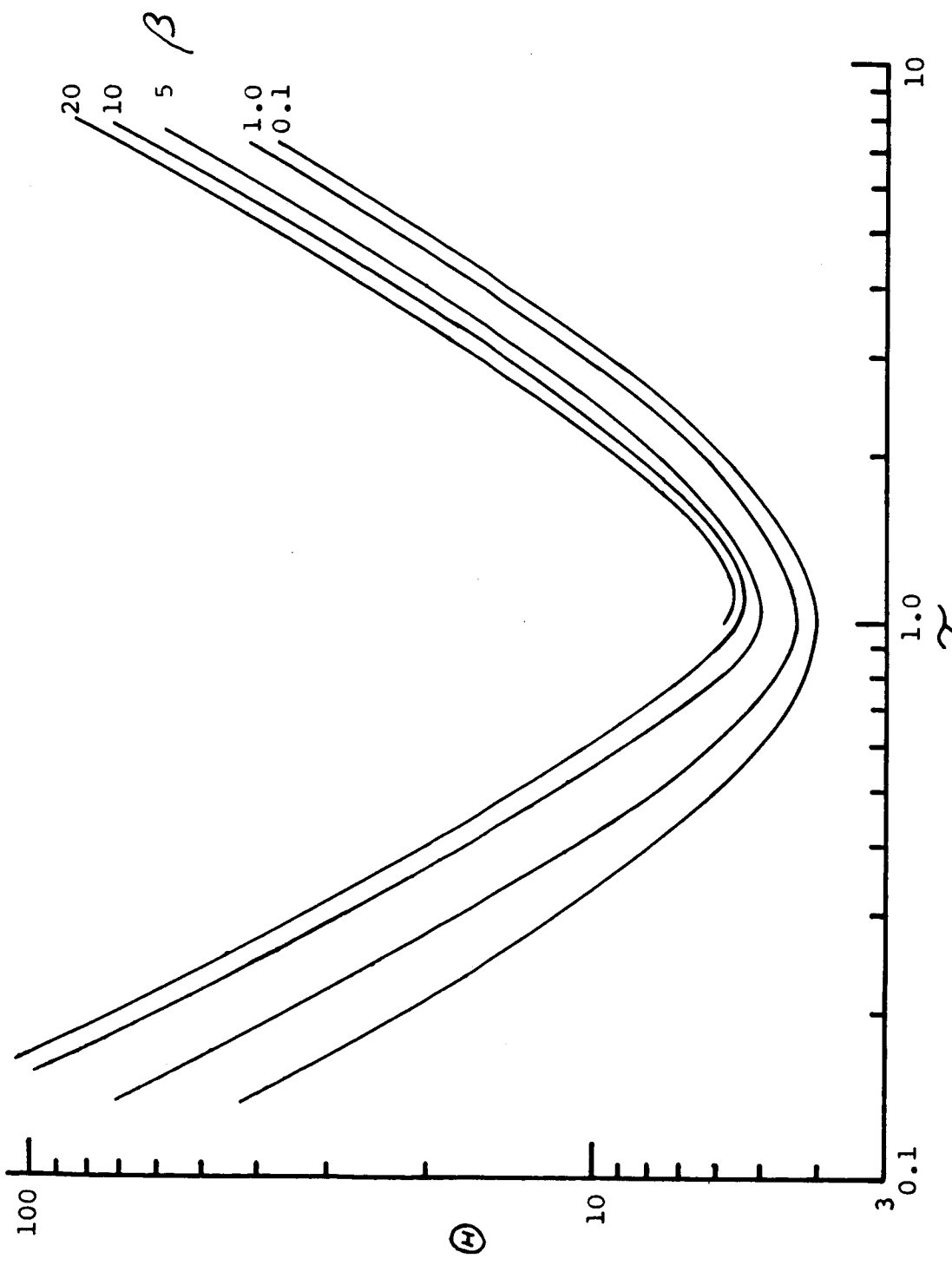

Fig. 9.--Time to Approach Steady State, Same Materials in Both Regions

that this time is independent of the overall temperature difference. With experimental data Figure 9 could also be used to determine contact conductance by measuring the time to reach steady state, for a system of known thickness and materials. These curves also show, through the β -parameter, under what conditions the contact conductance would significantly affect the response of the system.

As an example of the use of the curves, consider a system consisting of one inch of aluminum in contact with two inches of aluminum through a contact conductance of 280 Btu/hr.-ft.^{2}-^{o}F. This gives τ = 0.5 and β = 5. From Figure 9, Θ = 11.6 which gives θ = 69.6 seconds. The same system, with a contact conductance of 2800, would have τ = 0.5 and β = 0.5, which would give θ = 40.2 seconds.

An interesting and somewhat unexpected phenomenon is demonstrated by the curves of Figure 9. Consider a system of the same material with the same contact conductance (280 Btu/hr.-ft.^{2}-^{o}F) and same total length as the above example, but with equal thicknesses, a = b = 1.5 inches. Here τ = 1.0, β = 3.35, and the curves give Θ = 4.8. This results in a steady state time θ = 40.5 seconds. In other words the symmetrical system reaches its steady state sooner. The importance of the symmetry is further demonstrated by looking at

still another system which has the same materials and contact conductance as the above example, but which has equal thicknesses of $a = b = 2$ inches. The steady state time for this system is 69.0 seconds. It is seen that although this system has 25% more material than the 1 inch - 2 inch system its steady state time is approximately the same. It is this symmetry aspect which produces the minimum in the curves of Figure 9. These minima show that if $\tau > 1$ the dimensionless time is controlled by region 2 (the cooler side) and that region 1 controls when $\tau < 1$. While β affects the position of the curves, the minimum is almost independent of β.

For the cases in which the materials in the two regions are not the same it becomes necessary to present the information on two separate plots for each material combination. For example, in Figure 10 an aluminum-tin system (aluminum in region 1 and tin in region 2) is presented, whereas in Figure 11 the materials are reversed. Figures 12 and 13 show the correlations for a stainless steel-tin system. While it would be desirable to present all this information in one or two plots, it should not be surprising in view of the complexity of the system that this may not be possible. It may be possible to accomplish this through

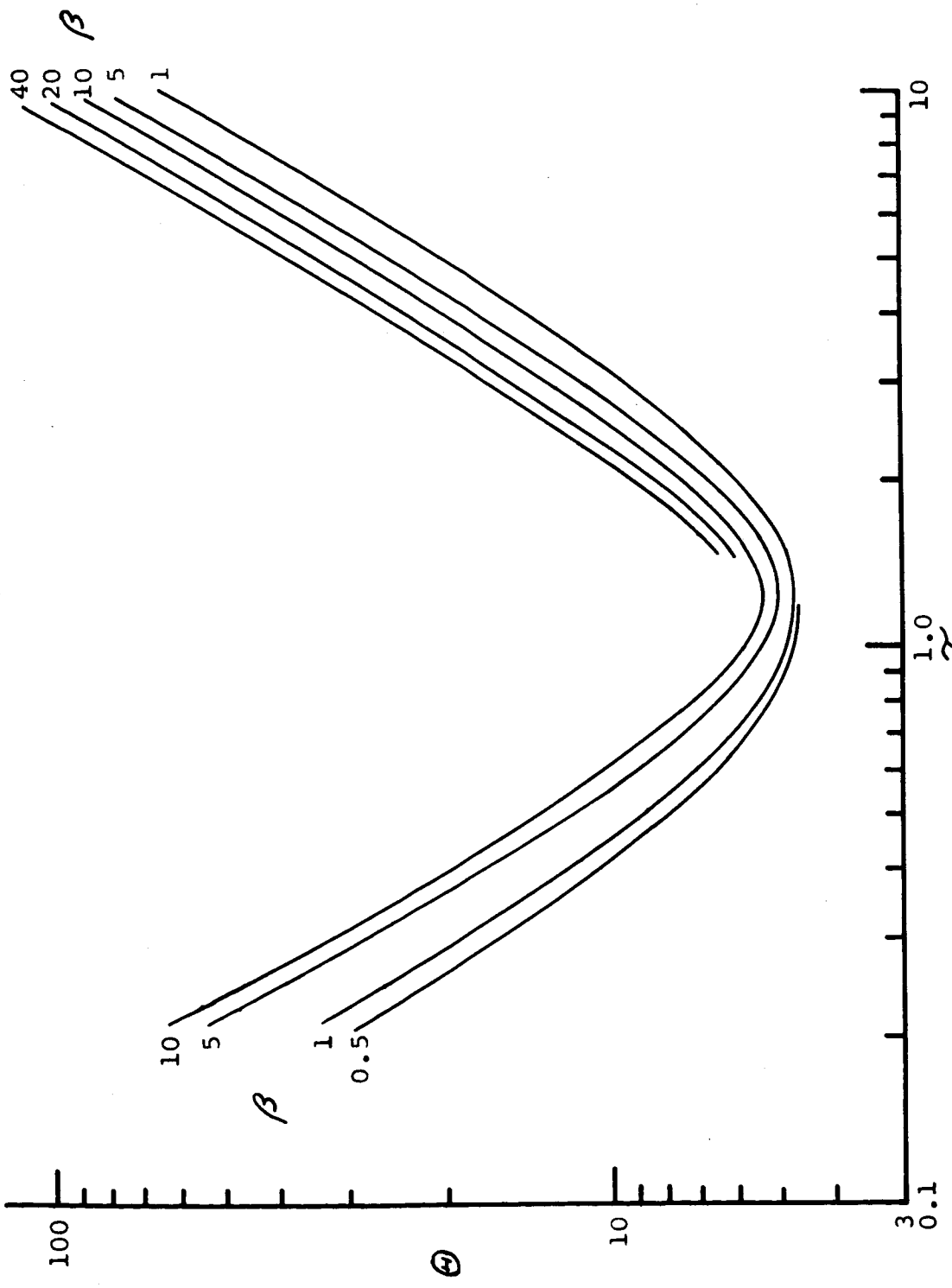

Fig. 10.--Time to Approach Steady State, Aluminum-Tin System

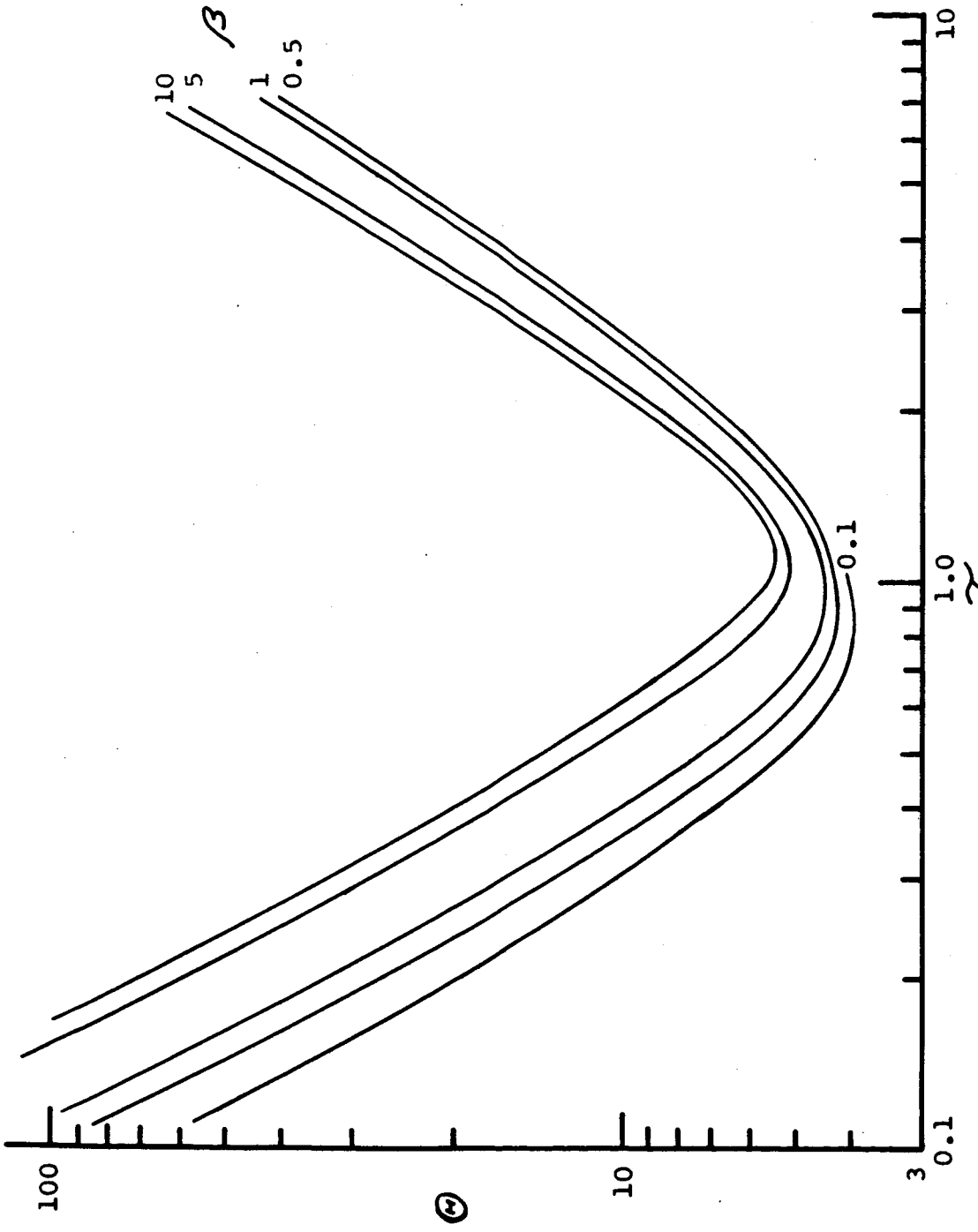

Fig. 11.--Time to Approach Steady State, Tin-Aluminum System

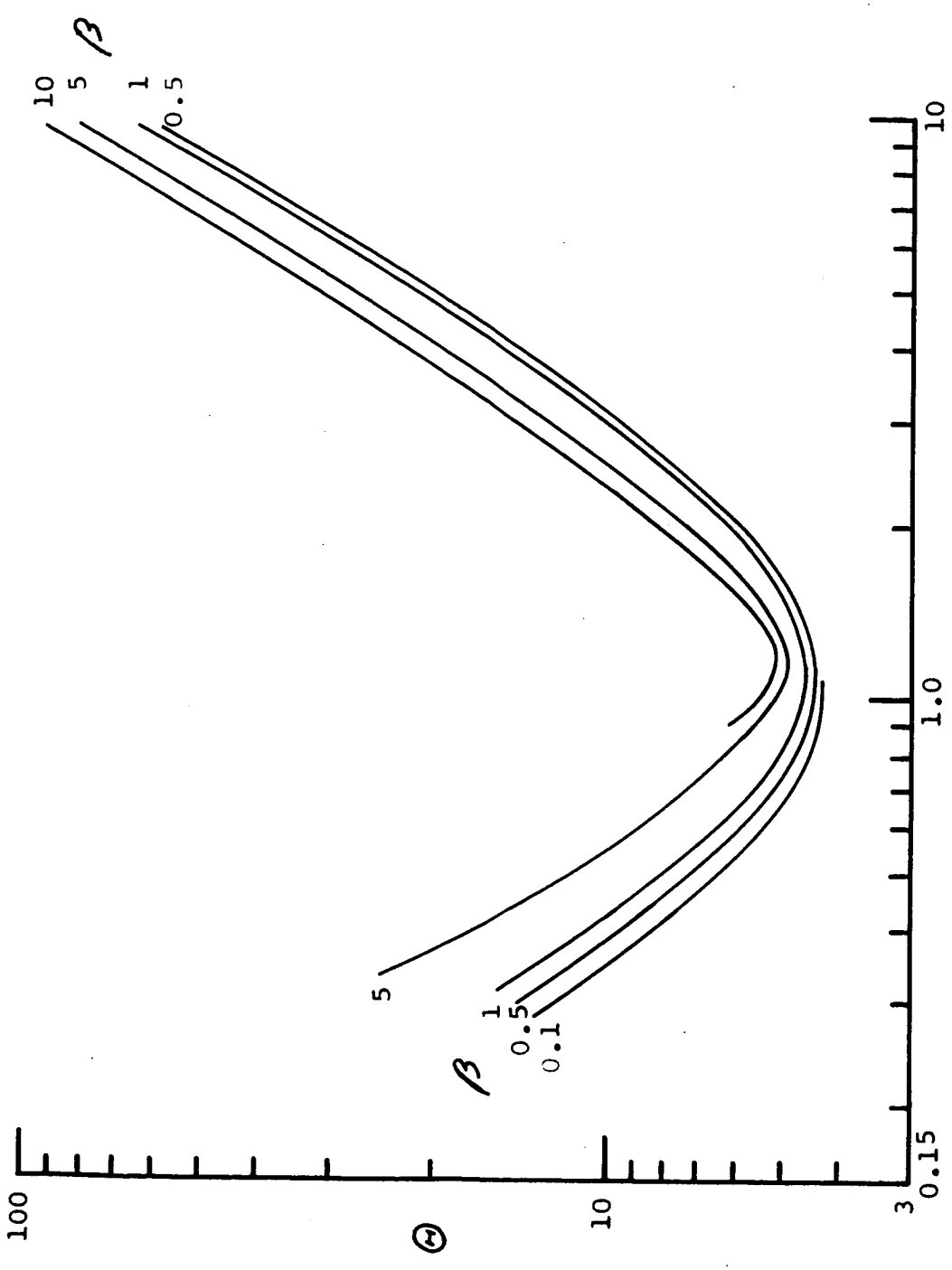

Fig. 12.--Time to Approach Steady State, Tin-Stainless Steel System

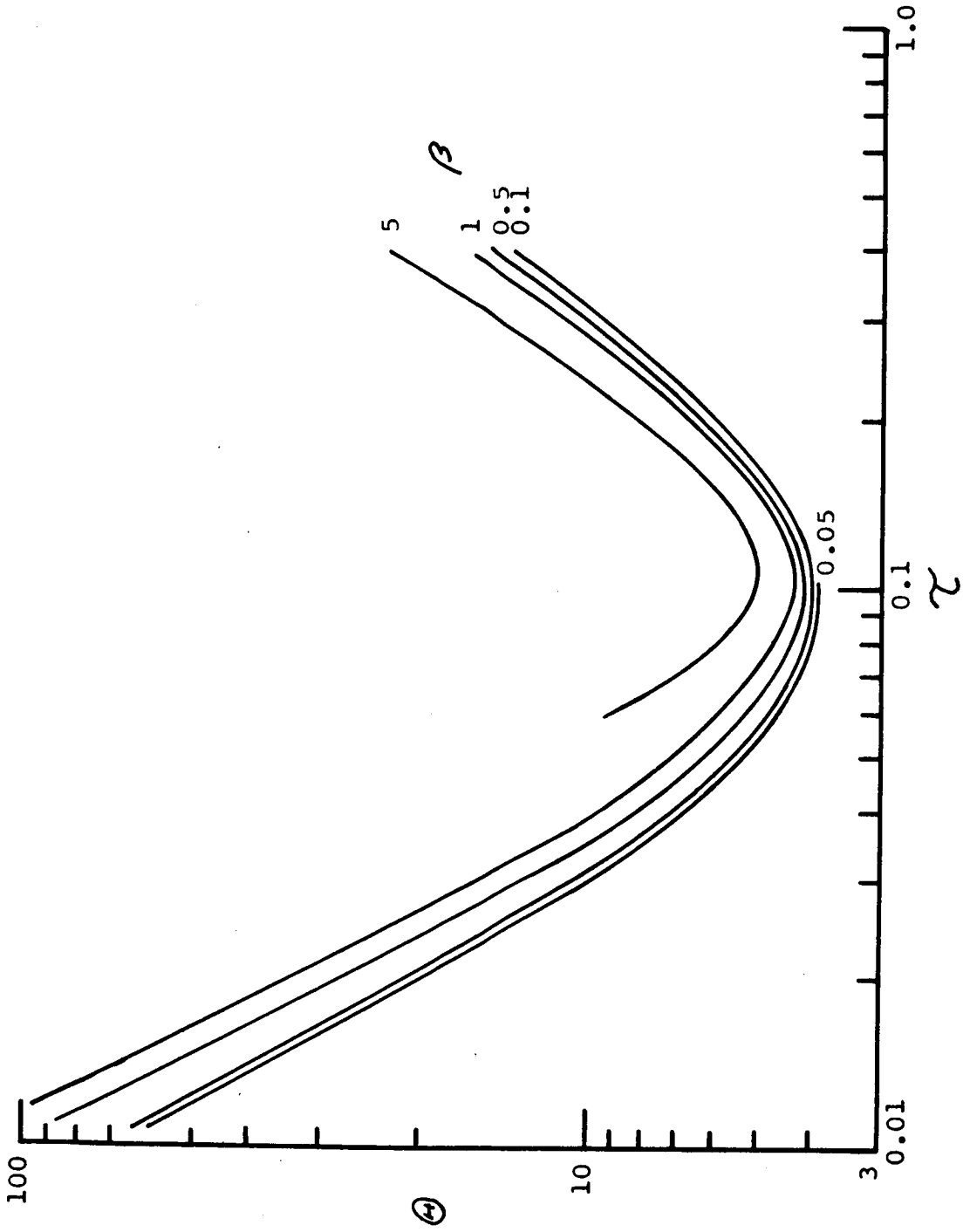

Fig. 13.--Time to Approach Steady State, Stainless Steel-Tin System

finding another parameter and/or combining two or more parameters. A possibility for an additional parameter, as indicated by the analytical solutions, is the ratio of the thermal conductivities. However, time did not permit further effort in this study. From the curves of Figures 10 and 11 it can be seen that the aluminum tin system demonstrates the same behavior and effects as were discussed regarding Figure 9. However, for these dissimilar metals the minima do show more of shift away from $\tau = 1$ as β varies. The curves for the stainless steel-tin system, i.e., Figures 12 and 13 show a large change in the minima locations when the materials are reversed. In Figure 12, where the better conductor is in region 1, the minima show a shift with β, but still occur in the neighborhood of $\tau = 1$. When the materials are reversed the minima locations shift to the vicinity of $\tau = 0.1$.

The overshoot phenomenon, mentioned above, represents the cases in which the temperature drop across the contact exceeds, or "overshoots," its steady state value during the transient portion before the steady state is reached. This phenomenon is illustrated in Figure 14 for a system consisting of aluminum and stainless steel with equal thicknesses of 1 inch for contact conductances of 200 and 1000 Btu/hr.-

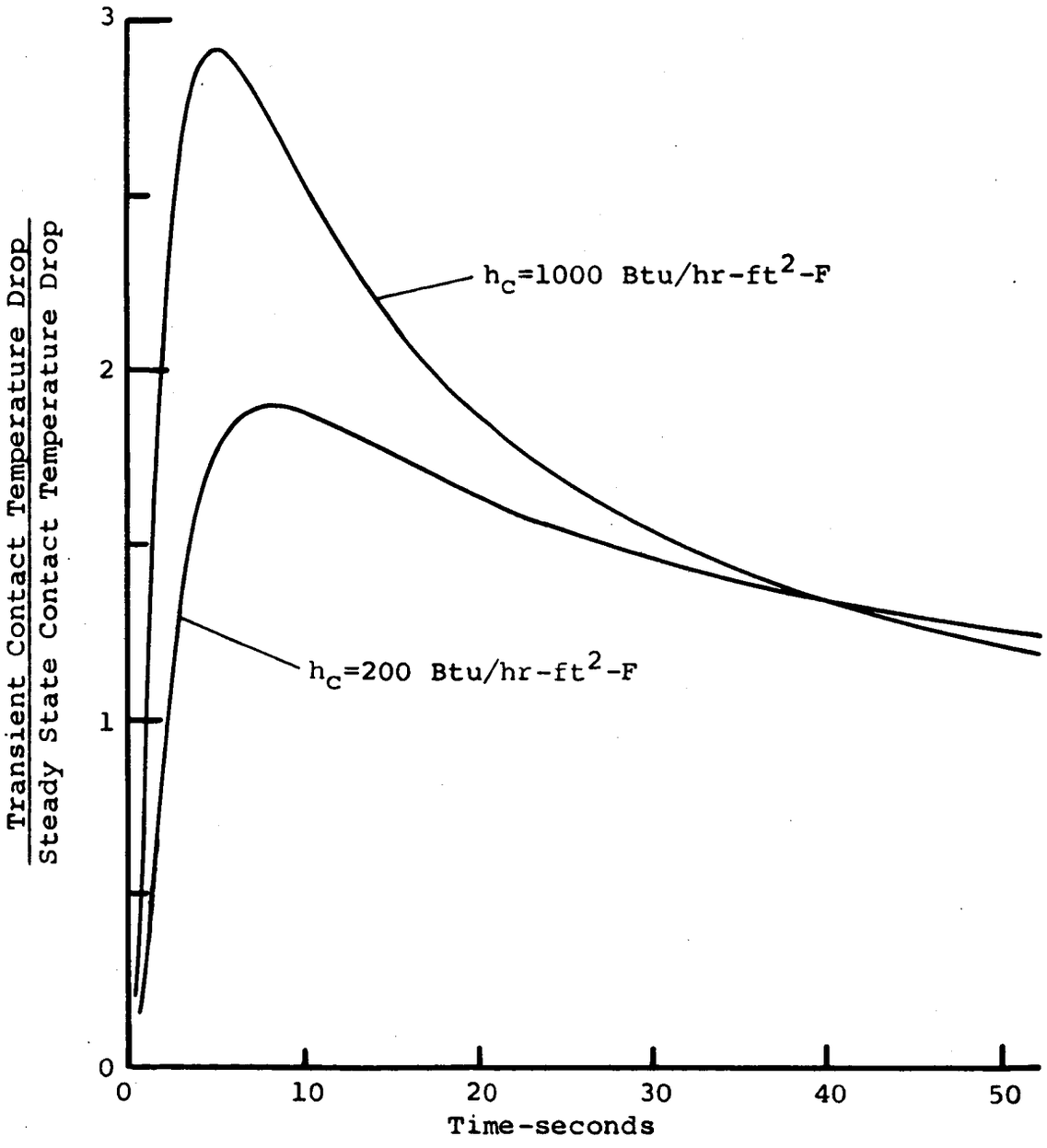

Fig. 14.--Contact Temperature Drop Overshoot

ft^2-^oF. Figure 14 is a plot of the ratio of the contact temperature drop to the steady state temperature drop, as a function of time. Both curves approach a value of unity as the system approaches steady state. For this particular case the overshoot amounts to approximately 290% for the higher contact conductance value and 190% for the lower value. It was found that for the cases studied the overshoot occurs for $\tau > 1$, regardless of whether the same or different materials make up the system. Although no general correlation of this interesting phenomenon was attempted, it was realized that it is clearly a characteristic for the transient behavior and was used in the comparison of the experimental and theoretical work in section VI.

All of the above work is for the situation corresponding to case A, i.e., an initially uniform temperature and a sudden temperature rise at $x = 0$. Figure 15 illustrates the type of transient behavior that occurs for the situation of case B. In Figure 15 the temperature distribution is plotted for several values of time for an equal thickness ($a = b = 1$ inch) aluminum system. The system was initially experiencing a steady state heat flux with a contact conductance of 1000 Btu/hr.-ft^2-^oF. The contact conductance was suddenly lowered to 300 Btu/hr.-ft^2-^oF. Figure 15 shows the

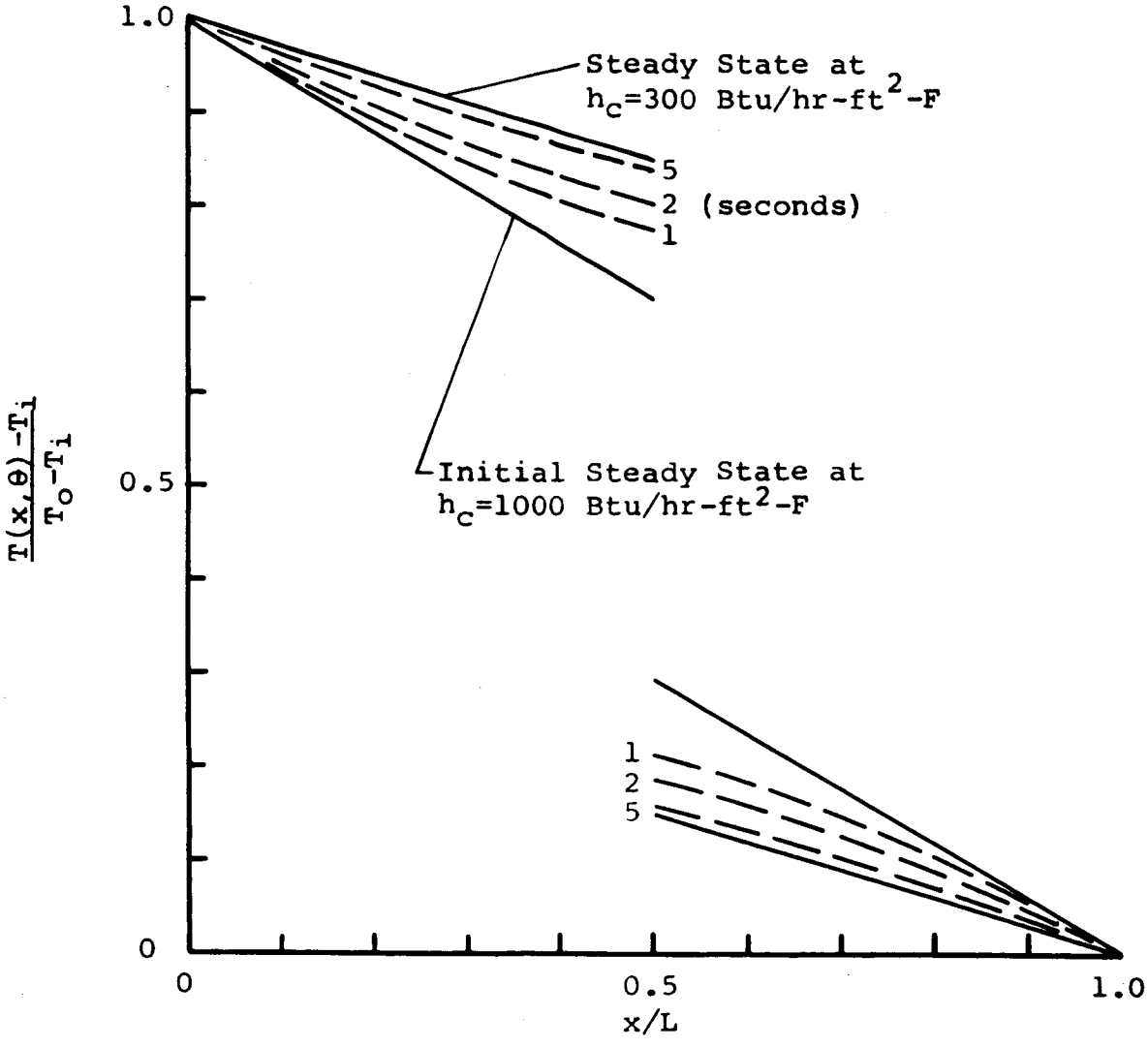

Fig. 15.--Effect of Suddenly Changing Contact Conductance

resulting temperature profiles for 1, 2 and 5 seconds and both steady states. Although a large number of such cases were studied for the purpose of designing laboratory experiments, no general correlation was attempted.

A glance at the solutions for cases C and D above shows that they represent very complex phenomena. They are quite useful solutions and can be applied to any particular combination of materials for which information is desired. Indeed, they are used in section VI for the comparison of the experimental results. However, anything approaching a general correlation will require a great deal of study and considerable computer time.

Summary of Theoretical Study

Analytical solutions for the time dependent temperature distributions for some problems of one-dimensional two-region systems separated by an interface with contact resistance have been derived. These solutions have been checked on a computer by a fine-network numerical technique and found to be accurate. The results of a computer study made with these solutions was presented in the form of dimensionless correlations for the practical quantity, time to approach steady state. An illustration of the contact over-

shoot, which is recognized as a characteristic of transient response, was also given.

V. EXPERIMENTAL PROGRAM

Objective

The objective of the experimental program was to design and operate an apparatus which would provide test data on the transient response of one-dimensional, composite metal systems with contact resistance when subjected to thermal transients. Primarily, this test data was desired for the purpose of checking the applicability of the theoretical solutions of section IV to real composite systems. To this end an attempt was made to create experimental conditions which approached, as closely as possible, the theoretical boundary conditions.

Types of Experiments

Basically the experimental program consisted of measuring the temperature distribution as a function of time in two metallic cylinders in contact while they were undergoing thermal transients. Figure 16 is a sectional drawing of the test section portion of the experimental apparatus. The other primary quantities measured were the axial force pressing the two cylinders together and the temperatures of the

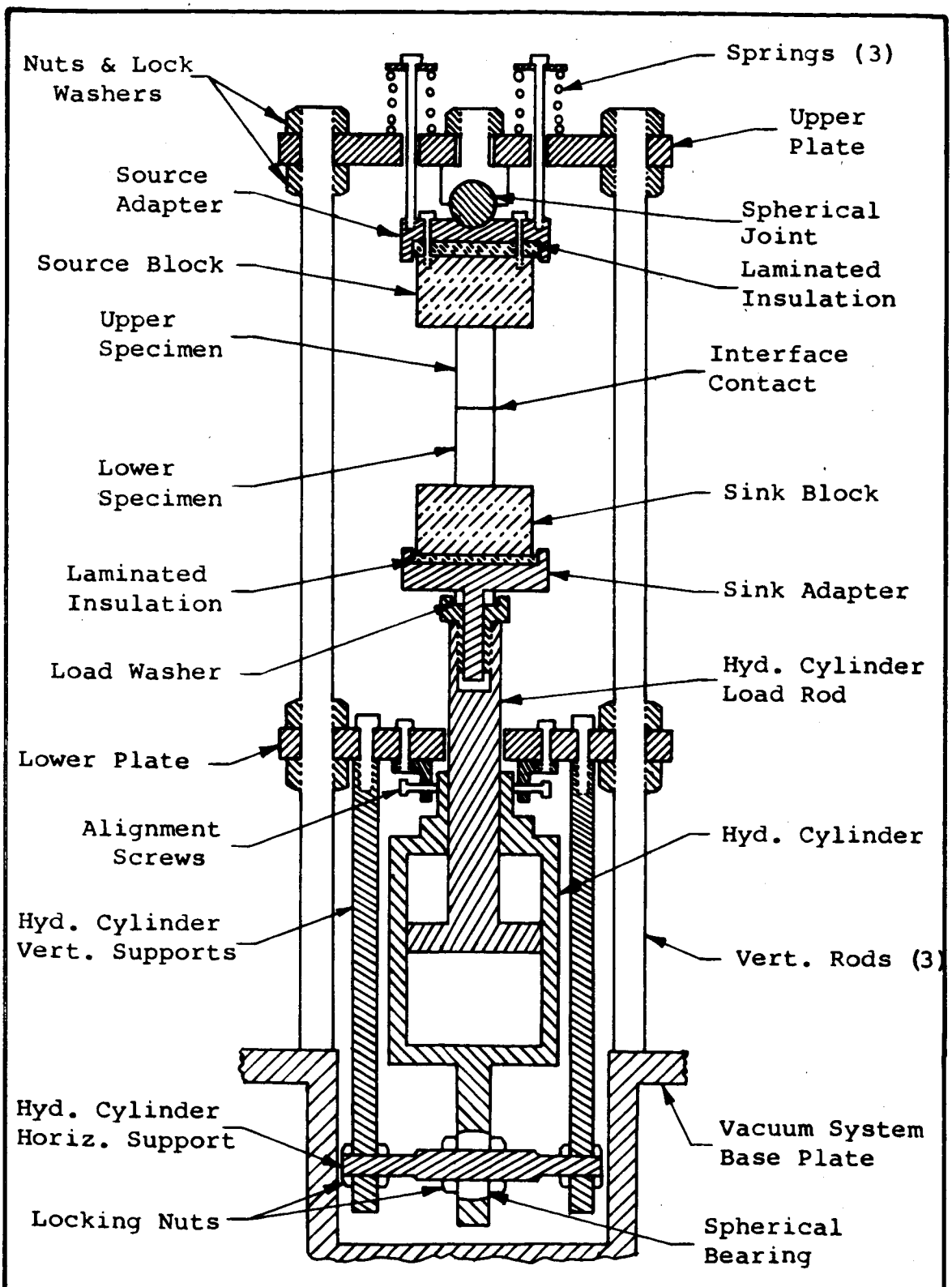

Fig. 16.--Sectional View of Test Section

heat source and sink blocks.

The thermal transients were produced by disturbing the one-dimensional heat transfer through the test specimens. Three test variables were employed in producing these disturbances: 1) the source block temperature; 2) the axial force on the contact surfaces; and 3) the environmental air pressure of the heat transfer system. Three different types of disturbances were studied. These consisted of holding two of the above test variables constant and varying the third rapidly from one fixed value to another, and then holding it constant.

The basic features of each type of test using the above test parameters are described below. The various portions of the apparatus which are referred to in these descriptions are shown in Figure 16. The equipment and exact procedures are described in detail later in this section.

All of the different types of test were designed so that they could be run sequentially. Therefore, each type of test is designated by the word "phase" and a number which denotes its place in the standard test sequence.

Phase 1. This test corresponds to the theoretical case C of section IV. The test began in a vacuum with a uniform temperature, in both specimens, equal to the sink

block temperature. Then the sink block and samples were raised by the loading system so that the upper specimen was held against the hot source block with a constant force. Data were recorded while the system responded and sought a steady state.

Phase 2. After the completion of phase 1, phase 2 was started by applying a step change in the force holding the specimens in contact. This test corresponded to the theoretical case D with a sudden increase in contact conductance.

Phase 3. This test consisted of reversing phase 2. After phase 2 was completed the contact force was suddenly dropped back to its original value. This test corresponds to the theoretical case D with a sudden decrease in contact conductance.

Phase 4. When phase 3 had reached steady state phase 4 was started by suddenly letting air back into the test chamber. The correspondence with the theoretical was the same as phase 2 except that the increase in conductance was achieved by adding air to the contacts at constant contact force.

Phases 5 and 6. These tests were repeats of phases 2 and 3 except that the samples were in air at atmospheric pressure instead of a vacuum.

The above brief descriptions demonstrate the basic philosophy of the experimental program and the correspondences intended to meet the stated objectives. Figure 17 is a photograph which provides an overall view of the basic test apparatus. Details of the test samples, equipment, and procedures are presented below.

Test Specimens

Test samples were constructed of 2024-T351 aluminum, Armco Iron, and type 303-MA stainless steel. All samples were made of one-inch diameter bar stock and had nominal lengths of either one or two inches. Each specimen contained five thermocouples nominally placed at the per-cent-of-length values shown in Figure 18. Actual measured dimensions of all test specimens were recorded and are presented in Appendix A, in which other pertinent sample data are also shown. The procedures used to prepare the test specimens are given next.

The sample material was first placed in a lathe, very lightly turned and then polished to make the cylindrical surface as reflective as possible. This was done to reduce both the absorption of radiation from the source block and the emission of radiation from the samples. The samples

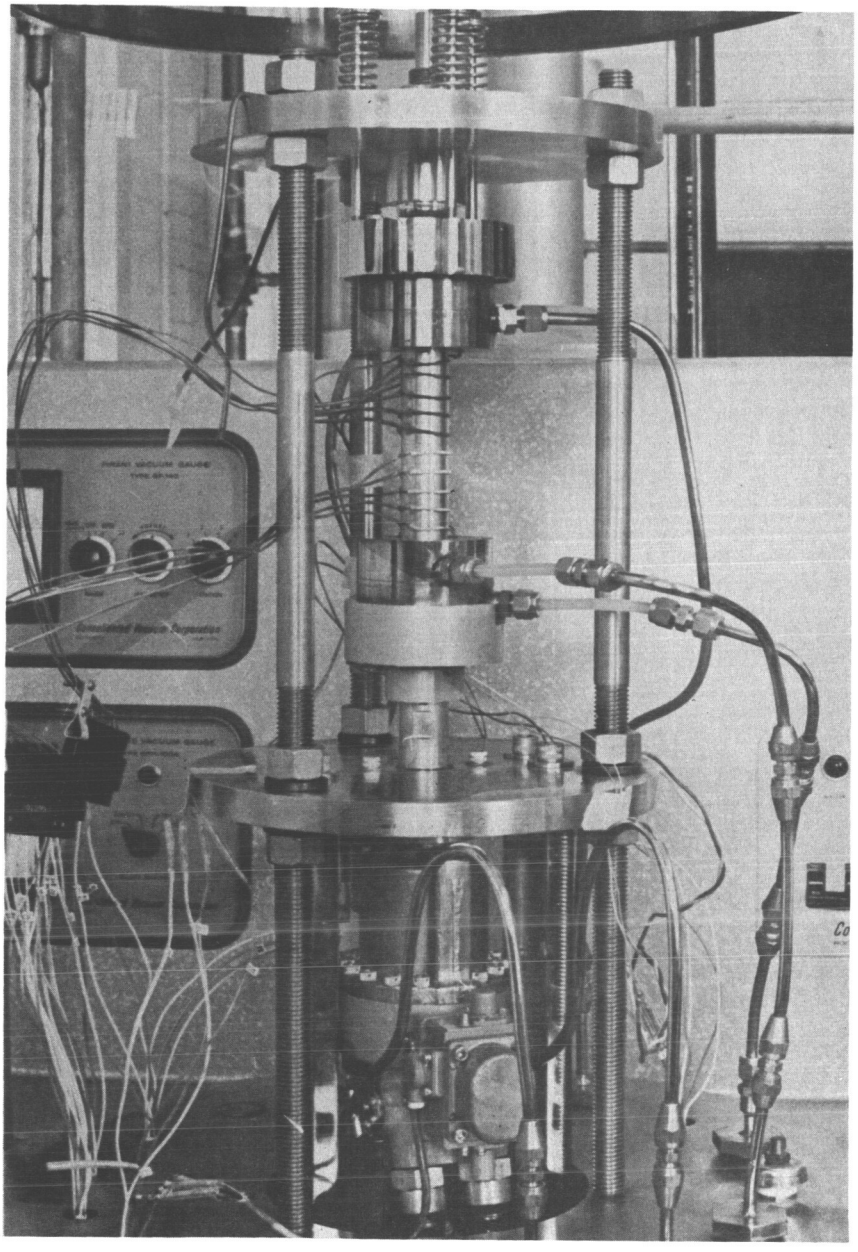

Fig. 17.--Photograph of Test Apparatus

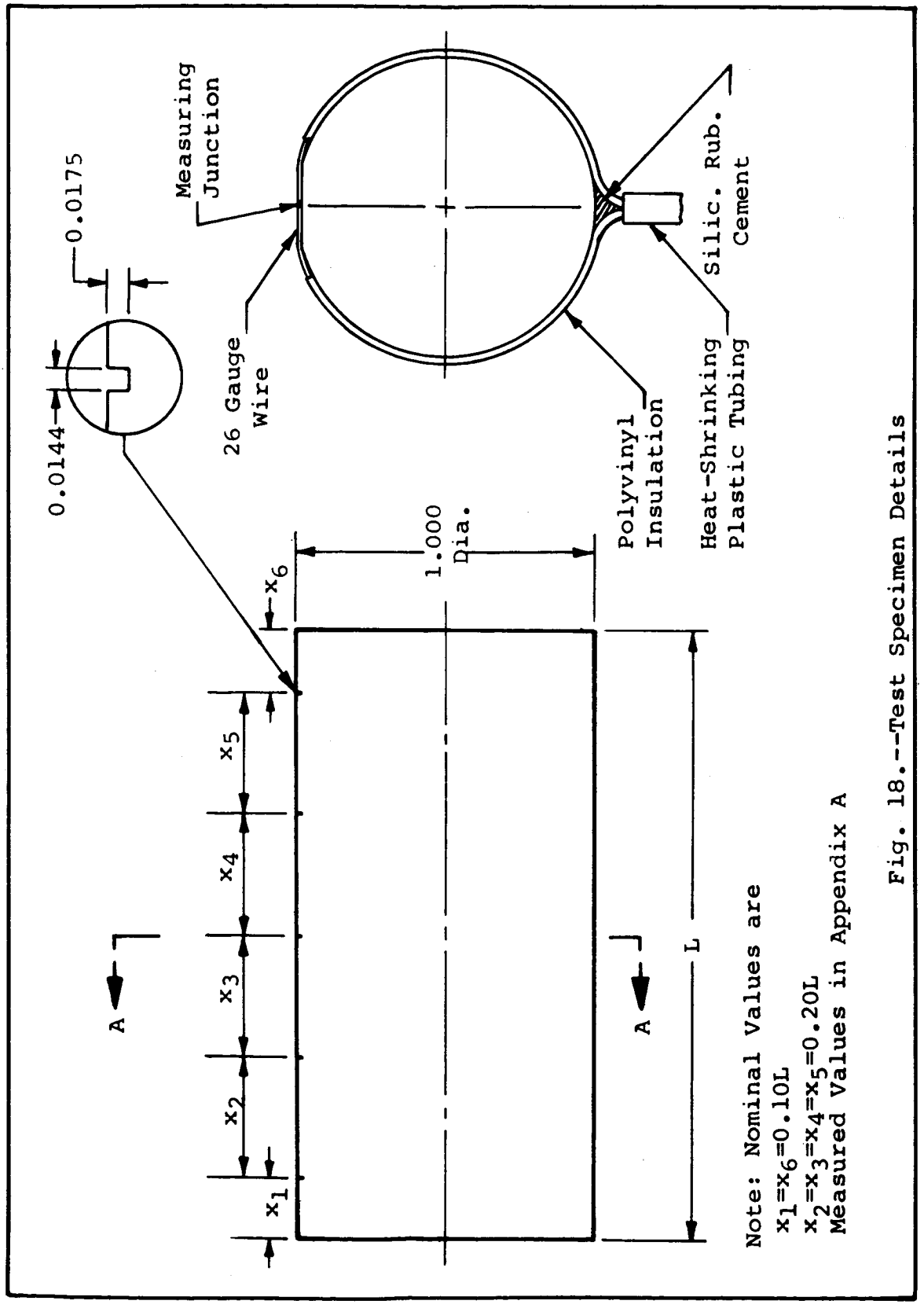

Fig. 18.--Test Specimen Details

were then cut to rough length in a draw-cut saw. These blocks were then put back into the lathe and both ends were turned to a smooth tool finish, leaving the total length about 0.010 inch longer than desired. The samples were taken to a commercial grinding shop where they were ground to a surface roughness of about 100 microinches (rms). The samples were then mounted in a shaper chuck, and the thermocouple slots were cut with a specially prepared shaper tool according to the scheme shown in Figure 18. After this, the samples were placed on a lapping table to be ground. All grinding was done by hand, starting with a number 240 grit and continuing with successively finer grits until the desired surface finish was obtained. The "outside" end of every specimen (the end that would be placed against a source or sink block) was ground in the final stage with an alumina powder. This resulted in surfaces with roughnesses of 3 - 6 microinches (rms).

Initially samples were prepared by machining the contact surfaces in a shaper to produce surfaces with parallel waviness of regular wavelength. However, test results on the samples prepared in this way showed extremely distorted temperature profiles. This was caused by the highly convex test surface produced by the shaping process. The deviation

was large enough in one case to be seen by the unaided eye when two such surfaces were held together. Thus the grinding process was used to prepare all samples for which data are reported here.

All surface roughness measurements were made using a Brush Surface Measuring System Model MS-5000. Surface records were made and kept on each sample tested. The average surface roughness of each contact surface is given in the sample data in Appendix A.

An attempt was made to measure the microhardness of the contact surfaces. However the surface roughness made it impossible to identify the edges of the indentations clearly. Consequently, microhardness measurements were made on polished flats on small cylinders of the sample materials. These measurements were made on a Tukon Model LL microhardness tester. Diamond Pyramid Hardness Numbers were obtained on the three sample materials for indenter loads of 0.50, 0.75 and 1.00 kilogram. These data are also given in appendix A.

Preparation of the test specimens was completed by installing the thermocouples. As noted previously the thermocouples were installed in shallow slots rather than drilled holes (see Figure 18). The idea for this type of instal-

lation originated at the National Bureau of Standards in experimental thermal conductivity work by Watson and Robinson [252]. The reasons for using slots are threefold. First, it is difficult to establish good thermal contact between a thermocouple bead and the bottom of a drilled hole. Secondly, a drilled hole produces a larger interruption in the sample cross section. Finally there is more uncertainty about the axial location of the thermocouple junction in a hole. The first two problems above can have disastrous effects on transient temperature measurements. Early in the test program a one-piece sample (no interface contact) was constructed with a number of holes drilled to the centerline on one side and an equal number of slots cut on the other side at the same axial locations. All the holes and slots were instrumented with thermocouples and a phase 1 type test was run. The temperature readings of the hole thermocouples showed large lags behind the slot thermocouples, as much as $30^{o}F$ about half way to steady state. Although this result was proof enough in favor of the slots, further comment is in order. Since the slots were cut with a width slightly less than the diameter of the thermocouple wire a very tight fit resulted from forcing the thermocouples into the slots. This provides intimate metal-to-metal contact and eliminates

the contact resistance problem. The slots were small and completely filled with thermocouple metal thus reducing the interruption of cross section and making the change in thermal capacity very small. Also, the press fit nature of the slot type installation makes the accuracy of the bead location equal to the accuracy of the slot location; whereas a hole must be drilled oversize and thus produces an additional possibility of error. The slot locations were measured just prior to thermocouple installation on the micrometer-equipped sample stage of the Tukon Hardness tester. In this way slot locations (center of the slots) could be measured to $\pm$ .002 inch. Measured slot locations of all test specimens are shown in Appendix A.

In the transient type experiments of interest here the heat flow through the specimen cannot be measured directly. In order to calculate the contact conductance it is necessary to evaluate the flux from the thermal conductivity of the materials and the measured slopes of the temperature profiles. Since the conductance values thus depend directly on the thermal conductivity it was necessary to have accurate data for the thermal conductivity. To provide this information a program was carried out by Mr. D. R. Williams in which the thermal conductivities of the materials used in

this work were accurately measured. The details of the measurement method are presented in Mr. Williams' thesis [250]. The thermal conductivity data were fitted with linear least-squares curve fits over the temperature range of interest in this study. The values of thermal diffusivity for the specimen materials were estimated from data available in the open literature for similar alloys. Due to lack of information these values were assumed to be constant. The thermal properties are shown, along with the other sample data in Appendix A.

Temperature Measurement

All temperature measurements were made using Chromel-Constantan thermocouples. The thermocouples were all made from the same spool of wire purchased from the Thermo-Electric Company. Number 26 gauge wires (0.0159 inch dia.) with a polyvinyl insulation were used to form all the measuring junctions. A smaller wire than this would be desirable from the standpoint of conduction error, however, this size was the smallest that could be butt-welded efficiently. Each test required 14 thermocouples in all: 2 each in the sink and source blocks and 5 each in the two test specimens. The same source and sink block thermocouples were used for all

tests. Their measuring junctions were formed by twisting and soldering, and they were installed by soldering into one-eigth-inch deep drilled holes in the copper blocks, as indicated in Figure 19.

Each test specimen had its own set of five thermocouples which were not removed after the initial installations. The specimen thermocouple measuring junctions were formed by butt-welding the Chromel and Constantan ends together with a small resistance welding unit. This process is definitely an art. After some experimentation the proper power settings and method of preparing the wire ends was found. The resulting thermocouples had a good, welded measuring junction and no bead, thus providing a uniform diameter for installation in the slots. Installation was also found to be an art, and, after practicing on some dummy samples, the following procedure was found to be successful. With the sample held in a small vise, the thermocouple reference junction was centered over the slot and tamped into the slot. For the tamping a single-edged razor blade whose sharp edge had been ground off was held against the wire and struck with a light hammer. After the wire was inserted to the bottom of the slot the upper edges of the slot were folded over on the wire to insure the security of the wire. Fi-

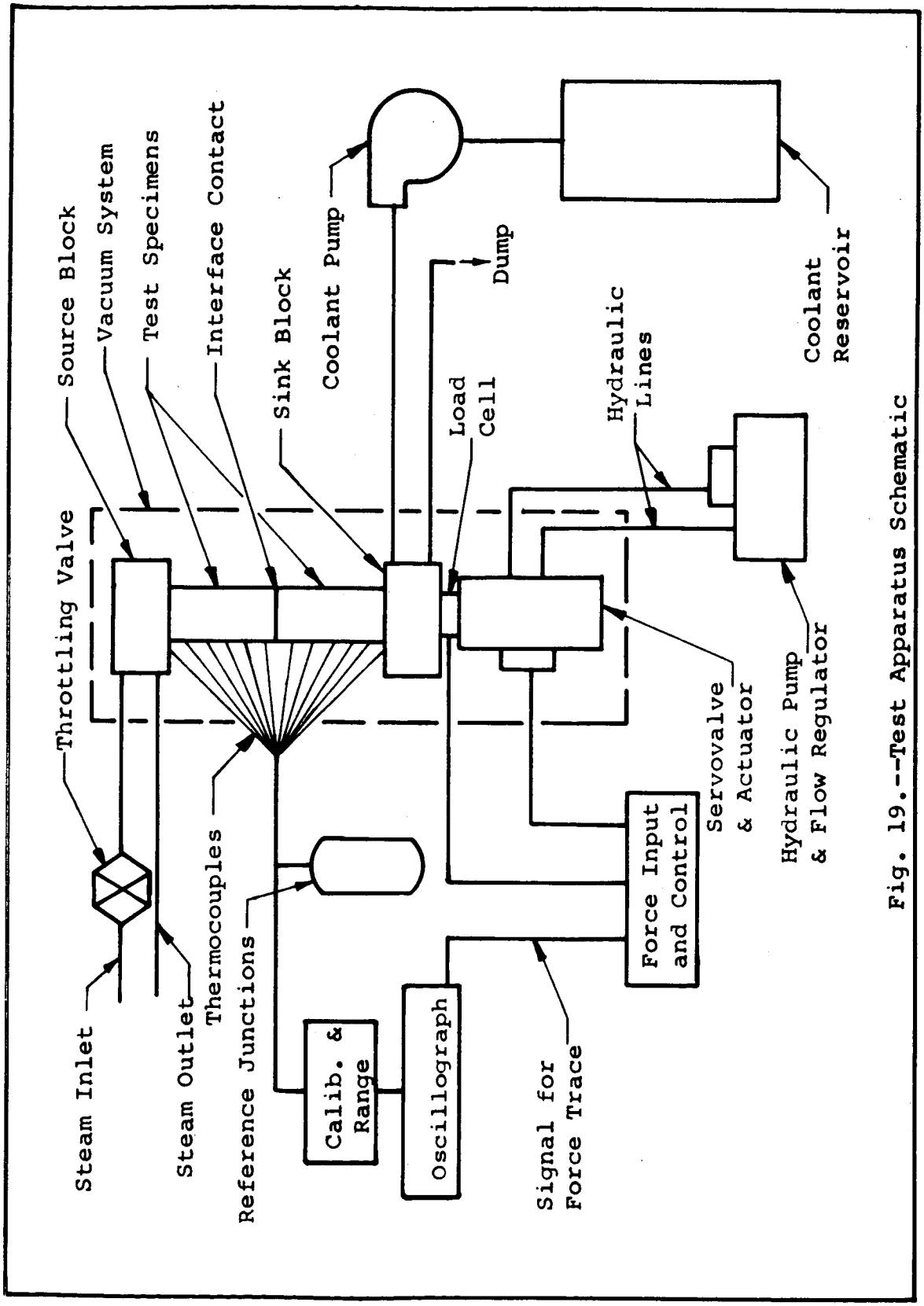

Fig. 19.--Test Apparatus Schematic

nally, the wires were wrapped around the sample and a short piece of heat-shrinking plastic tubing was shrunk over the two wires. At the point where the two wires met at the sample surface (opposite the slot) a small dab of silicone rubber cement was used to prevent relative motion between the wires and the specimen (see Figure 18).

This last step in thermocouple installation brings up an important point. Since transient temperature measurements were to be made, it was necessary to minimize the amount of extra material touching the samples, because additional material would add to the heat capacity and affect the transient response. For this reason the samples could not be insulated as they usually are in steady-state work.

The thermocouple circuits are shown schematically in Figure 19. Since each sample had its own set of thermocouples, all thermocouples were connected with gold plated socket-and-pin connectors near the base plate of the vacuum system to the lead wires from the reference junctions. Care was taken in the location of the connectors to insure that they were at a uniform temperature to prevent any additional thermocouple effect due to the dissimilar metals. The lead wires to the 32°F reference junction were Number 14 gauge Chromel-Constantan wires to reduce the electrical resistance.

The 10 thermocouples had electrical connection via the metal samples. No further electrically common connections could be allowed in order to prevent the thermocouple wires from forming current loops and thus giving erroneous voltages. Consequently, each thermocouple had its own separate reference junction. These junctions were made of the 14 gauge wire and electrically insulated by plastic tubing and silicone rubber. All junctions were kept together by means of a rubber band and held in the middle of a large insulated container which was packed, top-to-bottom, with crushed ice and water.

The requirement of simultaneous, transient temperature measurement precludes the use of a potentiometer for taking test data. All data were recorded on a Honeywell Model 1508 "Visicorder" at paper speeds of 0.1 or 0.2 inch/second depending on the samples being tested. Thermocouples used in this way have a small electrical current flowing at all times. Thermocouple reference tables are based on a balanced voltage reading and could not be used in this application. It was thus necessary to calibrate all the thermocouples of each specimen set over the range of temperatures to be incurred in the test. In order to provide the flexibility required by the variation of temperature range for

each thermocouple and to provide impedance matching for the galvanometers it was necessary to put a pair of variable, series-parallel resistors in each thermocouple circuit. These variable resistors were all located in a small metal cabinet which was located, electrically, between the reference junctions and the galvanometer inputs. By adjusting both resistors in each circuit the desired galvanometer deflection and impedance matching could both be achieved.

Galvanometer ranging was accomplished by putting the specimens in position in the test apparatus, establishing a steady state heat flow through the samples and adjusting the ranging resistors to obtain the desired deflections. After the ranging was set the thermocouples could be calibrated. Calibration was performed using the samples and instrumentation in the same configuration as they would be in for a test. This was accomplished by using a portable calibration bath which could be set up adjacent to the test fixture. The arrangement of this insulated bath is shown in Figure 20. With all thermocouple circuitry in the configuration it was to be used in during the tests, the samples were placed in the metal cans and covered with aluminum filings and insulation. The oil bath was constantly stirred by a paddle wheel. Bulk changes in the oil temperature were produced by flowing

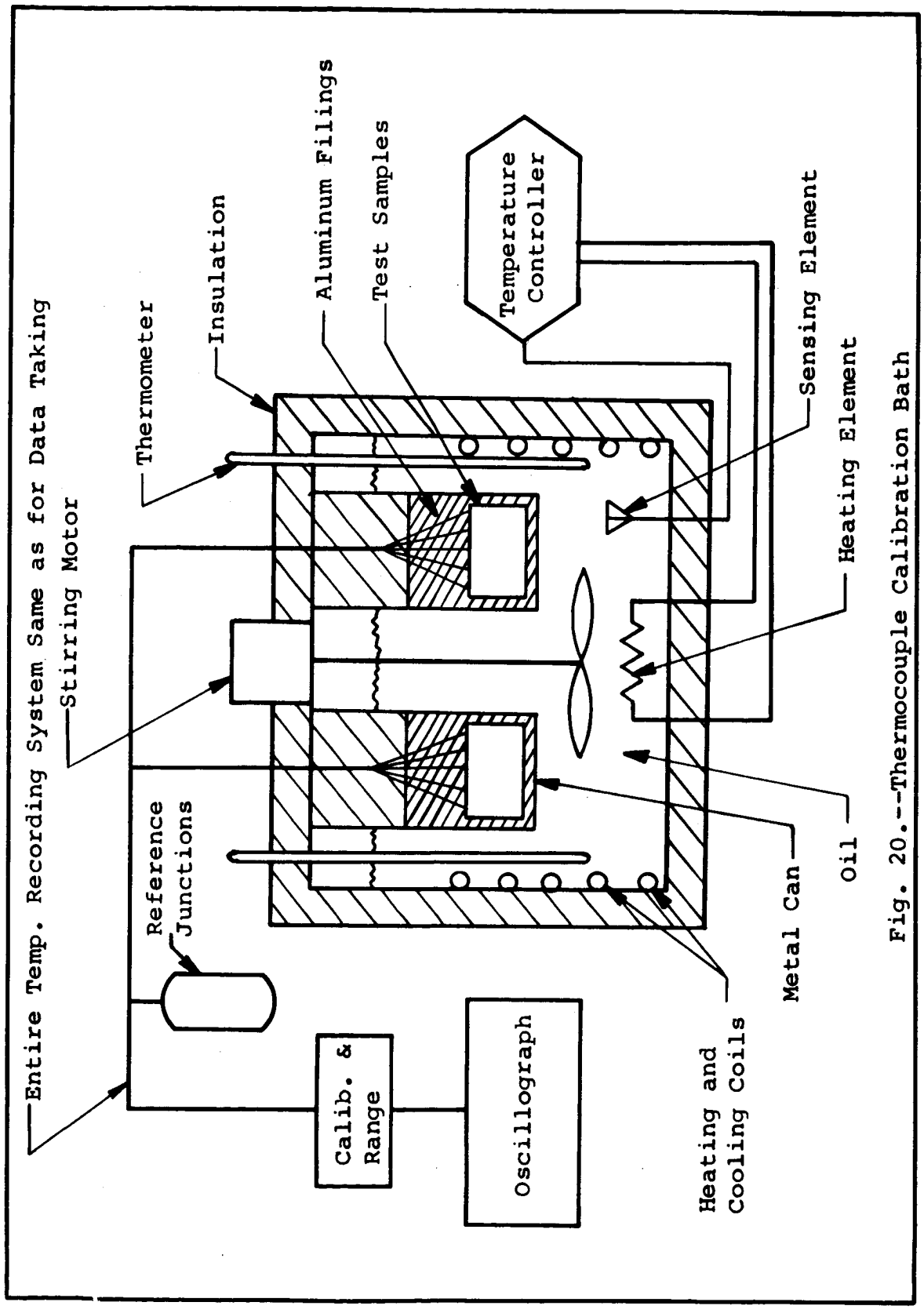

Fig. 20.--Thermocouple Calibration Bath

steam through the lines for heating, and water through the lines for cooling (see Figure 20). When the desired temperature of a given calibration point was neared the oil bath temperature was controlled automatically by a Honeywell "Thermoniter" unit and two 150 watt electrical heaters. A set of calibrated ASTM standard thermometers, used to provide temperature measurements over the full calibration range, were employed as indicated in Figure 20. To provide a check on the actual sample temperatures, and to provide a means of determining when the specimens had reached equilibrium, the center thermocouples of each specimen were monitored on a potentiometer. This was accomplished by disconnecting the leads (of these two thermocouples) to the ranging unit and connecting the potentiometer leads in their place. Thus connected, the ranging resistors and galvanometers were completely removed from the circuits. The temperatures of these two thermocouples were determined by converting the balanced voltage reading of the potentiometer using a set of NBS conversion tables. The two readings were always within about $0.1^{\circ}F$ of each other and usually were within the same tolerance of the thermometer reading. After the temperature readings had stabilized, the two center thermocouples were put back into the recording circuit and a

record was made of all the galvanometer deflections. This process was repeated until all the desired calibration points had been taken.

Since there was an electrical current flow in this application the temperature versus deflection curves were slightly non-linear. Two typical calibration curves are shown in Figure 21. All deflections, for calibrations and test runs, were read from the oscillograph records with a scale ruled to 0.01 inch. The calibration readings were punched on cards which were processed by a computer program to fit a least-squares second order polynomial through the calibration data of each thermocouple. These polynomials were used by the test data reduction program to calculate temperatures from the test data deflection readings. The solid lines in Figure 21 are the curve fits for the calibration data shown there. Each set of test specimens was calibrated prior to the running of its respective test series.

Source and Sink Blocks

During the experiments the test specimens were held between the source and sink blocks as shown in Figures 16 and 17. These blocks were constructed of OFHC copper and were hollow with inlet and outlet ports. A detail drawing

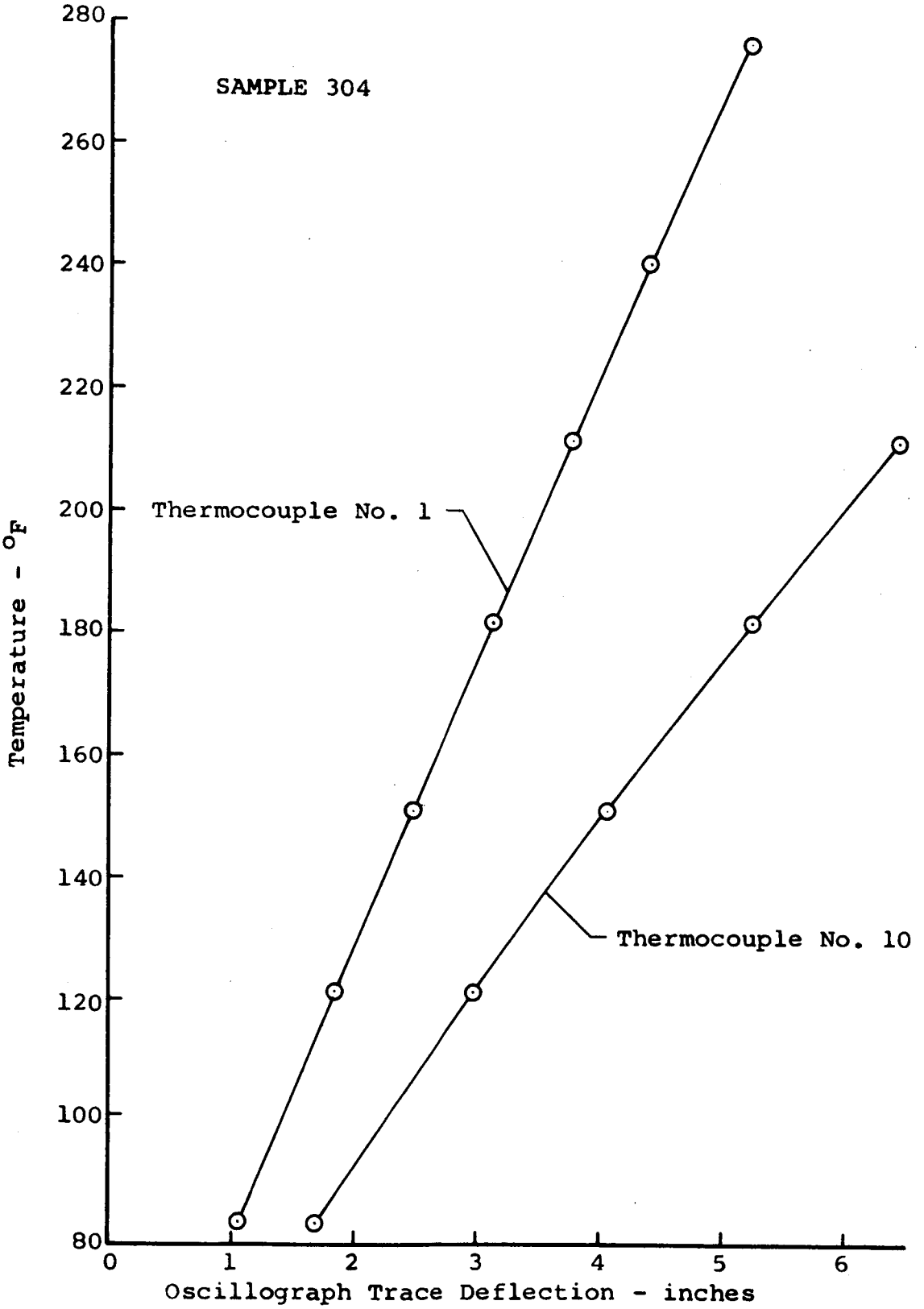

Fig. 21.--Typical Thermocouple Calibrations

of the blocks is given in Appendix C. The sink block temperature was held constant during the experiments by flowing room temperature water from a large tank. Steam from the building heating system was used to maintain the source temperature constant; the temperature was adjustable over the range of 290-310°F by means of controlling the pressure using a throttling valve. During the experiments source temperatures of 300-304°F were used. The source and sink temperatures were measured by Chromel-Constantan thermocouples as indicated previously. These thermocouples were from the same spool of wire as the specimen thermocouples. Because good accuracy found for this wire, as indicated above, the temperature-deflection calibrations of these thermocouples were made using the NBS table conversions. The procedure used was again that of disconnecting temporarily to use the potentiometer. The steam and water temperatures were varied over the small ranges of interest to provide these calibration points. Second order curve fits for these calibrations were made and used in the manner described above.

Test Fixture and Loading System

The basic test fixture, shown schematically in Figure 16, consisted of two 3/4-inch thick plates connected by

three 3/4-inch diameter rods. This basic framework was made of type 304 stainless steel. Detail drawings of all the test fixture components are shown in Appendix C. The two parallel plates were used to mount the sample holding and loading components, and were adjustable by means of the three threaded connecting rods to accommodate different total specimen lengths. The source block was held by an adapter and thermally insulated to reduce heat loss to the test fixture. As shown in Figure 16, this adapter transmitted the applied force through a spherical joint to the upper plate, to which it was connected by three small helical springs. This arrangement was used to insure that any small misalignment in the test column would not cause the contact surfaces to be loaded unevenly. A second, similar adapter was used to hold the sink block. This adapter rested on the load cell (Lockheed Electronics Model WR75-025 Load Washer) which in turn rested on the loading rod of the hydraulic cylinder. This test fixture assembly rested on the base plate of the vacuum chamber as shown in Figure 17. All instrumentation and fluid lines were passed through the base plate with standard vacuum type feed-throughs. The vacuum system was a Consolidated Vacuum Corporation Model CV-108 vacuum unit.

The force control system is basically a closed-loop electro-hydraulic servomechanism. Figure 22 is a schematic drawing of the main components of the system. A double ended hydraulic cylinder applies the force to the test specimens. The cylinder is supplied with a constant pressure, constant flow stream of hydraulic oil by a pump and flow regulator. A proportional type servovalve controls the pressure differential across the piston of the hydraulic cylinder and thus controls the force applied to the test samples. The cylinder and servovalve combination is a Moog Servocontrols, Inc. Model 1725G servoactuator. This servoactuator was originally designed as an engine positioner for the Titan I missile and as such was made to operate using piston position for feedback. This system was modified to allow the use of applied force for feedback.

As shown in Figures 16 and 19, the applied force is transmitted through the force cell. The force cell is a strain gage device. It is used as one leg of a resistance bridge so that the unbalanced bridge voltage is proportional to the applied force. This voltage is used as a feedback signal as indicated in Figure 22. By means of a potentiometer an input signal is supplied to a summing junction at a polarity opposite to the feedback signal. The difference

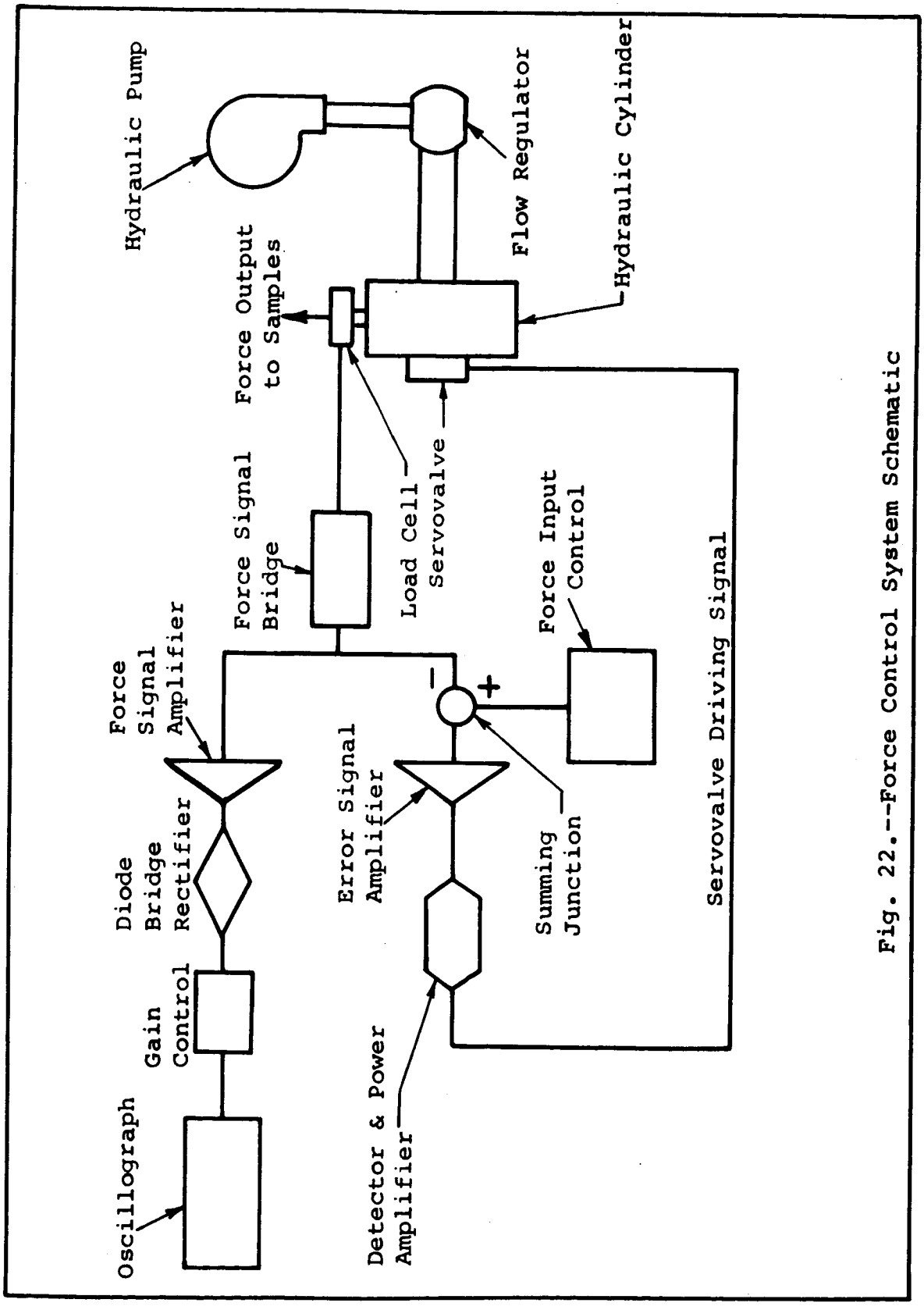

Fig. 22.--Force Control System Schematic

between these two voltages is the error signal which is amplified and used to drive the servovalve. Thus when the feedback is equal to the input the servovalve holds the desired force on the system. The input control consists of two potentiometers connected by a two position switch. This arrangement allowed the step change in input force to be accomplished. Tests made on the system showed that the response time to the step change was of the order of milliseconds, thus, for practical purposes the load changes were instantaneous.

In addition to providing a feedback signal for the controller the force cell signal was also amplified and rectified for use in recording the force on the samples during the experiments. A complete set of electrical circuit diagrams for the force control system are given in Appendix D. The force trace on the oscillograph was calibrated by placing another load cell between the source and sink blocks and comparing the trace deflection to the output of this second load cell, which had been calibrated on a compressive testing machine.

Experimental Procedure

The following is a brief outline of the procedures

used in operating the test apparatus to obtain the data for the various phases.

After the thermocouple circuits had been calibrated the samples were removed from the calibration bath and cleaned. Each end of both specimens was cleaned with acetone and absolute ethyl alcohol. The outside ends of both samples were coated with a thin film of Dow Corning silicone grease to reduce the contact resistance between the specimens and the source and sink block surfaces. Then the specimens were placed in the test apparatus.

Phase 1. The samples were pressed together between the source and sink blocks with a pressure of about 10 psi. By a valving arrangement cooling water was circulated through both blocks for about 10 minutes to bring the samples to a uniform temperature. Next, the samples and sink block were lowered by the force system so that the upper (hot side) specimen no longer made contact with the source block. The vacuum bell jar was then lowered and test chamber evacuation started. While the system was pumping down the cooling water was kept flowing through the sink block but was shut off from the source block. Normally it required about 20 minutes to pump the test chamber down to the range of 1-5 microns hg. This pressure range was used be-

cause it was low enough to make the interstitial gas conduction small, and because it was easily obtainable with a mechanical pump. When the desired test chamber pressure was reached the oscillograph was started and the steam to the source block was turned on. About 20 seconds was required to bring the source block up to the desired temperature. Finally, an input signal to the force controller raised the sink block and test specimens, bringing the upper specimen into contact with the hot source block. All data were continuously recorded on the oscillograph record throughout all phases of the tests.

Phase 2. When phase 1 was completed the contact pressure was raised suddenly to a new constant value by flipping the two position switch on the force controller. The control system maintained a constant pressure until a new steady state was reached.

Phase 3. The contact pressure was returned to its original (lower) value by flipping the control switch back to the first position. This constant pressure was maintained until the steady state was reached.

Phase 4. The vacuum pump was turned off. With the force control system maintaining the same constant pressure, air was allowed to enter the system by opening a hand valve.

This produced an increase in contact conductance and the system sought a new steady state. The test data show that this was effectively a very rapid change. That is, the temperature profiles show a response like that of the phase 2 tests. This provides experimental verification of the theoretical predictions of Aaron and Blum [2] that the "threshold" ambient pressure, above which the contact conductance is little affected by ambient pressure, is very low.

Phases 5 and 6. These phases were accomplished in the same manner as phases 2 and 3, respectively. However, the changes in contact conductance produced by changing the contact pressure were different due to the presence of air.

Data Reduction Procedure

As mentioned above, all data were recorded continuously on an oscillograph. The trace deflections of each measured quantity were manually read from the oscillograph records with a scale ruled to 0.01 inch. The time intervals at which data were read varied with the specimens being tested. During the early portion of each experiment smaller time intervals were used because changes were more rapid. As the rate of change became slower the "data times" were more widely spaced. Typical data time intervals were as

follows: every 2 or 4 seconds for the first 20 seconds, 5 or 10 seconds for the next 40 seconds, 20 or 40 seconds for the next 120 seconds, and then every 50 or 100 seconds depending on the total time. The oscillograph was equipped with an automatic timing system which placed lines on the oscillograms every second. This system, which used an RC circuit, was checked and found to be slightly fast. For convenience the data were processed using the timing line time and then the small correction factor was applied to all the final results. The deflection reading of all 15 traces were read for each data time and recorded in a log book. These data were then punched onto cards to be read into the data reduction computer program. For all the test data reported here this amounted to approximately 2300 data cards.

The data reduction computer program was written in FORTRAN and used on the Control Data Corporation's Model 1604 and 3400 computers. The following is a brief outline of the steps performed by the data reduction program.

1. Read in the required specimen data, such as thermal conductivity, exact sample length and thermocouple locations.
2. Read in the thermocouple and force trace calibration data, i.e., coefficients of the least-squares

curve fits.

3. Read in the experimental data cards.
4. Calculate the temperatures and contact pressure at each data time using the calibration results.
5. Print out all the above information in tabular form.
6. Perform transient analysis. This consisted of making least-squares curve fits through the temperature profiles for each data time and extrapolating these to the boundaries to calculate the contact surface temperatures. Then the contact heat flux was calculated from the local slope of the temperature profiles and the thermal conductivity. Finally, the contact temperature drops were calculated from the extrapolated profiles, and the contact conductance was determined from these temperature drops and the heat flux.
7. Print out the results of the transient analysis in tabular form.

The above outline provides an indication of the large amount of work necessary to reduce the data of an experiment of this type. It is estimated that manual reduction of the data presented in this work would have required several

months. Some further remarks are in order regarding item 6 of the above program. The least-squares curve fits for the temperature profiles used in the program were second order polynomials. This form was chosen after a study was made in which several functional forms of curve fit were tried on some of the experimental data. The second order polynomial consistently gave the smallest average deviation of the forms tried. Higher order polynomials and other functional forms were tried but were found either to give larger deviations or to possess bad extrapolation behavior. For example, with five temperatures one might fit a fourth order polynomial and obtain zero deviation, but the curve may rise or fall sharply outside the fitted range and produce meaningless extrapolations.

As discussed later in section VI, the test results were evaluated on a basis of time to approach steady state or time to reach maximum overshoot. These times were determined from hand made plots of the transient analysis. This was necessary because the temperature drop across a specimen versus time is an S-shaped curve making it difficult to use a curve fit. By hand plotting, smooth curves could be drawn through the data points for the extrapolated temperature at each end of a specimen versus time. The time at which a par-

ticular temperature difference occurred was determined by using a drafting divider.

The test data and results obtained using the above procedures are presented and discussed in section VI. A brief evaluation of the accuracy of the experimental results concludes this section.

Experimental Accuracy

A discussion of possible sources of error in the primary measured quantities is presented first. The effect of the errors on the calculated quantities is then evaluated.

The procedure used to calibrate the contact pressure trace was described above. The slope of the pressure trace (psi per inch of deflection) was approximately 30 psi/inch. With a reading accuracy on the scale used of $\pm$ .01 inch the contact pressure accuracy would be $\pm$ 0.3 psi. To this should be added the accuracy of the calibration device which was approximately $\pm$ 0.5 pound and therefore about $\pm$ 0.7 psi in terms of contact pressure. Thus the contact pressures should be good to at least $\pm$ 1 psi.

For the temperature data, that part of the possible error due to reading accuracy depends on the range setting of the galvanometer trace. The thermocouple nearest the

source had the largest deflection slope (^{o}F per inch of deflection) since it had to measure the highest temperature. This slope was approximately $45^{o}F$/inch which would give a reading accuracy of $\pm$ $0.45^{o}F$. The thermocouple nearest the sink had a slope of about $30^{o}F$/inch, or a reading accuracy of $\pm$ $0.3^{o}F$. The average deviation of the calibration curve fits from the calibration data was about $\pm$ $0.3^{o}F$. The temperature profile curve fits showed average deviations from the data which varied with time from about 0.6 to $0.2^{o}F$, the former occurring at early data times and the latter as steady state was neared. Assuming an average value of $0.4^{o}F$ for this deviation and assuming that the probable error is the square root of the sum of the squares, the probable error in a calculated temperature is around $\pm$ $0.6^{o}F$. Thus a calculated temperature difference is probably only good to about $\pm$ $1^{o}F$.

The contact conductance was calculated by dividing the contact heat flux by the contact temperature drop. The heat flux was calculated as the product of the local temperature profile slope and the thermal conductivity. Actually, the average of this product on both sides of the interface contact was used in these calculations. Symbolically,

$$h_c = \frac{\left[k \frac{dT}{dx}\right]_{HOT\ SIDE} + \left[k \frac{dT}{dx}\right]_{COLD\ SIDE}}{2\,(\Delta T)_c} \qquad (V\text{-}1)$$

The thermal conductivity data is believed to be within ± 4% [250]. It is practically impossible to evaluate the accuracy of the temperature profile slopes during the transients and it can only be estimated in the steady state. However, only steady state values of conductance were used in the correlation of test results presented in section VI. In the steady state the temperature profiles are essentially linear. Assuming the worst situation, namely all the temperatures in one half of a specimen are high and those in the other half are low, would give an error of about 0.5°F/inch in the slope. The lowest slope measured was about 4°F/inch but it was usually around 20-30 °F/inch

The percentage accuracy of the calculated contact conductance depends somewhat on the level of conductance, primarily because of the contact temperature difference (see equation V-1). As an illustration consider the steady state value of phase 1 of run 405-2. This represents the lowest value of interface conductance calculated in these experiments. The contact conductance was calculated as 29 Btu/hr.-ft.^{2}-°F. The contact ΔT was 142.9°F and the slopes were

8.6°F/inch on the hot side and 76.7°F/inch on the cold side. Thus the possible percent error in ΔT is about 0.6% and the possible percent error in the slopes were about 5.8% and 0.6%. All errors combined would give a result of about ±10% for the contact conductance. For this same run the hot end conductance (conductance for the contact between the source block and the upper specimen) was calculated as 848 Btu/hr.-ft.^{2}-°F from a ΔT of 4.8°F. The possible error in ΔT is now about 20% giving a conductance accuracy of about 25%.

The highest value of interface conductance calculated in the present data (2505 Btu/hr.-ft.^{2}-°F) was on phase 5 of run 304-8. The contact temperature drop was 21.0°F, the slopes were 28 and 60.5 °F/inch. The probable error in ΔT would be about 5% and for the slopes about 2% and 1%. This again results in about ± 10% for the conductance. For this experiment the hot end conductance was calculated to be 5063 Btu/hr.-ft.^{2}-°F. with a ΔT of 10.4°F, or, in other words, about ± 15% for the conductance.

Based on this approach, it is believed that the conductance values are good to about 10% at best and probably average closer to 15%. It should be noted, however, that in some cases on the 405 series the contact temperature drop on the (grease filled) end contacts was so low that the calcu-

lated conductances exceeded computer print format. In some of this series even negative values were calculated for the end conductances, which demonstrates the problem of ΔT accuracy. However, a check of the data shows that any calculated end conductance below about 5000 Btu/hr.-ft^2-$^\circ$F is probably at least within $\pm$ 20%.

Although these estimates of data accuracy certainly leave a lot to be desired one is hard-pressed to find many experimental contact conductance works that show a better accuracy. Some suggested changes for possible future work which might improve upon the overall data accuracy are offered in section VII.

VI. EXPERIMENTAL RESULTS

The experimental data obtained in the present work are presented in this section. All data were obtained employing the equipment and procedures described in the previous section. As used in this section, the word "data" refers to the printed output of the computer data reduction program. This data consisted of the following: (1) temperature distributions in the two test samples and the source and sink block temperatures; and (2) the quantities which were calculated from the temperature distributions and thermal properties, all at specified time intervals. The latter group includes the contact temperature drop, ΔT_c, and the three contact conductances h_c, h_1 and h_2 (see Figure 7). These data are presented below in four separate groupings according to the important point emphasized and the type of test.

Contact Conductance as a Function of Time

One of the first effects noticed in analyzing the test results was the apparent variation of the contact conductance coefficient with time. A plot is shown in Figure 23 of the calculated contact conductance coefficient versus time

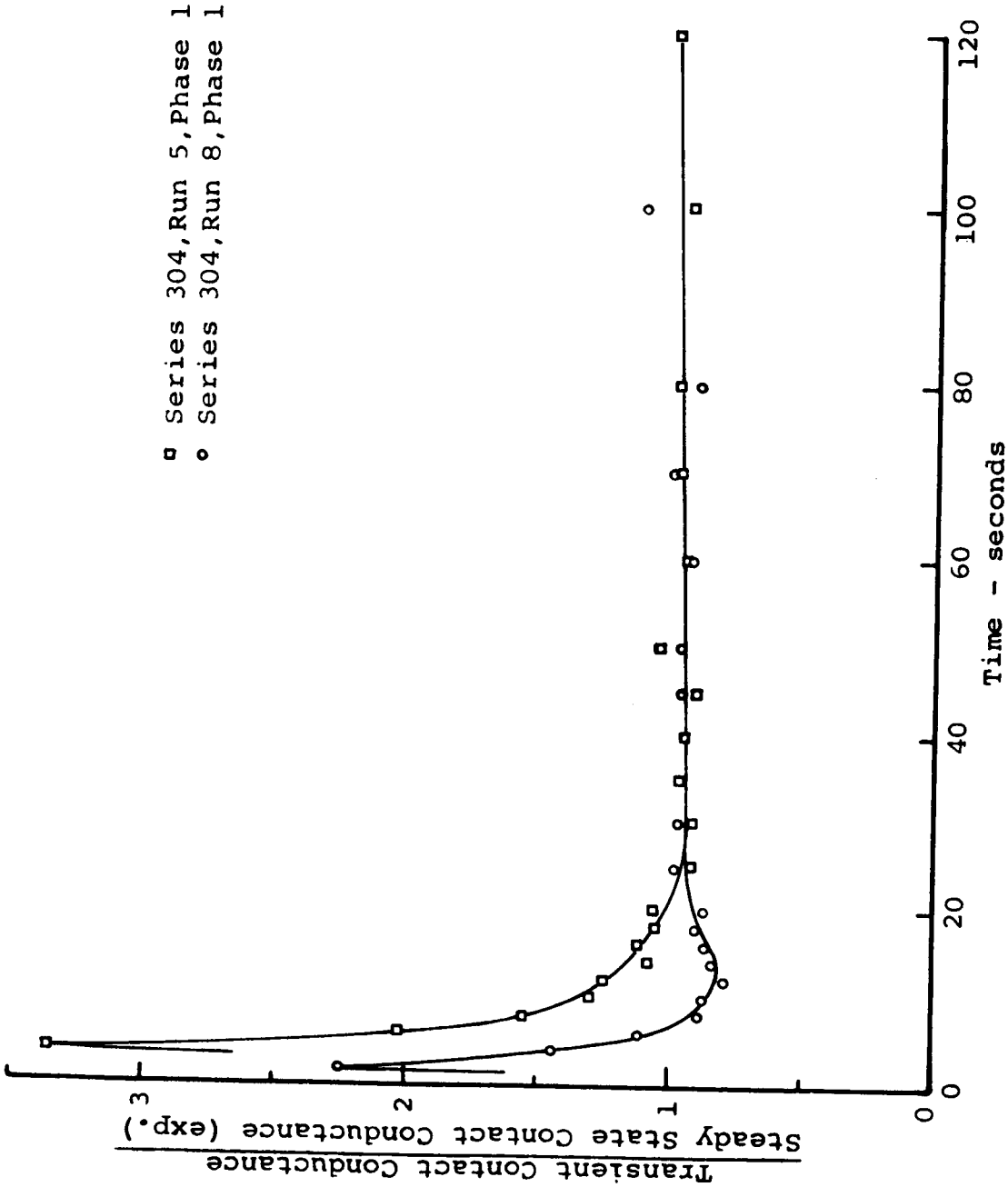

Fig. 23.--Calculated Contact Conductance as a Function of Time

for two typical test runs. The sharp variations shown in Figure 23 were unexpected, and it was decided to attempt to determine whether such variations were real or whether they were a result of the calculation procedure. For this perpose several sets of data were generated with the theoretical solution for a constant contact conductance. These data consisted of the theoretical temperatures at the locations in the samples where the temperatures were measured in the experiment, at the time intervals used in the experiments. Next, these data were punched on cards and fed into the data reduction computer routine just as if they were experimental test data. The results of two such check runs are shown in Figure 24. It can be seen that even though the data used were generated using a constant contact conductance, the data reduction program calculates a conductance which varies with time in much the same manner as shown in Figure 23 for experimental data. As a further check on this effect, some of the same data was run through another computer program written by Dr. James Beck of Michigan State University [249]. Dr. Beck's program employs a different method of calculating the conductance coefficient. However, the results were the same. That is, this program predicted the same kind of variation for both experimental and theoretical

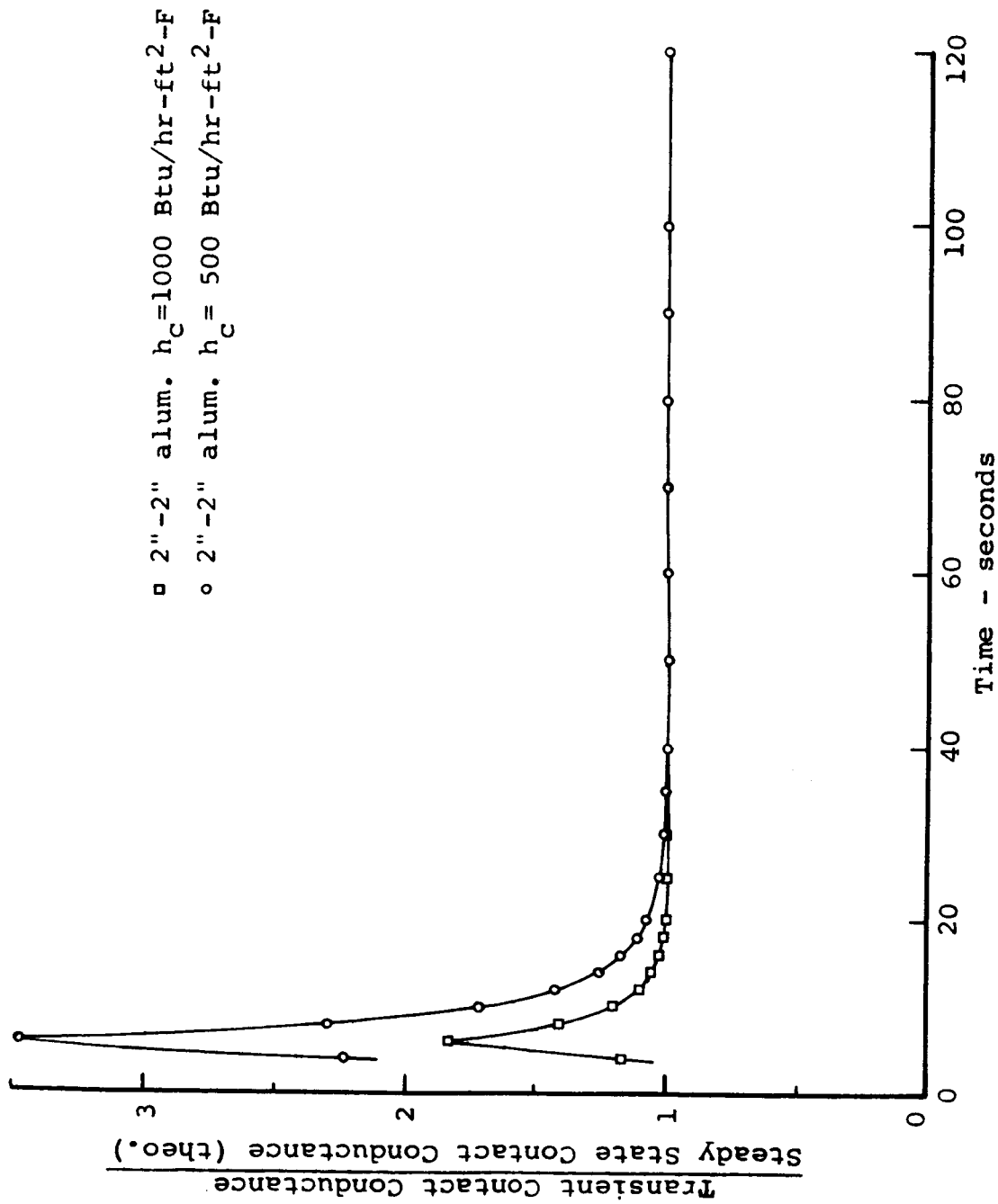

Fig. 24.--Check Runs With Theoretical Data

data. This evidence is not conclusive proof that the indicated variation in contact conductance is a result of the calculation procedure, but it does show that such a variation is calculated when none exists.

There is nothing in any of the theoretical work on contact conductance [55,58,85,143] to suggest a variation as strong as the one indicated in Figure 23. The only variation that might be suggested by the theories of contact conductances is a slight variation due to the changing mean interface temperature. Figure 23 shows that after the initial sharp variation has settled out there is a gradual rise. This rise is of the order of that found by others studying the effects of mean interface temperature [24,27,47,140].

Of the reported works which have measured contact conductance by a transient means [26,46,60,127,190,231] only one [190] has indicated a variation of the order indicated in Figure 23. The others have either not mentioned observing any variation [60], found it to be of the nature of scatter [26,46,127], or found that it was a result of mean temperature increase [231]. Schauer and Giedt [190] measured the contact conductance between two thin strips during transient heating. Their method and results were discussed in section IV. They found a sharp increase in contact conduct-

ance which occurred over a period of approximately 100 milliseconds. The present writer feels that their results may be questionable. However, assuming that they are valid would suggest that any sharp variations in contact conductance would have disappeared long before any time at which data were recorded in the present experiments.

In view of all of the above evidence it is the writer's opinion that the contact conductance variation indicated in Figure 23 is not real but is a result of the calculation method. This can be explained as follows. During the early data times the contact heat flux is small and the resulting contact temperature drop, ΔT_c, is small. This results in low accuracy for the calculated contact conductance because the error incurred in extrapolating the curve fits of the temperature profiles is not small compared to the calculated ΔT_c. In fact, in some cases, the early-time conductance values were calculated to be negative as a result of the low accuracy in the contact temperature drop. Another source of error in the early conductance calculations is the temperature profile slopes. Apparently the early-time temperature profiles vary too sharply near the contact plane to be closely fit by the curve fit used. As a part of the data reduction routine the average deviation of the temperature pro-

files were also calculated at each data time. The deviation was always worse during the early times and improved for later times. For example, the data of the phase 1 portions of the 304 series showed deviations of around $0.6^{\circ}F$ at the early times and decreased to around $0.1^{\circ}F$ for the later times. The slope accuracy problem is made worse by the fact that the cold-side specimen temperature profile is slower in developing because of the contact resistance. Even after the calculated temperature drop across the contact has become sufficiently large (to prevent its being calculated to be negative) this second source of error may still be present. As the heat flow increases, the calculated ΔT_c becomes more accurate and the profiles become more amenable to the curve fitting. This results in better contact conductance values as evidenced by the above-mentioned check runs of Figure 24. From an "information theory" point of view the above remarks might be summarized by saying that during the early times, when the heat flux is low, the five thermocouples in each specimen do not provide sufficient information to calculate the contact conductance. This suggests that better values might be obtained by employing more thermocouples in each specimen to provide a better knowledge of the actual temperature profiles. As

discussed in the previous section, it was sometimes possible to use only four of the five thermocouple readings in a test specimen due to the distortions caused by the contact surfaces. In view of the above discussion this probably compounded the early time conductance calculation problem.

In summary it is stated that the small gradual rise in calculated contact conductance at the later times, indicated in Figure 23, is believed to real. The sharper variations at the earlier times are believed to be only a result of the calculation method. Thus, the evaluations and comparisons of the data which are presented below are based on the contact conductance values calculated when a steady state had been reached.

Comparison With the Results of Other Investigators

As a means of providing a rough, overall check on the accuracy of the data obtained in this study, the values of contact conductance as a function of contact pressure were compared to results published by other investigators. These comparisons are shown in Figures 25 and 26.

In Figure 25 the vacuum data of the 304 series are compared to some data obtained by Fried [92] and Clausing and Chao [58]. The specimens used in the 304 series were

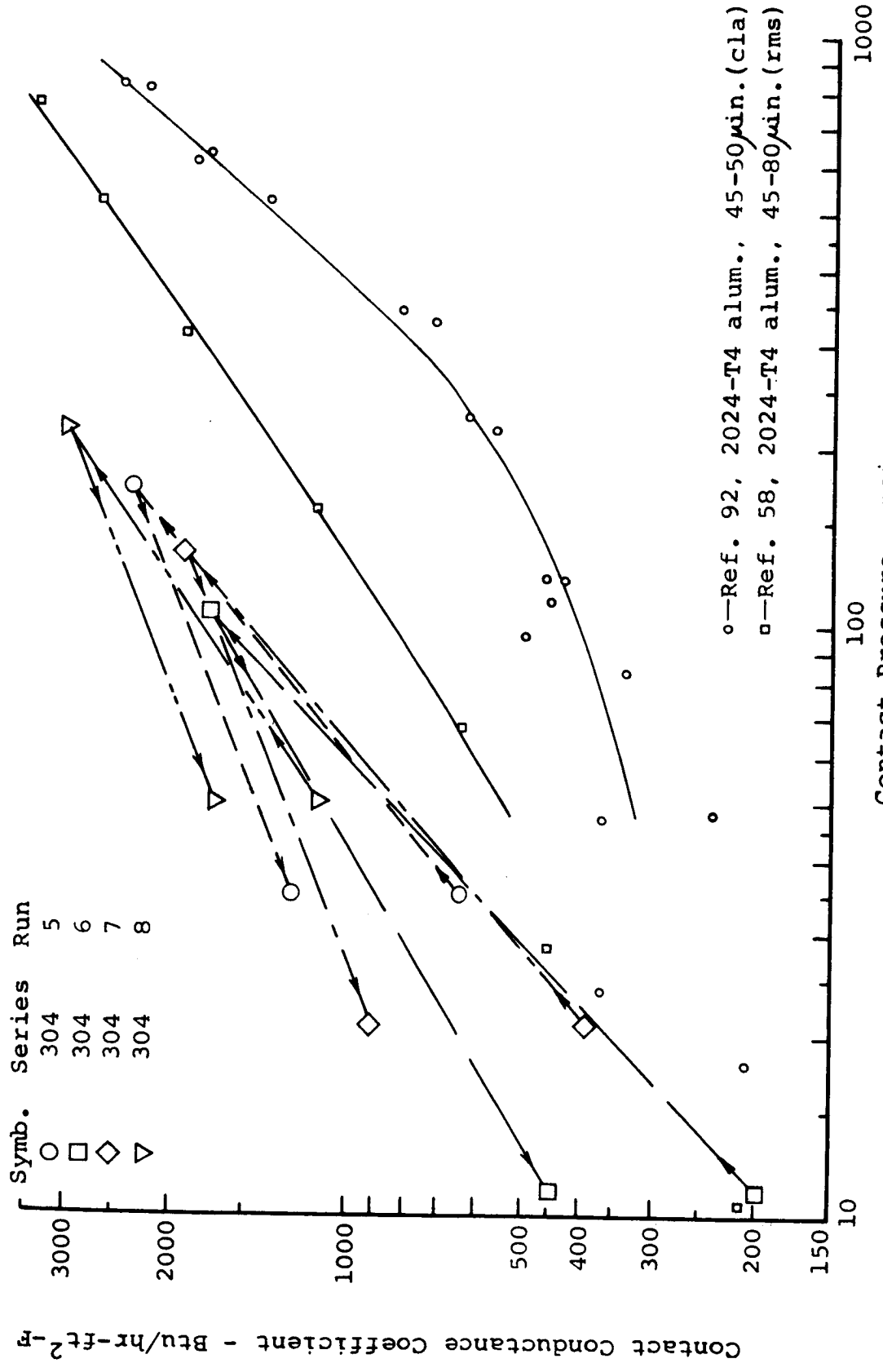

Fig. 25.--Comparison With Data of References 58 and 92

made of 2024-T351 aluminum with surface roughnesses of 70 and 75 microinches (rms). The cited data of Fried were obtained for 2024-T4 aluminum for surface roughnesses of 45 and 50 microinches (cla), and that of Clausing and Chao were for 2024-T4 aluminum for 45 and 80 microinches (rms). Based on the surface roughnesses the comparison indicates that the present data are reasonable. The absence of data on flatness deviation for the present data and Fried's data make a more valid comparison impossible. However, since the accuracy of the present steady-state data, which was discussed in the previous section, is at least as good as that of the other investigators, and since considerable scatter is known to exist in all the literature [103,124], the above comparison is adequate to demonstrate that the present data are reasonable.

In Figure 26 the in-air results of the 7A4 series are compared to the data of Fenech and Rohsenow [85]. The specimens of the 7A4 series were 2024-T351 aluminum and Armco Iron with surface roughnesses of 30 and 75 microinches (rms), respectively. The data of Fenech and Rohsenow are for specimens of aluminum (alloy unspecified) and Armco Iron with surface roughnesses stated to be 150 microinches maximum (no average given). The comparison shown in Figure 26 is, again,

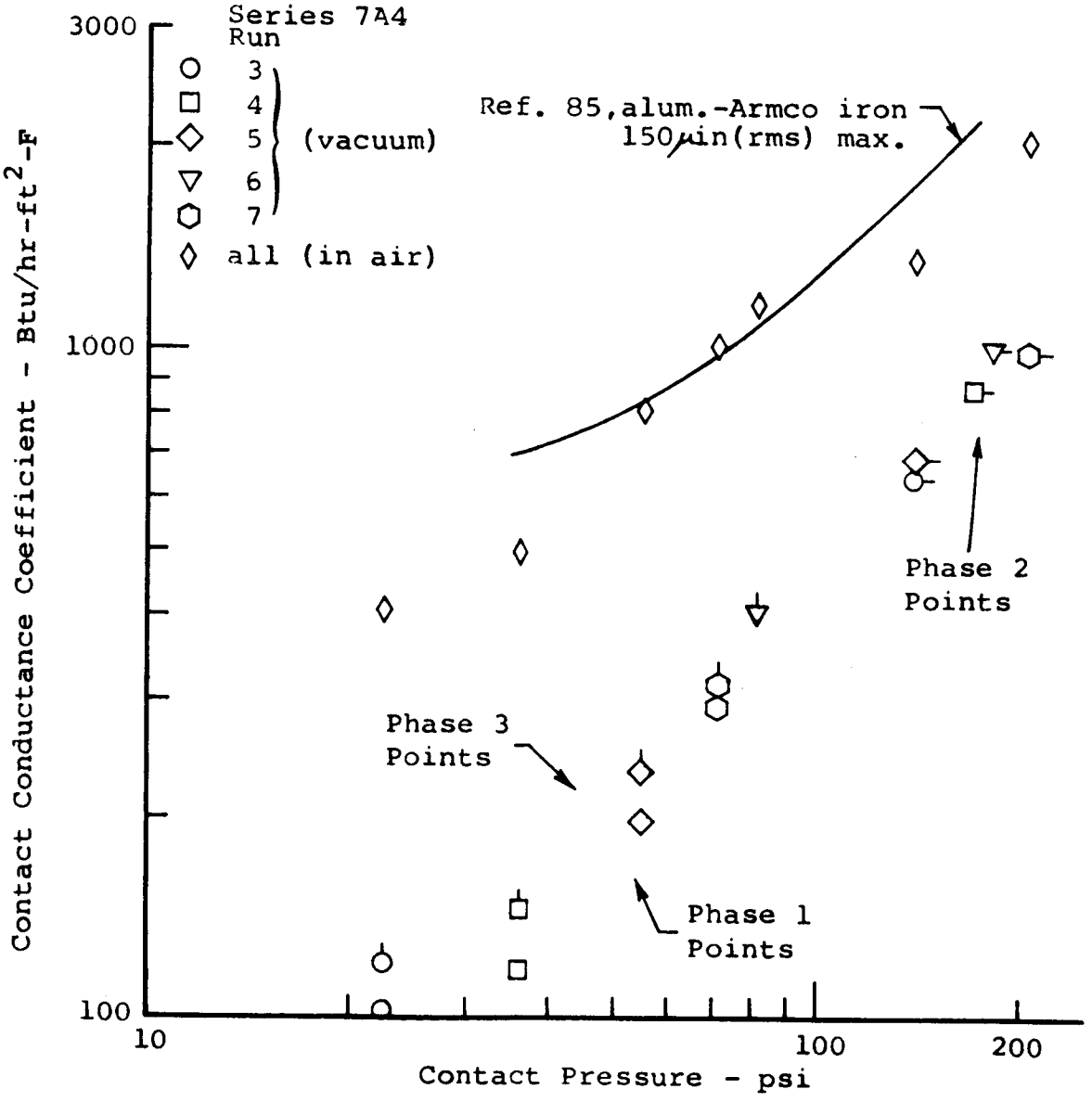

Fig. 26.--Comparison With Data of Reference 85

only offered as an indication of reasonableness.

As indicated in the above discussion, it is very difficult to make a better comparison of the test data because of the impossibility of matching even the most important parameters of materials, surface roughness and contact pressure range.

Before proceeding to the main point of interest in the present work, there is one other observation which bears mentioning. The data of series 304, shown in Figure 25, illustrate quite clearly the hysteresis effect mentioned earlier. Going from a given contact pressure to a higher contact pressure and then returning to the original value again is seen to result in a higher value of contact conductance at the same pressure. This result has been observed by others [85,92,233] but their tests were always run by continually increasing and then continually decreasing the contact pressure. The present results show that even when the initial contact pressure is well below the maximum value to which the surface has been subjected, the effect is still present.

The vacuum data of the 7A4 series are also shown in Figure 26. The effect of "breaking in" the surface is demonstrated in these data. These data are for a set of spec-

imens whose surfaces had been exercised in previous tests, whereas the data shown in Figure 25 were for the first tests made on those surfaces. Comparing Figures 25 and 26 shows that the hysteresis effect was considerably reduced by having the surfaces well broken in. This affords an example of another variable in contact conductance - surface loading history.

Comparison of Experimental Results with Theory

The primary purpose of the present study was to determine whether the one-dimensional theoretical solutions obtained in section IV could be used to predict, with sufficient accuracy, the transient behavior of a one-dimensional two layer solid with contact resistance in the interface. To this end, a series of tests were run in which the boundary conditions were made to closely approximate those of the theoretical solutions. The results of these experiments are compared to the corresponding theoretical cases below.

Phase 1 Results

As indicated in the discussion in section IV, the time to approach steady state is believed to be a parameter which is characteristic of transient behavior, as well a practical one. For this reason the time to approach steady state is

one of the parameters chosen as a basis for comparing the experimental results with theory, For use in those comparisons the time to approach steady state was defined to be the time at which the temperature drop across the slowest reacting portion of the system was within one "time constant" of its steady state value, i.e., to within e^{-1}, thus the fraction is $1-e^{-1} \approx .632$. It was necessary to go to a lower value than the 0.99 fraction used in the theoretical correlation to reduce the sensitivity to experimental error. The 99% criterion is more meaningful from a practical standpoint, but in this regime the rate of change of temperature drop with time is very low and small errors in temperature measurement would result in large time errors.

The results of the comparisons of the Phase 1 data are presented as plots of time to approach steady state versus interface contact conductance. The actual experimental values are tabulated in Appendix **B.** Those values shown in the plots reflect slight adjustments in the times made as follows. For each run of a given series, i.e., set of specimens, the contact conductances on the ends of the specimens (the outer boundaries) were different due to the different contact pressures on each run. It was desired to show the data in a form that could be compared to a single

theoretical curve for each series, rather than a point-for-point comparison which could not be meaningfully plotted. The test data were plotted on a "map" of theoretical data which consisted of a plot of time to approach steady versus interface contact conductance for various values of the end conductance. From this plot it was found that the experimental data exhibited about the same slopes as the theoretical for dependence on the end conductances. Thus the experimental times to reach steady state were adjusted by adding or subtracting a small amount. This amount is the difference in time found from the theoretical curves, at the experimental value of interface conductance, in going from the end conductance measured in each experiment to a value which was the approximate average for the complete series. In this way experimental values of steady-state time versus interface conductance for the same end conductance could be determined for each test series and compared with theory. It is emphasized that, as can be seen in Appendix A, the adjustments were usually small and should not affect the validity of the comparison. This is indicative of the fact that when the end conductances, h_1 and h_2 are large compared to the interface conductance, h_c, they do not exert as large an influence on the time. This was the case in all

the present data.

The resulting comparisons made in the above-described manner are shown in Figures 27 through 31 for the six sets of samples tested. In these figures the solid lines represent the theoretical predictions made using the theoretical solution corresponding to Case C of section IV. A constant thermal conductivity calculated from the experimental data [250] at the average specimen mid-point temperatures used in the theoretical solution. The experimental data points are plotted with symbols. It can be seen that the agreement between theory and experiment is better for some test series than for others. The worst comparison is for the 304 series, shown in Figure 27. The agreement for the 904 series is somewhat better, as seen in Figure 28. Figure 29 shows the comparison is still better for the 407 and 47A series, both on a straight difference and percentage difference basis. The best agreement was found for the 7A4 and 405 series, as shown in Figures 30 and 31. It is obvious that the agreement is better for the slower reacting systems. It is believed that this can be explained by the failure of an experimental boundary condition to match the theoretical boundary condition - specifically, the step rise in the source temperature. It was observed that during the experi-

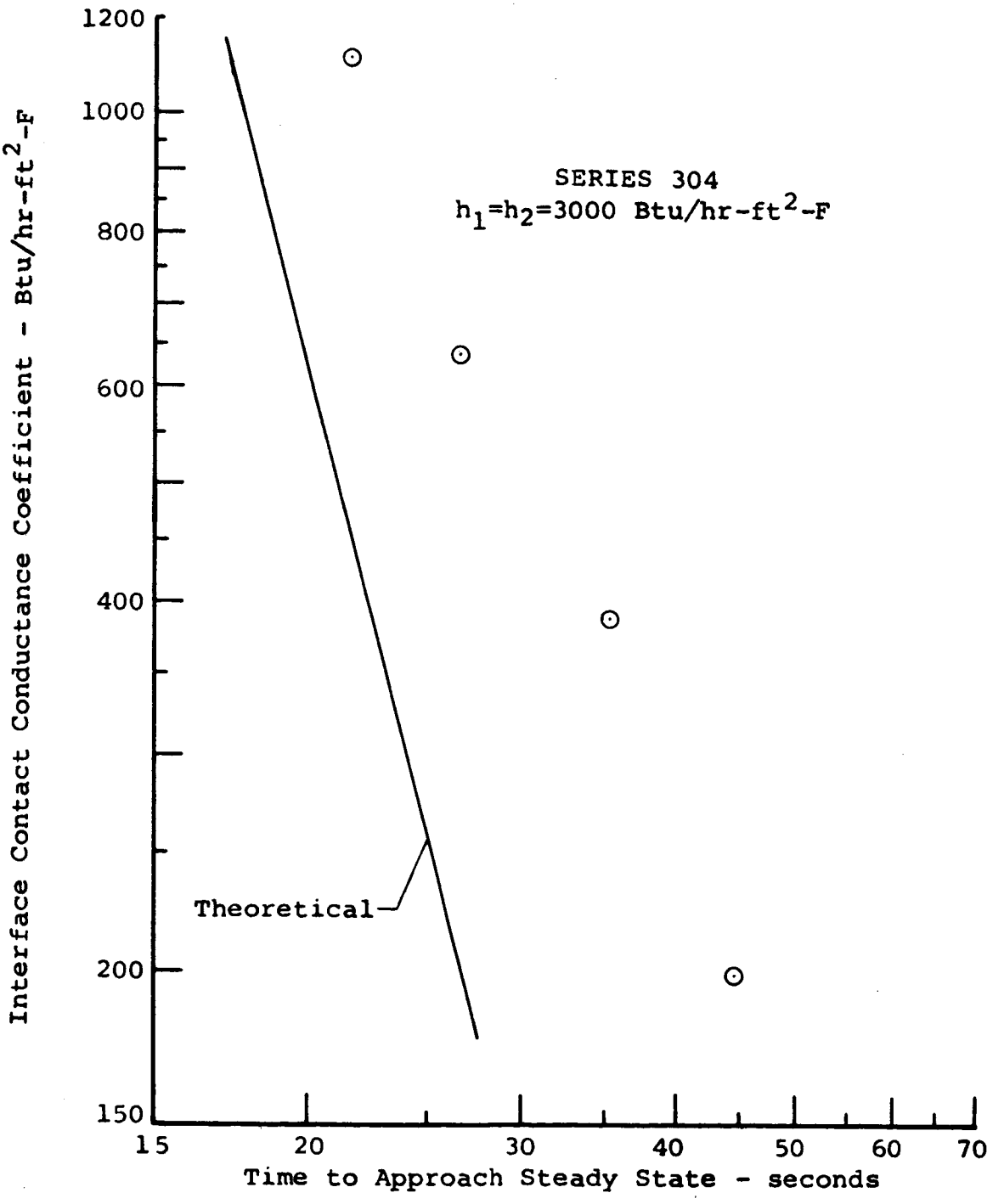

Fig. 27.--Time to Approach Steady State for Series 304-Phase 1

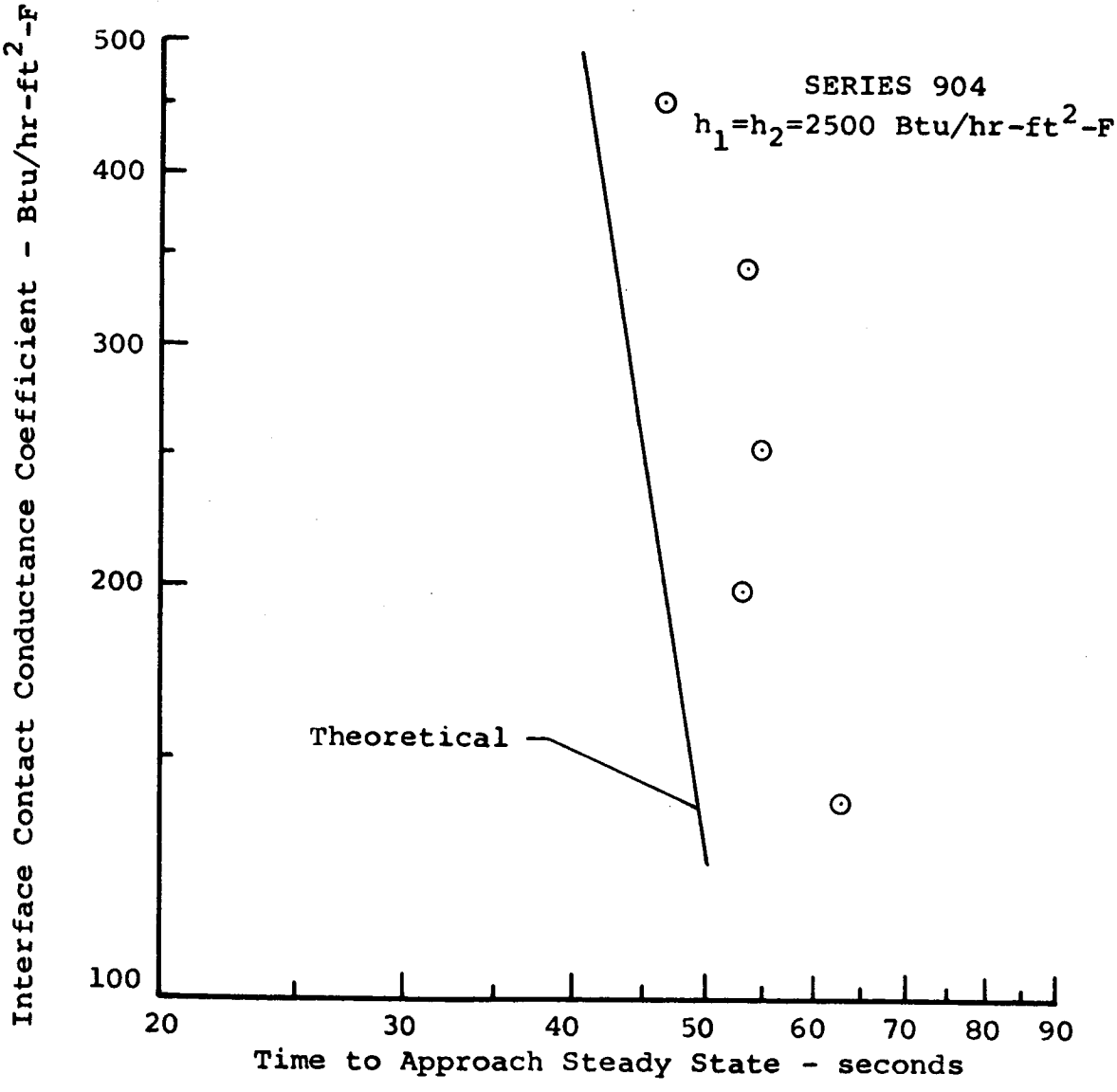

Fig. 28.--Time to Approach Steady State-Series 904 Phase 1

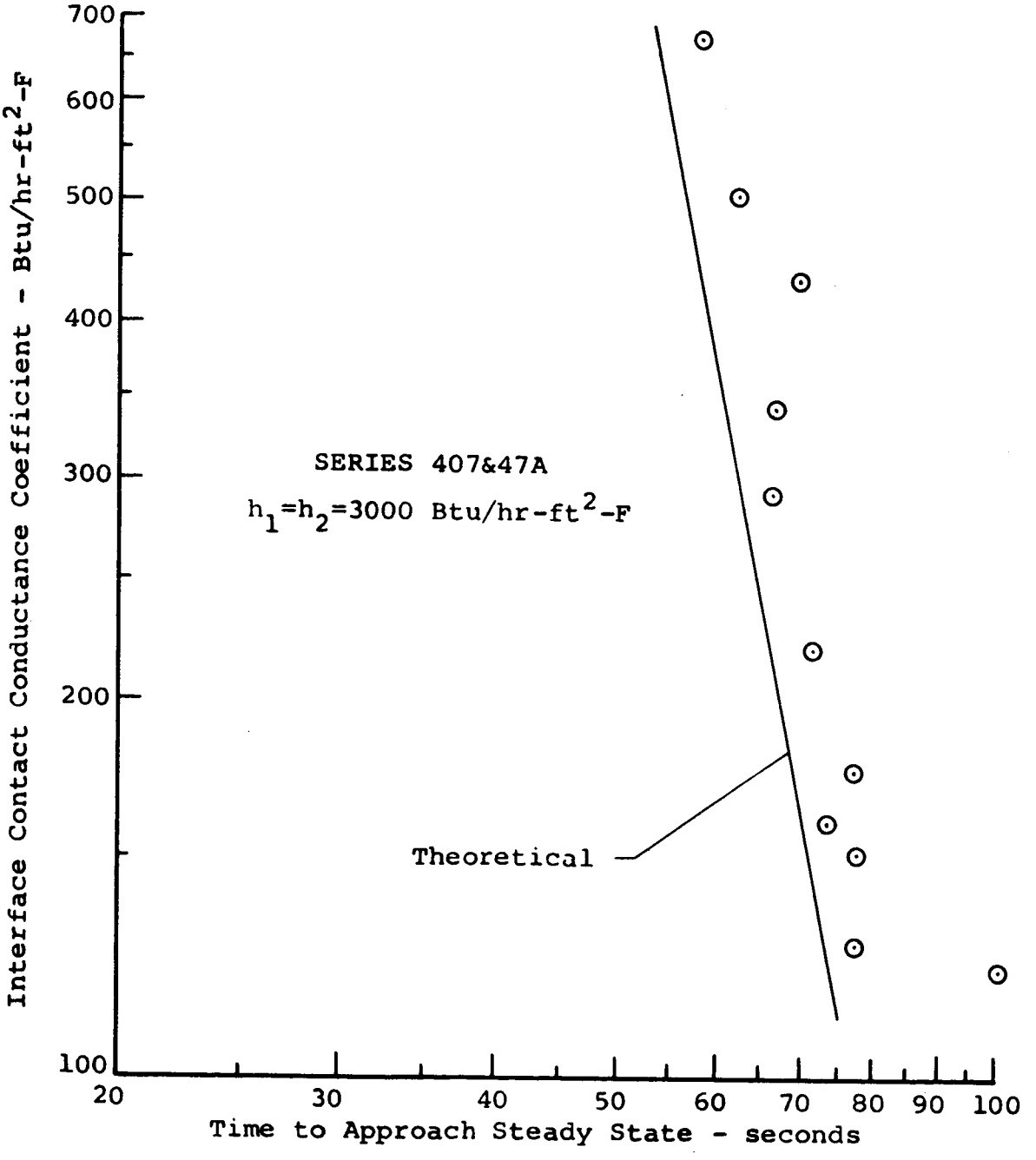

Fig. 29.--Time to Approach Steady State-Series 407 and 47A Phase 1.

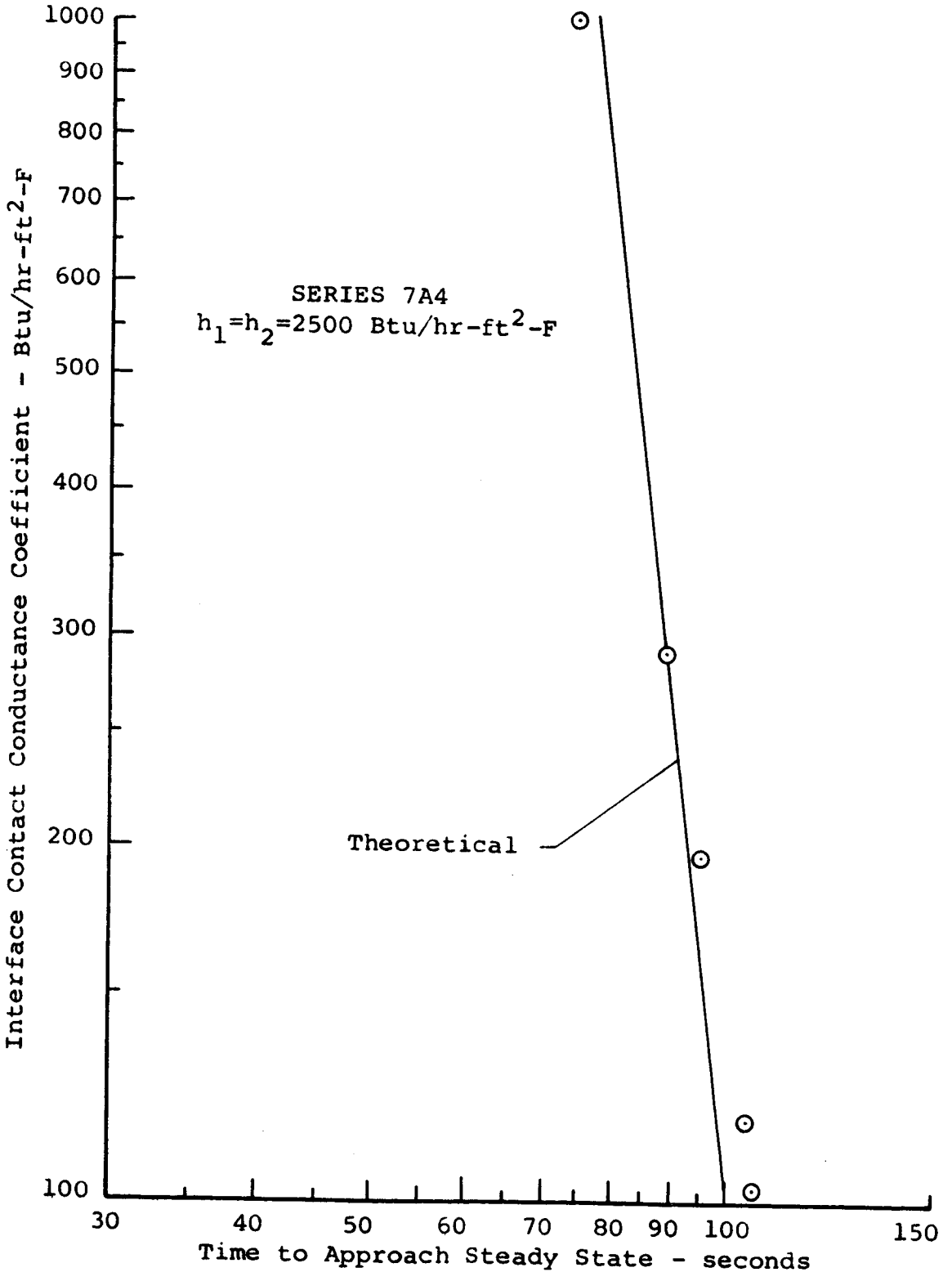

Fig. 30.--Time to Approach Steady State-Series 7A4 Phase 1

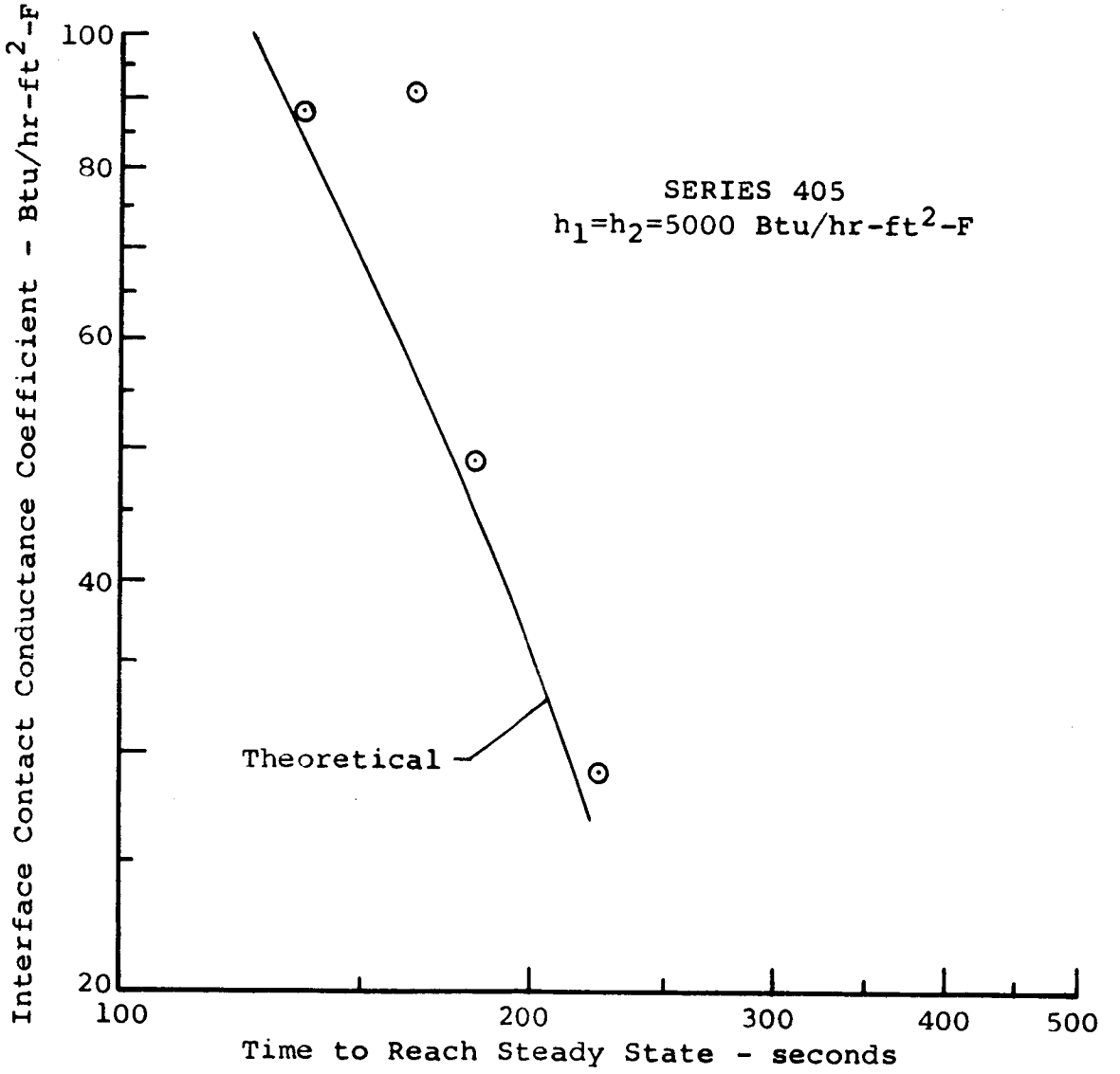

Fig. 31.--Time to Reach Steady State-Series 405 Phase 1

ments the temperature of the source block (copper block-steam system) would "dip" slightly when the upper specimen is brought into contact with it because of the finite capacity of the source block. The dip amounted to about 4 - 6°F at the maximum and required approximately 10 - 30 seconds to vanish completely, depending on the system. In other words the overall driving force (total ΔT) was low for the early part of each experiment. As can be seen in Figures 27 - 31, and as would be expected, the error thus produced is largest for the systems with the lowest total resistance, which would also have the lowest time to reach steady state. This point is illustrated by comparing the Figures 30 and 28, the former is for a 2-inch Armco Iron specimen above a 2-inch aluminum specimen (series 7A4), where as the latter is for two 2-inch aluminum samples (series 904). The Armco Iron sample being a poorer conductor than aluminum does not cause as much of a dip in the source temperature. The dip also does not last as long and this time represents a smaller portion of the time to reach steady state. Thus the error produced is much smaller. Similar arguments explain why the agreement was better for two 2-inch aluminum specimens, Figure 28, than for a 1-inch above 2-inch aluminum set, Figure 27; as well as why the Armco Iron-aluminum specimens, Figure

30, compared better than the reversed aluminum-Armco Iron specimens, Figure 29. For the 2-inch aluminum above 2-inch stainless steel series, Figure 31, the dip was about the same as for the 904 series, but the time represented a much smaller part of the steady state time, which resulted in better agreement. The result of this argument is that the agreement between theory and experiment is good for those experiments which more closely matched the theoretical boundary conditions.

It should be emphasized here that Figure 29 contains the results of two test series, 407 and 47A. These series used the same specimens except that the surface of the Armco Iron specimen was re-ground to produce a different surface roughness (see Appendix A). Also, as indicated in Figure 29, two of the runs for the 407 series were made in air. This provided two additional means of varying the interface contact conductance, h_c, and thus furnished a further check on the validity of h_c as a correlating parameter. No effect due to surface finish or the presence of air was noted.

For another comparison between theory and experiment the overshoot in the interface contact temperature drop was used. As explained in section IV, under the condition that

$$\tau = \frac{b}{a}\sqrt{\frac{\alpha_1}{\alpha_2}} > 1 \qquad \text{(VI-1)}$$

the temperature drop across the interface contact (ΔT_c) exceeds or overshoots its steady state value for a while during the transient period. The quantity used for comparison in this phenomenon is the time required for the transient ΔT_c to reach its maximum value. In the theoretical work it was found that this time depended on h_c. The experimental values of this parameter are shown in Appendix B. Small adjustments were also made to this parameter, in the manner discussed above, to provide a set of experimental data for a single value of the end conductance, h_1 and h_2, for each series. The results are plotted in Figures 32 through 34, in which the theoretical curves are drawn as solid lines and the experimental points are plotted as symbols. It can be seen that the agreement follows about the same pattern as in the time to approach steady state comparison. Note that the error is such (as in the previous case) that the experimental observations appear to be somewhat slower than the theoretical. That is, the experimental time of maximum overshoot occurs later than the theoretical time. This also seems to support the above argument in that a temporary dip in driv-

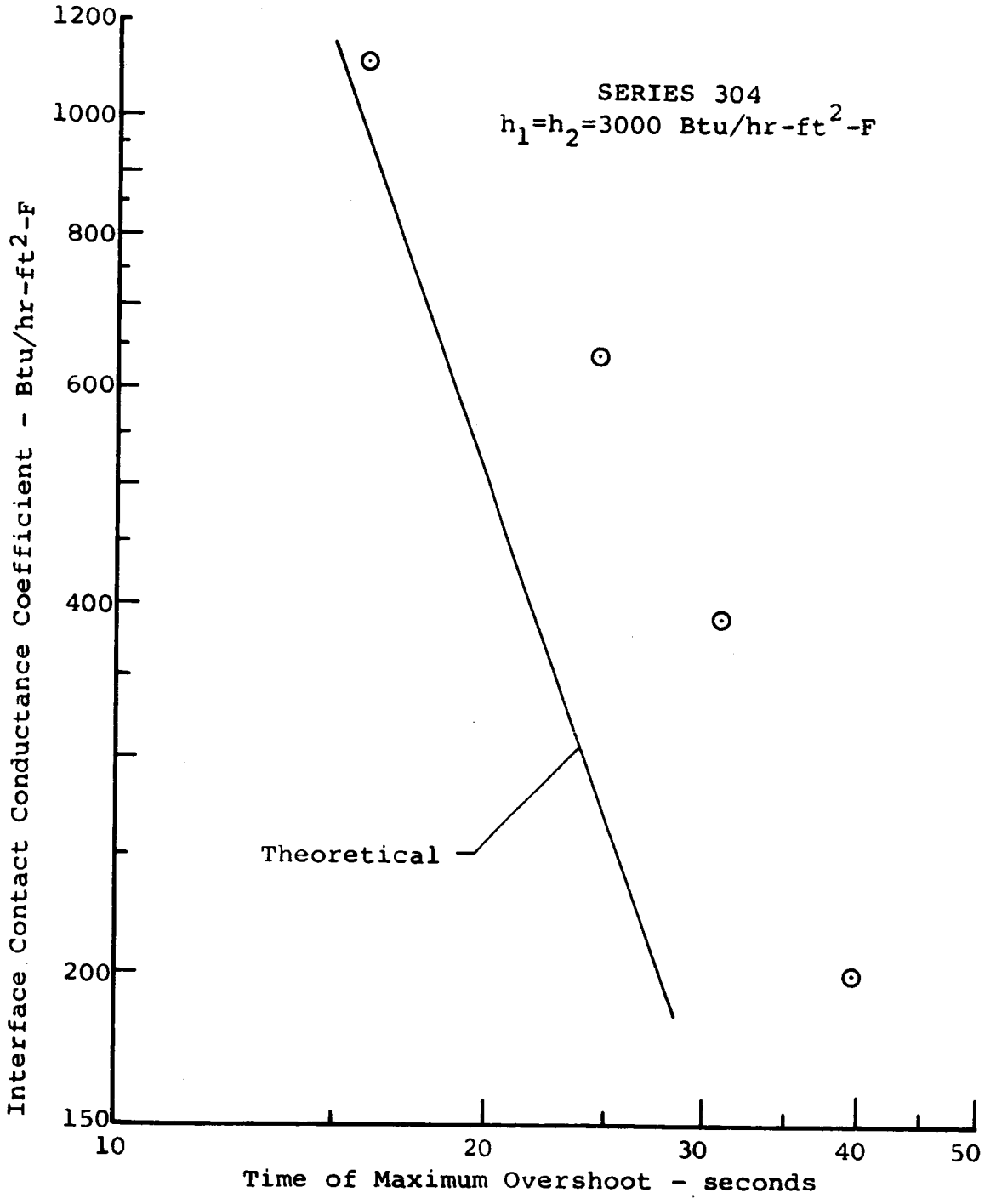

Fig. 32.--Time of Maximum Overshoot-Series 304 Phase 1

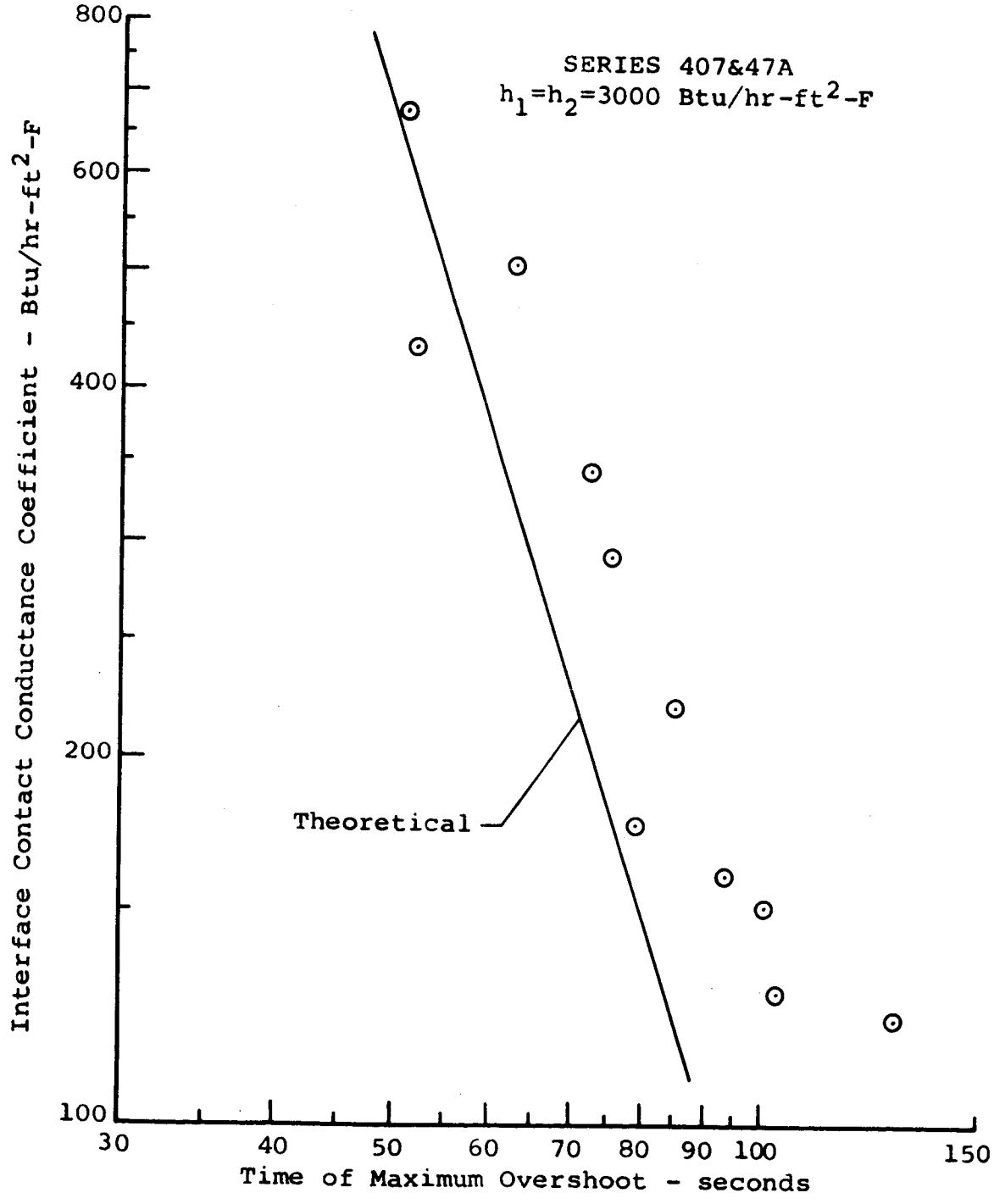

Fig. 33.--Time of Maximum Overshoot-Series 407&47A Phase 1

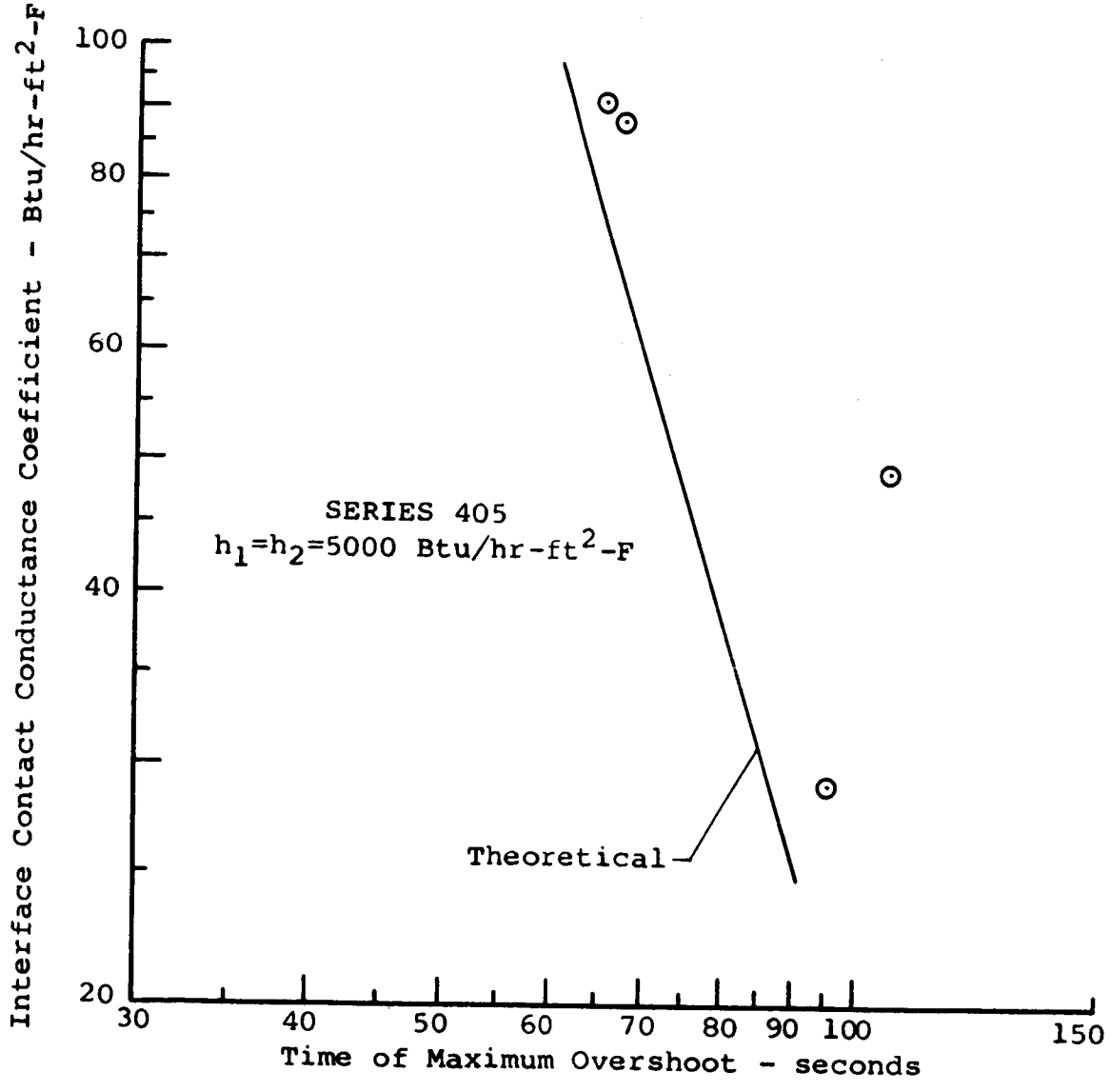

Fig. 34.--Time of Maximum Overshoot-Series 405 Phase 1

ing potential should have a delaying effect on the time to reach maximum overshoot. As in Figure 29, Figure 33 represents tests with two surface roughness combinations and tests in air and vacuum. Again no effects due to these quantities were noted.

As further evidence in the comparison it is pointed out that only four of the six series produced an overshoot in ΔT_c. For the two series in which $\tau < 1$ (904 and 7A4) no overshoot was found to occur, which agrees with the theoretical work.

The phase 1 results may be summarized as follows. The poorer comparison of the 304 and 904 series is attributed to the source temperature discrepancy explained above. For the 407-47A (same samples), 7A4 and 405 series the agreement between experiment and theory is considered to be very good, especially in view of the experimental complexity.

Results of Test Phases 2,3,4,5, and 6

After each phase 1 experiment had reached its steady state a sequence of other tests were made with the samples still in place. The details of the test procedures used were discussed in section V. Each of these tests corresponds to the theoretical Case D of section IV. That is, the system

has a steady state heat flow established, and at time zero the interface conductance, h_c, and the end conductances, h_1 and h_2, are suddenly changed to new, constant values. Each succeeding test was started after the preceding phase had reached its steady state. For phase 2 the change was produced by suddenly increasing the contact pressure and holding it constant. Phase 3 consisted of suddenly decreasing the contact pressure back to the original value (the value at the end of phase 1). The change was produced in phase 4 by suddenly letting air into the vacuum chamber. Phases 5 and 6 were the same as phased 2 and 3 except that the contact pressure changes were made with the specimens in air instead of a vacuum. This sequence of tests provided experimental data for comparison in which the changes in conductance were both increasing and decreasing, and which were produced by two separate means.

For this second type of test the parameter used for comparison of the experimental data and the theoretical solutions was the time to approach steady state; again, because it is an obvious and practical characteristic of transient behavior. However, in these cases the dependence of the time to approach steady state on the contact conductances at the three broudaries is much more complicated than

for the phase 1 case. The theoretical solution in section IV (Case D) shows that transient portion — and thus the time to approach steady state — depends not only on the final values of h_c', h_1' and h_2' (values after change) but also on the old values h_c, h_1 and h_2. It is apparent that such a dependence prohibits the results from being displayed in as simple a manner as was possible for the phase 1 data. Hence, it was decided, due to the complexity of the situation, that the only practical comparison that could be made was a point-for-point comparison. That is, to compare the experimental value of the time to approach steady state with the value predicted by the theoretical solution for the exact conditions of each individual run. The theoretical value for each run was found by putting the experimental values of the steady state contact conductances, h_c, h_c', h_1, h_1', h_2 and h_2', for that run into the computer programmed solution and calculating the theoretical time to approach steady state.

When the above scheme was first employed the same criterion for the time to approach steady state as was used in the phase 1 was used, namely, $1-\frac{1}{e}$, or 0.632. It was found that the resulting comparisons were very poor. The reason for this can be explained as follows. First, the

time to approach steady state for these cases is much smaller than for the phase 1 type transients, as can be seen in the tabulated data. For, example, the theoretical times to approach steady state for the 904 series (two 2-inch aluminum specimens) were all below 1.5 seconds using the 0.632 criterion. Secondly, a problem arises in curve fitting the early time temperature profiles as it did in the phase 1 case. The problem is that when the contact conductances are changed suddenly the temperature distribution is the vicinity of the contacts responds very quickly, thereby producing a sharp change in temperature profile near the boundaries. Thus the curve fit, which cannot match this change, produces erroneous boundary temperatures when extrapolated. This means that if the time to approach steady state occurs quickly enough it is bound to be erroneously determined. To circumvent this problem it was decided to go to a fraction larger than 0.632 for the criterion. This allows the temperature profiles time to smooth out so that the extrapolation of the curve fits to the boundaries more accurately represents the true boundary temperatures. A fraction of 0.800 was arbitrarily chosen. It was felt that anything larger than this might cause accuracy problems due to the small temperature-time slopes which occur as steady state is

approached. Since there is nothing to suggest that there is anything "holy" about any particular number this change of criterion should not have any effect on the outcome to the results.

Therefore, the experimental and theoretical times to approach steady state were all recalculated on the basis of the 0.800 criterion for all the test runs. The complete test results are presented in Appendix B. Since a point-for-point comparison was made the results pertinent to the comparison for these data are presented in Tables 4 through 6. In these tables the test runs and phases are identified and the values of the initial and final conductances are given. The experimental and theoretical times to approach steady state and the difference between them are also given in the tables. The difference shown in each entry is the experimental value minus the theoretical value. As can be seen the comparisons show both plus and minus differences. This indicates that the differences are of a scatter nature, in contrast to the phase 1 results, which tended to be off in one direction. This observation adds further evidence in support of the argument given in the discussion of phase 1 results regarding the source temperature dip; because, in these phase 2, etc., experiments the temperature of the

TABLE 4.
Comparison for Series 304 & 7A4

		Contact Conductances (Btu/hr-ft^2-^{o}F)						Steady St. Time		Diff.
		Interface		Hot End		Cold End		Exp.	The.	
Run	Ph.	In'l	Fin.	In'l	Fin.	In'l	Fin.	Sec.	Sec.	Sec.
304-5	2	638	2319	3523	4900	3402	4500	5.7	5.44	+0.3
	3	2319	1238	4900	4169	4500	4195	8.7	9.40	-0.7
	4	1238	1975	4169	4366	4195	4305	7.2	7.08	+0.1
304-6	2	199	1707	1200	4444	1838	4366	9.5	8.08	+1.4
	3	1707	446	4444	1993	4366	2923	10.7	13.74	-3.0
	4	446	1092	1993	2345	2923	3738	11.1	6.42	-4.7
	5	1092	2441	2345	4220	3738	4606	9.2	10.60	-1.4
304-7	2	389	1893	1972	4932	3225	4747	7.7	9.30	-1.6
	3	1893	907	4932	2818	4747	3825	11.0	11.74	-0.7
	4	907	1549	2818	3510	3825	4077	9.7	10.38	-0.7
	5	1549	2637	3510	4745	4077	4917	8.7	7.08	+0.9
304-8	2	1111	2987	4571	5925	4904	5679	7.2	6.76	+0.4
	3	2987	1657	5925	4697	5679	5400	9.2	10.50	-1.3
	4	1657	2505	4697	5063	5400	5431	6.1	9.24	-3.1
	5	2505	3553	5063	5776	5431	6007	4.4	5.64	-1.2
7A4-3	2	102	640	952	4870	1063	3408	27.1	21.08	+6.0
	3	640	121	4870	2123	3408	818	53.0	60.68	-7.7
	4	121	408	2123	2399	818	1077	32.9	37.09	-4.2
	5	408	1351	2399	4022	1077	3716	37.6	37.37	+0.4
7A4-4	2	117	868	1184	3357	1127	4129	28.1	24.77	+3.3
	3	868	146	3357	1771	4129	993	53.2	56.98	-3.8
	4	146	498	1771	1741	993	1297	35.8	37.91	-2.1
	5	498	2032	1747	3763	1297	4505	24.2	23.20	+1.0
7A4-5	2	196	686	1457	2417	2998	5101	25.1	22.32	+2.8
	3	686	234	2417	1752	5101	3481	38.8	43.14	-4.3
	4	234	808	1752	1725	3481	4055	31.0	33.01	-2.0
7A4-6	3	1000	402	3105	2195	5221	5711	25.2	22.10	+3.1
	4	402	1166	2195	2130	5711	5630	27.1	29.25	-2.2
7A4-7	2	292	990	1711	3425	5016	6446	9.5	10.78	-1.3
	3	990	316	3425	1838	6446	5800	26.1	21.68	+4.7
	4	316	1010	1838	2120	5800	6427	26.1	21.90	+4.2

TABLE 5.
Comparison for Series 407 & 47A

		Contact Conductances (Btu/hr-ft^2-^{o}F)						Steady St. Time		Diff.
		Interface		Hot End		Cold End		Exp.	The.	
Run	Ph.	In'l	Fin.	In'l	Fin.	In'l	Fin.	Sec.	Sec.	Sec.
407-1	2	128	328	1672	2643	2260	3420	40.7	43.14	-2.4
	3	328	138	2643	2459	3420	2507	46.5	56.90	-10.4
	4	138	519	2459	2248	2507	3135	27.2	31.63	-4.4
	5	519	1003	2248	2482	3135	3522	22.3	22.18	+0.1
407-2	2	151	304	1761	2845	3372	4490	46.5	48.22	-1.7
	3	304	169	2845	2983	4490	3220	42.6	48.78	-6.2
	4	169	489	2983	2449	3220	4272	30.0	31.29	-1.3
	5	489	853	2449	2618	4272	4441	29.1	31.01	-1.9
407-3	2	176	334	2207	2707	5306	4887	52.3	50.50	+1.8
	3	334	190	2707	2553	4887	4628	54.3	55.04	-0.7
	4	190	579	2553	2176	4628	4498	34.8	32.51	+2.3
	5	579	916	2176	2399	4498	4515	20.0	36.03	-16.0
407-4	2	293	493	2551	2956	4262	5665	29.7	33.75	-4.1
	3	493	290	2956	2887	5665	6534	40.1	51.18	-11.1
	4	290	1004	2887	2667	6534	6222	28.1	26.11	+2.0
407-5	2	122	380	1093	2875	6202	5921	46.7	50.92	-4.2
	3	380	133	2875	2592	5921	6670	48.9	64.67	-15.8
	4	133	511	2592	2340	6670	4515	32.0	39.67	-7.7
	5	511	1316	2340	2641	4515	5963	17.6	17.54	+0.1
407-6	2	675	1221	2120	2573	3126	5664	13.6	7.34	+6.3
407-7	2	433	1514	874	2601	4948	6746	41.6	47.20	-5.6
47A-1	2	160	354	1441	2278	1385	1988	33.0	36.07	-3.1
	3	354	111	2278	1959	1988	1992	60.0	72.61	-12.6
	4	111	506	1959	2079	1992	2019	32.1	35.89	-3.8
	5	506	1022	2079	2398	2019	2302	19.4	17.40	+2.0
47A-2	2	220	530	1839	2342	2384	3490	31.9	30.13	+1.8
	3	530	205	2342	2316	3490	3518	39.0	55.84	-16.8
	2A	205	1034	2316	3087	3518	5897	27.1	23.78	+3.7
	3A	1034	213	3087	2645	5897	4595	48.3	51.82	-3.5
	4	213	721	2645	2439	4595	4995	28.1	28.67	-0.6
	5	721	1843	2439	2912	4995	7472	14.5	13.80	+0.7
	6	1843	712	2912	2498	7472	6376	29.1	31.09	-2.0
47A-3	2	343	733	*	2382	5698	7249	39.7	-	-
	3	733	353	2382	2041	7249	8339	43.6	47.86	-4.3
	4	353	1094	2041	1783	8339	6614	18.4	18.36	+0.0
47A-4	2	506	1029	2364	2782	6388	8506	24.2	26.31	-1.9
	3	1029	582	2782	2586	8506	9153	38.8	38.83	+0.0
	4	582	1518	2586	2578	9153	8381	22.3	23.72	-1.4

* = No value.

TABLE 6.
Comparison for Series 405 & 904

		Contact Conductances (Btu/hr-ft^2-^{o}F)						Steady St. Time		Diff.
		Interface		Hot End		Cold End		Exp.	The.	
Run	Ph.	In'l	Fin.	In'l	Fin.	In'l	Fin.	Sec.	Sec.	Sec.
405-1	2	91	243	*	*	3482	4337			
	3	243	84	*	*	4337	3778			
	4	84	801	*	6744	3778	5616			
405-2	2	29	127	848	4766	853	1623	169.4	172.41	-3.0
	3	127	31	4766	1481	1623	796	243.0	317.55	-74.6
	4	31	343	1481	1079	796	1663	93.1	100.19	-7.1
405-3	2	49	168	*	*	6282	6290			
	3	168	49	*	*	6290	8437			
	4	49	711	*	7320	8437	5667			
	5	711	1036	7320	10001	5667	5631	116.1	121.96	-5.9
405-4	2	88	202	1705	2431	9604	7395	174.3	151.31	+23.0
	3	202	89	2431	2026	7395	15008	208.0	218.57	-10.6
	4	89	1015	2026	1885	15008	6537	71.6	70.63	+1.0
405-5	2	92	237	*	*	8304	6176			
	3	237	93	*	*	6176	9252			
	4	93	945	*	7192	9252	8190			
904-1	2	144	756	1014	3658	1407	2688	4.8	4.70	+0.1
	3	756	141	3658	1458	2688	933	9.7	6.92	+2.8
	4	141	291	1458	1762	933	2184	6.1	3.04	+3.1
	5	291	1274	1762	3685	2184	2778	3.0	2.74	+0.3
904-2	2	252	1064	1419	2943	2390	3487	3.9	3.34	+0.6
	3	1064	311	2943	2230	3487	2668	6.7	8.58	-1.9
	4	311	665	2230	2056	2668	2913	4.0	3.32	+0.7
	5	665	1846	2056	3197	2913	3883	2.9	1.82	+1.1
904-3	2	341	872	1682	2434	3618	4240	3.8	4.40	-0.6
	3	872	372	2434	1937	4240	3183	3.5	6.82	-3.3
	4	372	812	1937	1895	3183	3461	3.9	2.76	+1.1
	5	812	1844	1895	2558	3461	4105	3.5	2.08	+1.4
904-4	2	199	987	2128	2763	3361	4759	2.7	2.82	-0.1
	3	987	274	2763	2401	4759	3087	7.3	8.22	-0.9
904-5	3	461	283	2551	2308	4316	3771	7.8	9.88	-2.1
	4	283	663	2308	2380	3771	3599	5.3	4.84	+0.5

* = No value.

source was much more stable since it did not have to undergo such large changes in heat flux. On a percentage basis the longer times were found to compare better. It is pointed out that even with the 0.800 criterion some of the times are still very small. It is also noted that the differences for these smaller times (904 series) are mostly positive. Since the above-mentioned early time accuracy problems would tend to cause errors in this direction the effect may still have been present. In Table 6 it can be seen that the comparisons are made for only seven of the 405 series experiments. For the other tests shown there the end conductances could not be calculated accurately because the temperature drops were too small. This is unfortunate, but nothing can be done about it. The limitations of the experimental accuracy (discussed in Section V) prevent any reasonable estimate from being made. As an example, for a calculated ΔT of $2^{o}F$, a possible error of $\pm 1^{o}F$ makes it impossible to evaluate the contact conductance within 100%. For those runs in which this occurred no attempt was made to guess at the conductance values. Although an estimate was made for the hot end conductance on two of the phase 1 runs of the 405 series it could be seen from the theoretical work that the effect was small. However, in the present cases the

theoretical solution shows that the time to approach steady state depends on the difference between the initial and final values at each contact. The possible consequences of estimating both or even one conductance value are obvious. Thus only those runs for which calculated values were available were used in the comparison.

It is difficult to evaluate the comparisons in the tabular form. For this reason the data were plotted in the form shown in Figure 35. This figure is a plot of the experimental values of the time to approach steady state versus the corresponding theoretical values. Each series is represented by a different plotting symbol as shown on the plot. For a perfect correlation each point would lie on a 45^{o} line passing through the points (1,1), (10,10), etc. As a means of evaluating the results two bands are drawn on the plot representing an agreement of $\pm$ 10% and $\pm$ 20% based on the theoretical. There are a total of 92 points plotted in Figure 35. Of these only 18 lie outside the 20% band, and 8 of that 18 are on the 904 series, for which there is some doubt about the accuracy. Of the 92 total points, 48 of them lie within the 10% band. Although this comparison is indirect to the intended purposes, i.e., it could not be made in the form of a plot as a function of interface con-

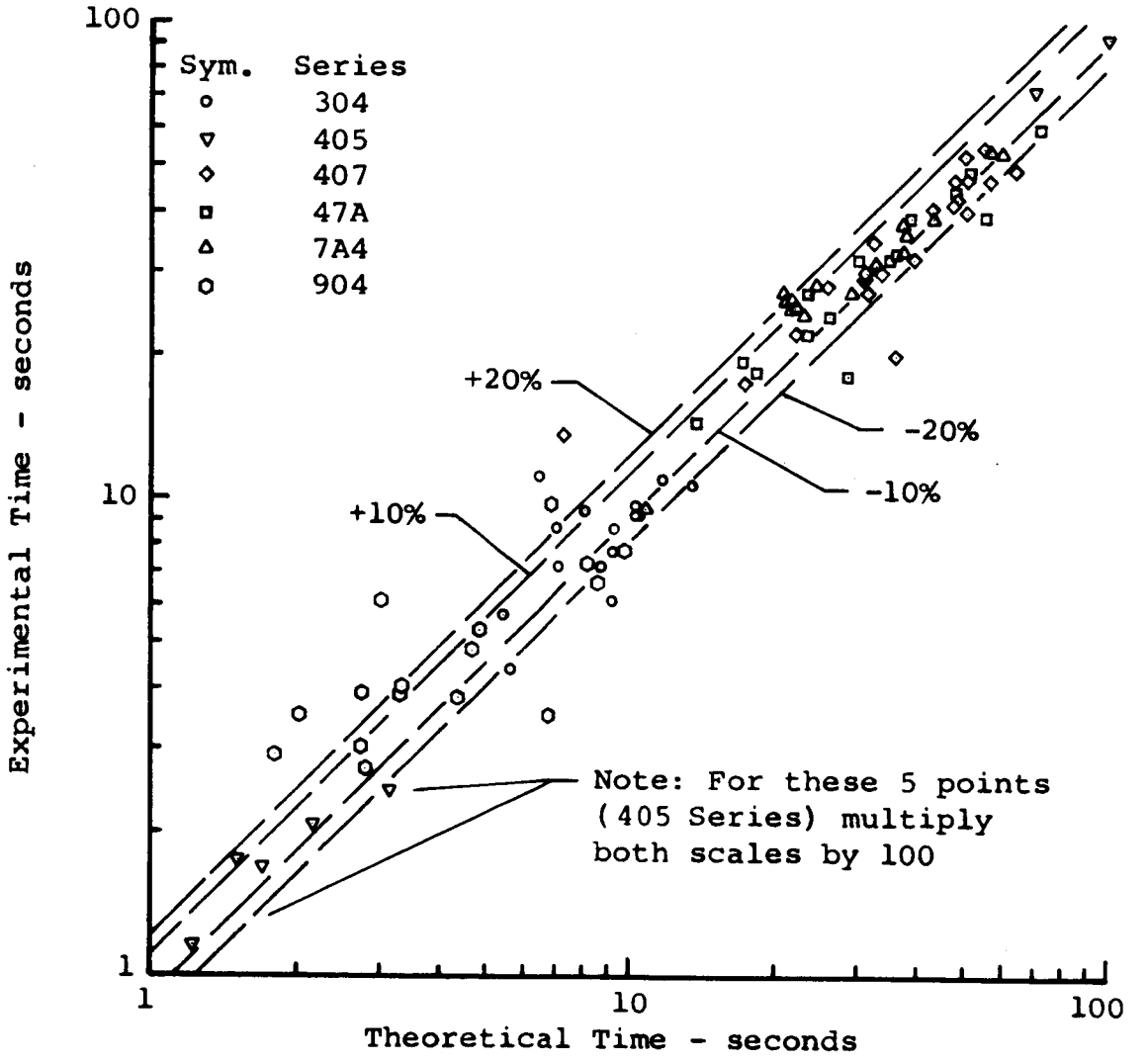

Fig. 35.--Time to Reach Steady State for All Series-Phases 2,3,4,5 and 6.

tact conductance, it is still believed to be a representative one.

In view of the above comparison it is the opinion of the writer that the correlation between the experimental behavior and the simple, constant property theoretical predictions for this second type of transient is very good. It is believed that these data are the first data on the transient thermal response of composite metals to be reported.

VII. SUMMARY, CONCLUSIONS AND RECOMMENDATIONS

Solutions have been derived for a class of boundary value problems for the time-dependent temperature distribution in a two layer, composite slab with contact resistance at the interface and contact or convective resistance on the outer boundaries. These solutions represent an original contribution to the field of conduction heat transfer.

The results of a limited parametric computer study using these solutions has been presented. This study includes a set of dimensionless correlations of an arbitrarily defined time to approach steady state and a discussion of some transient thermal characteristics which were observed for these types of systems.

To evaluate the usefulness of the above solutions for predicting transient response of real systems an experimental program was carried out. The experimental work consisted of measuring the transient temperature distributions in a series of test samples when subjected to thermal transients which approximated the boundary conditions used in the theoretical solutions. Test samples of aluminum, Armco-Iron,

and stainless steel were used to provide a large range of thermal properties. The test data provided by this experimental program were compared to the theoretical predictions. These data also represent an original contribution to conduction heat transfer.

For the case of a uniform initial temperature distribution and a sudden increase in one boundary medium temperature, the results were compared on the basis of time to approach steady state and the time of occurrence of maximum overshoot as functions of interface contact conductance. In general the agreement was found to be good. For those cases in which a noted discrepancey in the experimental boundary condition was believed to have only a small effect the agreement was very good — at least within 10%.

The results of a second set of experiments for the case of an initial steady state heat flow condition followed by a sudden change in contact conductance were also compared to the corresponding theoretical case. These results could only be compared on a basis of time to reach steady state for each individual test made because of the large number of variables involved. These comparisons showed that less than 20% of the experimental data differed from the theoretical by more than 20%, and that over 50% of the data was within

10% of the theoretical.

On the basis of the above comparisons it is concluded that the theoretical solutions presented could be used to predict the transient response of systems to which they are applicable to an accuracy sufficient for most engineering purposes. That is, with these solutions properly programmed on a digital computer, a knowledge of the required thermal properties and an estimate of the contact conductance from the existing literature, a design engineer could predict the transient response of a given system. Thus used an accuracy at least as good as his knowledge of the contact conductance could be expected.

Recommendations For Future Work

It is recommended that further experimental work be performed to provide additional verification of the above conclusions. It is believed that emphasis should be placed on the phase 2, 3, etc. experiments since these type of changes are representative of what happens when a space vehicle enters a planetary atmosphere. The following recommendations regarding future experimental work all involve improvement in procedures and technique to achieve better accuracy.

1. Steps should be taken to improve the stability of the source block temperature. While a larger source block with a larger condensing cavity should provide some reduction of this problem, consideration should be given to a fast response, thermostatically controlled electrical heat source.
2. For greater accuracy in the temperature profiles a larger number of thermocouples should be used, and the thermocouples near the boundaries should be placed as close to the boundary planes as possible. In order to achieve the latter it will be necessary to find a better method of contact surface preparation. The distortions of temperature profiles near the contact boundaries noted in the present study and by others [58,92] are the result of flatness deviations of the contact surfaces. Great care should be exercised in the surface preparation to achieve a high degree of flatness. Since rougher surfaces would also help this problem it is recommended that the surfaces be ground to optical flatness and then blasted to obtain non-oriented roughness as discussed by Henry [114].

3. It is also recommended that the thermocouple calibration procedure be changed to reduce the amount of time required for calibration. With the test specimens in place in the test fixture, the temperature distributions could be varied over the range of interest by varying the contact pressure and/or the source temperature. By use of a multi-connected switch all thermocouples could be calibrated with a single potentiometer in a manner similar to the method described in section V. This method would achieve the same accuracy for temperature measurements, but it has the advantages of being simpler and faster, and would concentrate the calibration points of each thermocouple into the range over which it would be used during the experiments.
4. Experimental work on thinner specimens would be desirable, and consideration should be given to this possibility.

Since the results of the present study are encouraging it would seem desirable to expend further effort in the theoretical work. It is recommended that this work be directed toward attempting to establish general correlations of the

temperature time distributions in a form similar to the well-known work of Schneider [251].

APPENDIX A
TEST SPECIMEN DATA

Sample No.	Material	Total Length	Thermocouple Spacing (see Fig. 18.) x_1	x_2	x_3	x_4	x_5	x_6	Avg. Surf. Roughness
3	2024-T351	0.994	0.099	0.200	0.201	0.199	0.200	0.095	70 μin (rms)
4	2024-T351	1.995	0.202	0.398	0.401	0.398	0.398	0.198	75 "
5	303-MA	1.990	0.198	0.398	0.402	0.398	0.398	0.196	3 "
7	Armco iron	2.017	0.217	0.400	0.400	0.400	0.400	0.200	3 "
7A	Armco iron	"	"	"	"	"	"	"	30 "
9	2024-T351	2.000	0.210	0.400	0.395	0.400	0.401	0.194	20 "

MATERIAL PROPERTIES

Material	Thermal Conductivity (Btu/hr-ft-°F), (t in °F)	Therm. Diff. (ft^2/hr)	Dia. Pyr. Hardness 0.5 kg	.75 kg	1.0 kg
2024-T351 alum.	62.49+0.0607t, 125<t<300	2.00	148.0	164.5	144.4
Armco iron	44.52-0.0243t, 100<t<300	0.60	208.5	200.4	181.0
303-MA st. stl.	7.997+0.0064t, 150<t<450	0.11	330.8	320.4	328.5

APPENDIX B-1
PHASE 1 RESULTS

Run No.	p_c	h_c	h_1	h_2	θ_{ss}	θ_{mo}	θ'_{ss}	θ'_{mo}	$h_{ad.}$
304-5	35	638	3523	3402	26.1	23.3	26.6	24.7	3000
6	11	199	1200	1838	49.4	49.4	44.5	39.7	3000
7	21	389	1972	3225	36.4	33.9	35.3	31.0	3000
8	50	1111	4571	4904	20.8	13.6	21.7	16.0	3000
405-1	32	91	*	3482	167.5	70.7	164.5	65.8	5000
2	13	29	848	853	245.0	155.0	224.0	95.8	5000
3	20	49	*	6282	181.0	101.7	182.0	105.5	5000
4	48	88	1705	9604	148.1	72.6	136.5	67.8	5000
407-1	32	128	1672	2260	82.8	114.3	77.4	103.5	3000
2	47	151	1761	3372	79.9	106.5	77.7	101.5	3000
3	64	176	2207	5036	75.0	77.5	77.1	79.3	3000
4	78	293	2551	4262	64.9	73.6	66.3	75.5	3000
5	22	122	1093	6202	99.7	135.5	101.0	129.0	3000
6	29	675	2120	3126	59.1	53.2	58.1	51.1	3000
7	5	433	874	4948	74.7	67.8	69.5	52.3	3000
47A-1	14	160	1441	1385	83.2	111.3	73.6	93.8	3000
2	30	220	1839	2384	74.5	92.9	71.4	85.1	3000
3	53	343	*	5698	66.8	67.8	66.8	72.5	3000
4	76	506	2364	6388	59.1	60.0	62.1	62.9	3000
7A4-3	22	102	952	1063	126.7	None	105.5	None	2500
4	36	117	1184	1127	122.0	"	104.5	"	2500
5	55	196	1457	2998	98.7	"	95.3	"	2500
6	193	1000	3105	5221	70.2	"	74.5	"	2500
7	71	292	1711	3425	89.0	"	89.1	"	2500
904-1	19	144	1014	1407	72.1	None	62.8	None	2500
2	31	252	1419	2390	58.1	"	54.8	"	2500
3	46	341	1682	3618	54.2	"	53.4	"	2500
4	63	199	2128	2761	52.3	"	53.2	"	2500
5	111	461	2551	4316	43.6	"	46.5	"	2500

p_c=contact pressure
h_c=interface conductance
h_1= hot end "
h_2= cold end "

θ_{ss}=time to reach steady state
θ_{mo}=time of maximum overshoot
Primes indicate adjusted times for $h_1=h_2=h_{ad.}$ *=No value.

APPENDIX B-2
PHASES 2,3, 4 AND 5 RESULTS

		CONTACT CONDUCTANCES (Btu/hr-ft^2-^{o}F)						Contact Pressure		θ_{ss}
		Interface		Hot End		Cold End		In'l	Fin.	
Run	Ph.	In'l	Fin.	In'l	Fin.	In'l	Fin.	psi.	psi.	sec.
304-5	2	638	2319	3523	4900	3402	4500	35	171	5.7
	3	2319	1238	4900	4169	4500	4195	171	35	8.7
	4	1238	1975	4169	4366	4195	4305	35	35	7.2
304-6	2	199	1707	1200	4444	1838	4366	11	105	9.5
	3	1707	446	4444	1993	4366	2923	105	11	10.7
	4	446	1092	1993	2345	2923	3738	11	11	11.1
	5	1092	2441	2345	4220	3738	4606	11	104	9.2
304-7	2	389	1893	1972	4932	3225	4747	21	132	7.7
	3	1893	907	4932	2818	4747	3825	132	21	11.0
	4	907	1549	2818	3510	3825	4077	21	21	9.7
	5	1549	2637	3510	4745	4077	4917	21	132	8.7
304-8	2	1111	2987	4571	5925	4904	5679	50	214	7.2
	3	2987	1657	5925	4697	5679	5400	214	50	9.2
	4	1657	2505	4697	5063	5400	5431	50	50	6.1
	5	2505	3553	5063	5776	5431	6007	33	164	4.4
7A4-3	2	102	640	952	4870	1063	3408	22	140	27.1
	3	640	121	4870	2123	3408	818	140	23	53.0
	4	121	408	2123	2399	818	1077	23	22	32.9
	5	408	1351	2399	4022	1077	3716	22	140	37.6
7A4-4	2	117	868	1184	3357	1127	4129	36	171	28.1
	3	868	146	3357	1771	4129	993	171	36	53.2
	4	146	498	1771	1747	993	1297	36	36	35.8
	5	498	2032	1747	3763	1297	4505	36	205	24.2
7A4-5	2	196	686	1457	2417	2998	5101	55	141	25.1
	3	686	234	2417	1752	5101	3481	141	55	38.8
	4	234	808	1752	1725	3481	4055	55	55	31.0
7A4-6	3	1000	402	3105	2195	5221	5711	193	81	25.2
	4	402	1166	2195	2130	5711	5630	81	81	27.1
7A4-7	2	292	990	1711	3425	5016	6446	71	206	9.5
	3	990	316	3425	1838	6446	5800	206	71	26.1
	4	316	1010	1838	2120	5800	6427	71	71	26.1

θ_{ss} = Time to reach steady state.

APPENDIX B-3
PHASES 2,3,4,5 AND 6 RESULTS

		Contact Conductances ($Btu/hr\text{-}ft^2\text{-}^oF$)						Contact Pressure		θ_{ss}
		Interface		Hot End		Cold End		In'l	Fin.	
Run	Ph.	In'l	Fin.	In'l	Fin.	In'l	Fin.	psi.	psi.	sec.
407-1	2	128	328	1672	2643	2260	3420	32	90	40.7
	3	328	138	2643	2459	2459	2507	90	32	46.5
	4	138	519	2459	2248	2507	3135	32	32	27.2
	5	519	1003	2248	2482	3135	3522	32	89	22.3
407-2	2	151	304	1761	2845	3372	4490	47	118	46.5
	3	304	169	2845	2983	4490	3220	118	47	42.6
	4	169	489	2983	2449	3220	4272	47	47	30.0
	5	489	853	2449	2618	4272	4441	47	118	29.1
407-3	2	176	334	2207	2707	5306	4887	64	150	52.3
	3	334	190	2707	2553	4887	4628	150	63	54.3
	4	190	579	2553	2176	4628	4498	63	63	34.8
	5	579	916	2176	2399	4498	4515	63	149	20.0
407-4	2	293	493	2551	2956	4262	5665	78	180	29.7
	3	493	290	2956	2887	5665	6534	180	78	40.1
	4	290	1004	2887	2667	6534	6222	78	78	28.1
407-5	2	122	380	1093	2875	6202	5921	22	72	46.7
	3	380	133	2875	2592	5921	6670	72	22	48.9
	4	133	511	2592	2340	6670	4515	22	22	32.0
	5	511	1316	2340	2641	4515	5963	22	72	17.6
407-6	2	675	1221	2120	2573	3126	5664	29	86	13.6
407-7	2	433	1514	874	2601	4948	6746	5	86	41.6
47A-1	2	160	354	1441	2278	1385	1988	14	58	33.0
	3	354	111	2278	1959	1988	1992	58	14	60.0
	4	111	506	1959	2079	1992	2019	14	14	32.1
	5	506	1022	2079	2398	2019	2302	14	57	19.4
47A-2	2	220	530	1839	2342	2384	3490	30	85	31.9
	3	530	205	2342	2316	3490	3518	85	30	39.0
	2A	205	1034	2316	3087	3518	5897	30	173	27.1
	3A	1034	213	3087	2645	5897	4595	173	30	48.3
	4	213	721	2645	2439	4595	4995	30	30	28.1
	5	721	1843	2439	2912	4995	7472	30	172	14.5
	6	1843	712	2912	2498	7472	6376	172	30	29.1
47A-3	2	343	733	*	2382	5698	7249	53	131	39.7
	3	733	353	2382	2041	7249	8339	131	53	43.6
	4	353	1094	2041	1783	8339	6614	53	53	18.4
47A-4	2	506	1029	2364	2782	6388	8506	76	178	24.2
	3	1029	582	2782	2586	8506	9153	178	76	38.8
	4	582	1518	2586	2578	9153	8381	76	76	22.3

θ_{ss} = Time to reach steady state. * = No value.

APPENDIX B-4
PHASES 2,3,4 AND 5 RESULTS

		Contact Conductances (Btu/hr-ft^2-^{o}F)						Contact Pressure		θ_{ss}
		Interface		Hot End		Cold End		In'l	Fin.	
Run	Ph.	In'l	Fin.	In'l	Fin.	In'l	Fin.	psi.	psi.	sec.
405-1	2	91	243	*	*	3482	4337	32	162	
	3	243	84	*	*	4337	3778	162	32	
	4	84	801	*	6744	3778	5616	32	32	
405-2	2	29	127	848	4766	853	1623	13	108	169.4
	3	127	31	4766	1481	1623	796	108	13	243.0
	4	31	343	1481	1079	796	1663	13	13	93.1
405-3	2	49	168	*	*	6282	6290	21	130	
	3	168	49	*	*	6290	8437	130	20	
	4	49	711	*	7320	8437	5667	20	20	
	5	711	1036	7320	10001	5667	5631	20	130	116.1
405-4	2	88	202	1705	2431	9604	7395	48	144	174.3
	3	202	89	2431	2026	7395	15008	144	47	208.0
	4	89	1015	2026	1885	15008	6537	47	47	71.6
405-5	2	92	237	*	*	8304	6176	30	157	
	3	237	93	*	*	6176	9252			
	4	93	945	*	7192	9252	8190	30	30	
904-1	2	144	756	1014	3658	1407	2688	19	162	4.8
	3	756	141	3658	1458	2688	933	162	19	9.7
	4	141	291	1458	1762	933	2184	19	19	6.1
	5	291	1274	1762	3685	2184	2778	19	162	3.0
904-2	2	252	1064	1419	2943	2390	3487	31	161	3.9
	3	1064	311	2943	2230	3487	2668	161	30	6.7
	4	311	665	2230	2056	2668	2913	30	30	4.0
	5	665	1846	2056	3197	2913	3883	30	187	2.9
904-3	2	341	872	1682	2434	3618	4240	46	129	3.8
	3	872	372	2434	1937	4240	3183	129	46	3.5
	4	372	812	1937	1895	3183	3461	46	46	3.9
	5	812	1844	1895	2558	3461	4105	46	191	3.5
904-4	2	199	987	2128	2763	3361	4759	63	191	2.7
	3	987	274	2763	2401	4759	3087	191	64	7.3
905-5	3	461	283	2551	2308	4316	3771	111	65	7.8
	4	283	663	2308	2380	3771	3599	65	65	5.3

θ_{ss} = Time to reach steady state. * = No value.

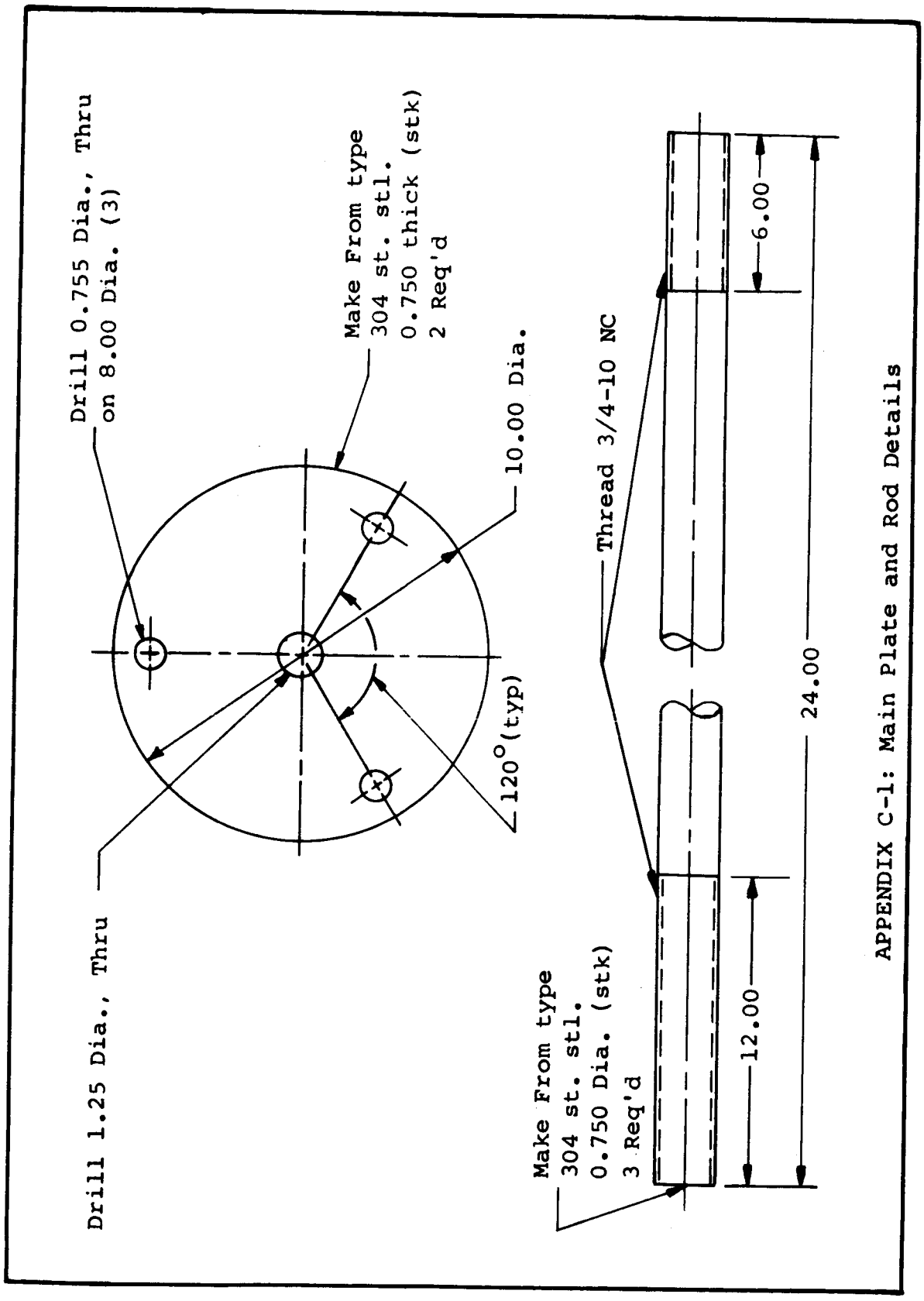

APPENDIX C-1: Main Plate and Rod Details

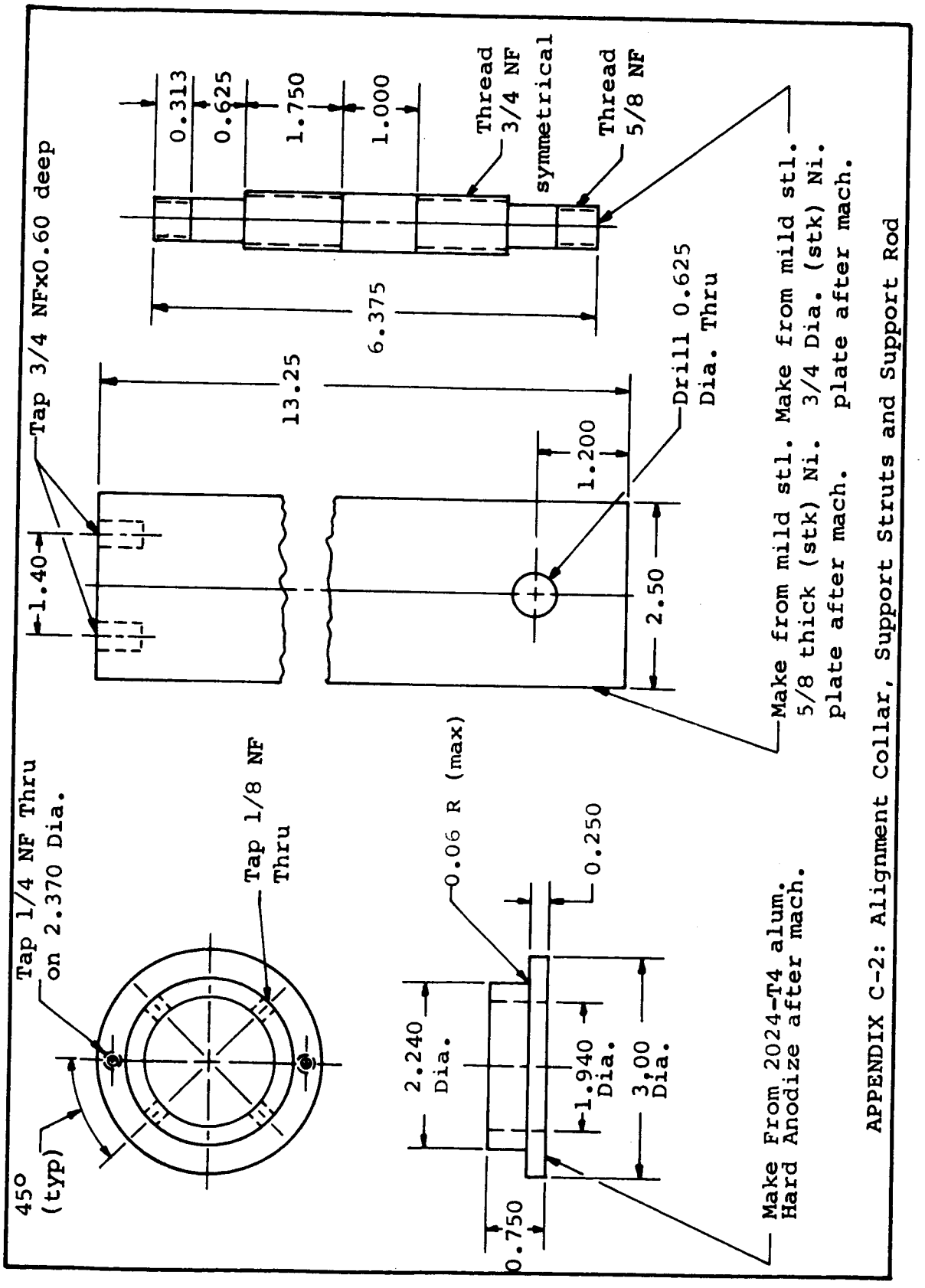

APPENDIX C-2: Alignment Collar, Support Struts and Support Rod

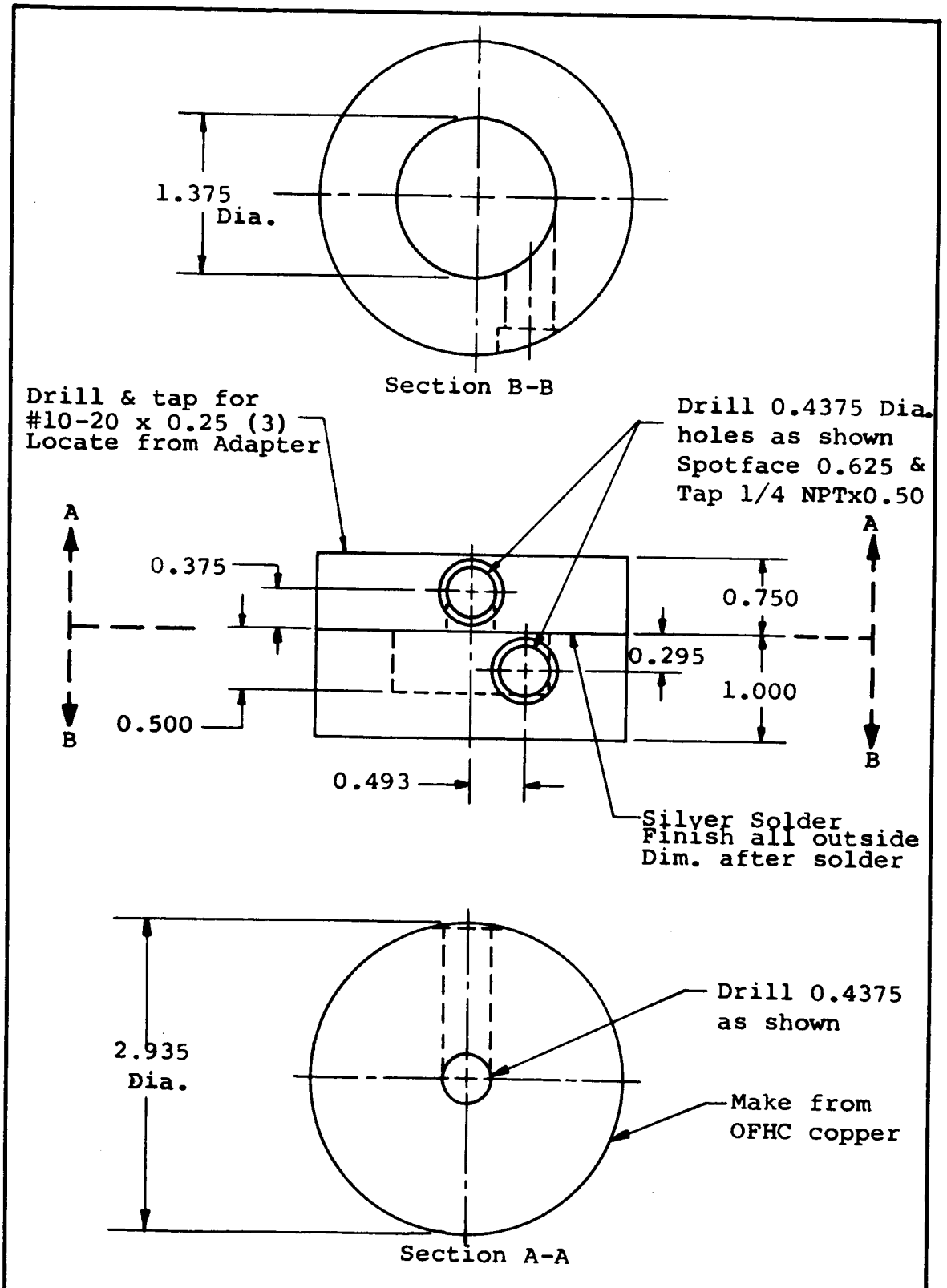

Appendix C-3: Source and Sink Blocks

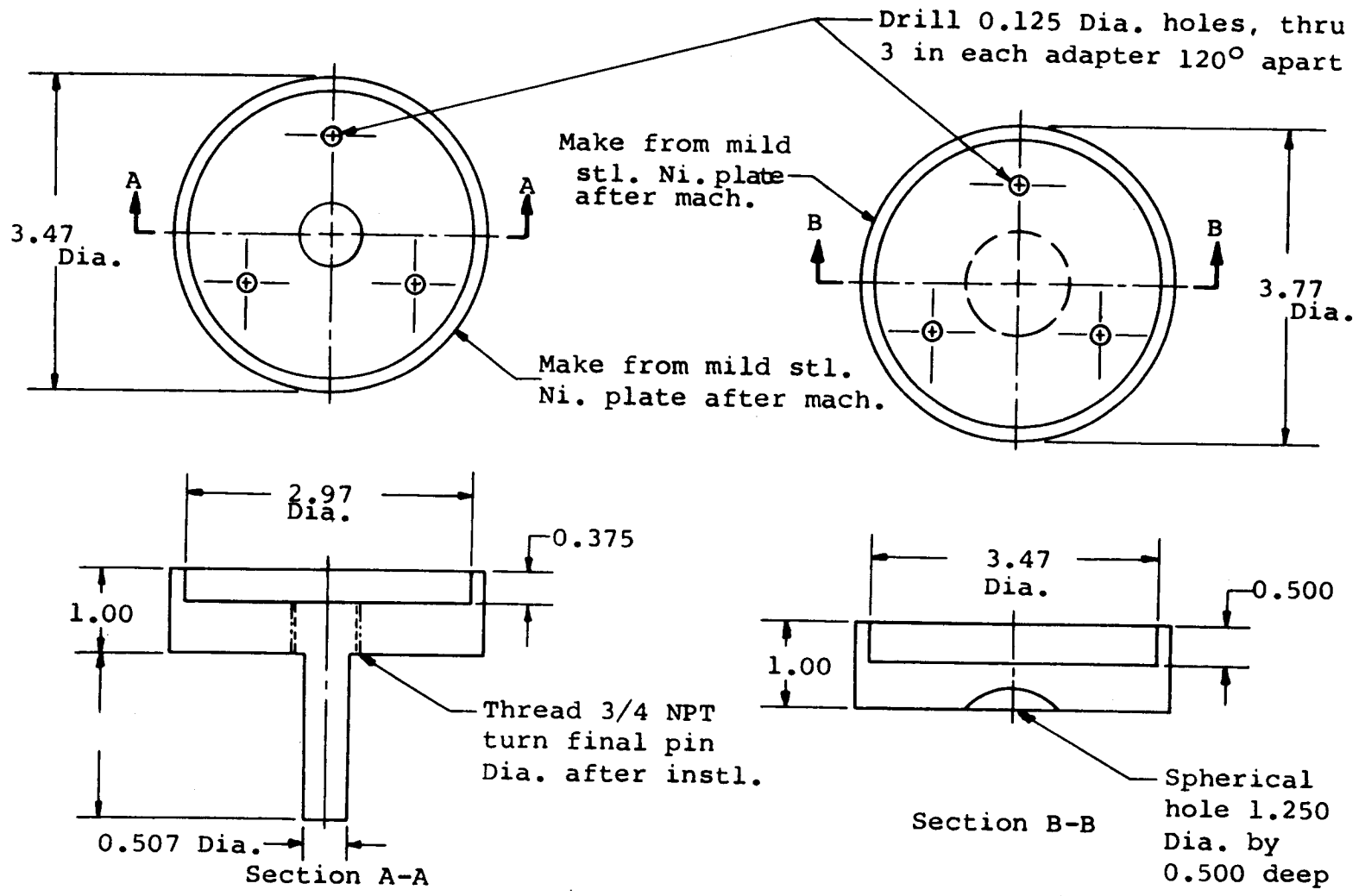

Appendix C-4: Source and Sink Block Adapters

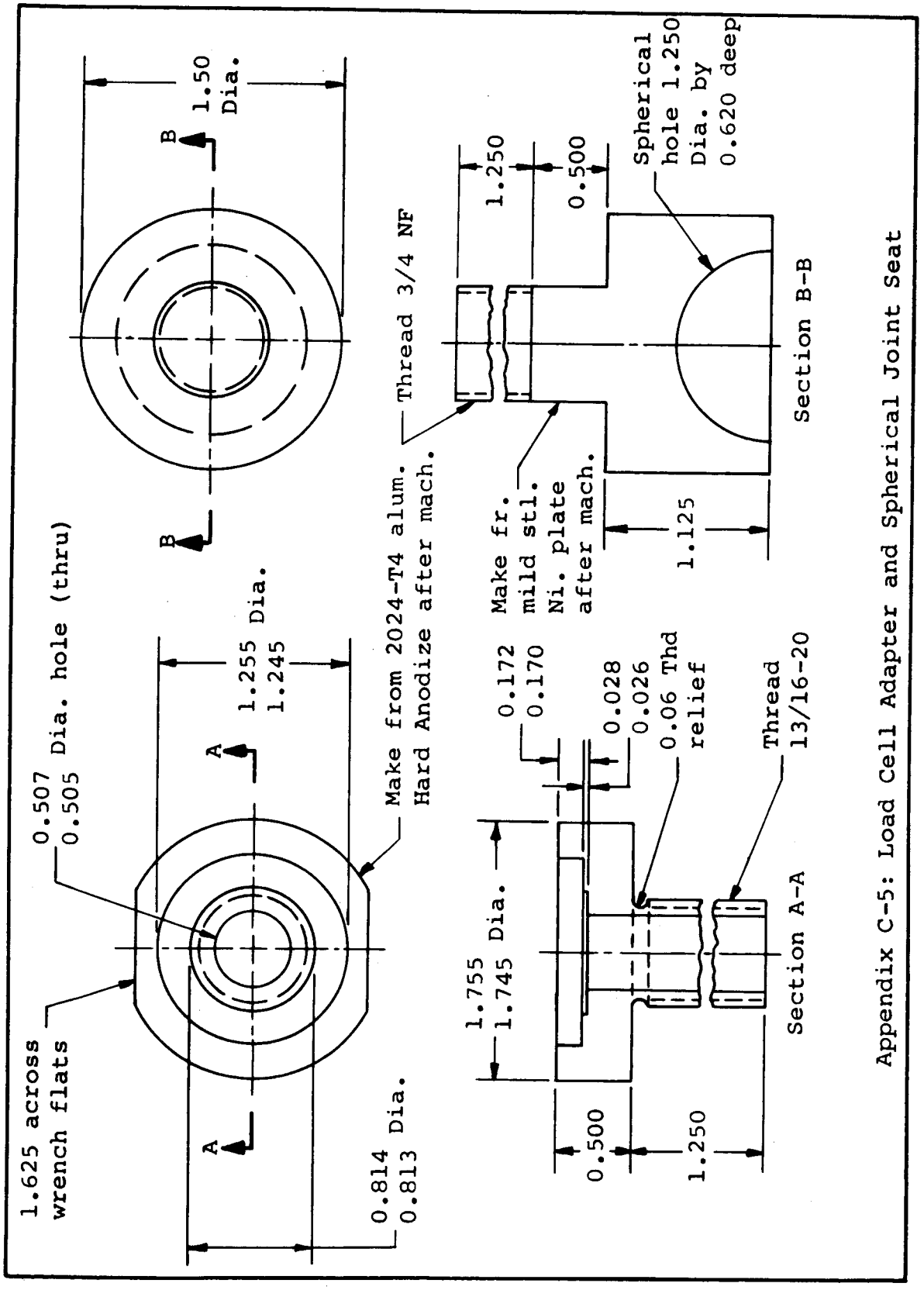

Appendix C-5: Load Cell Adapter and Spherical Joint Seat

#1

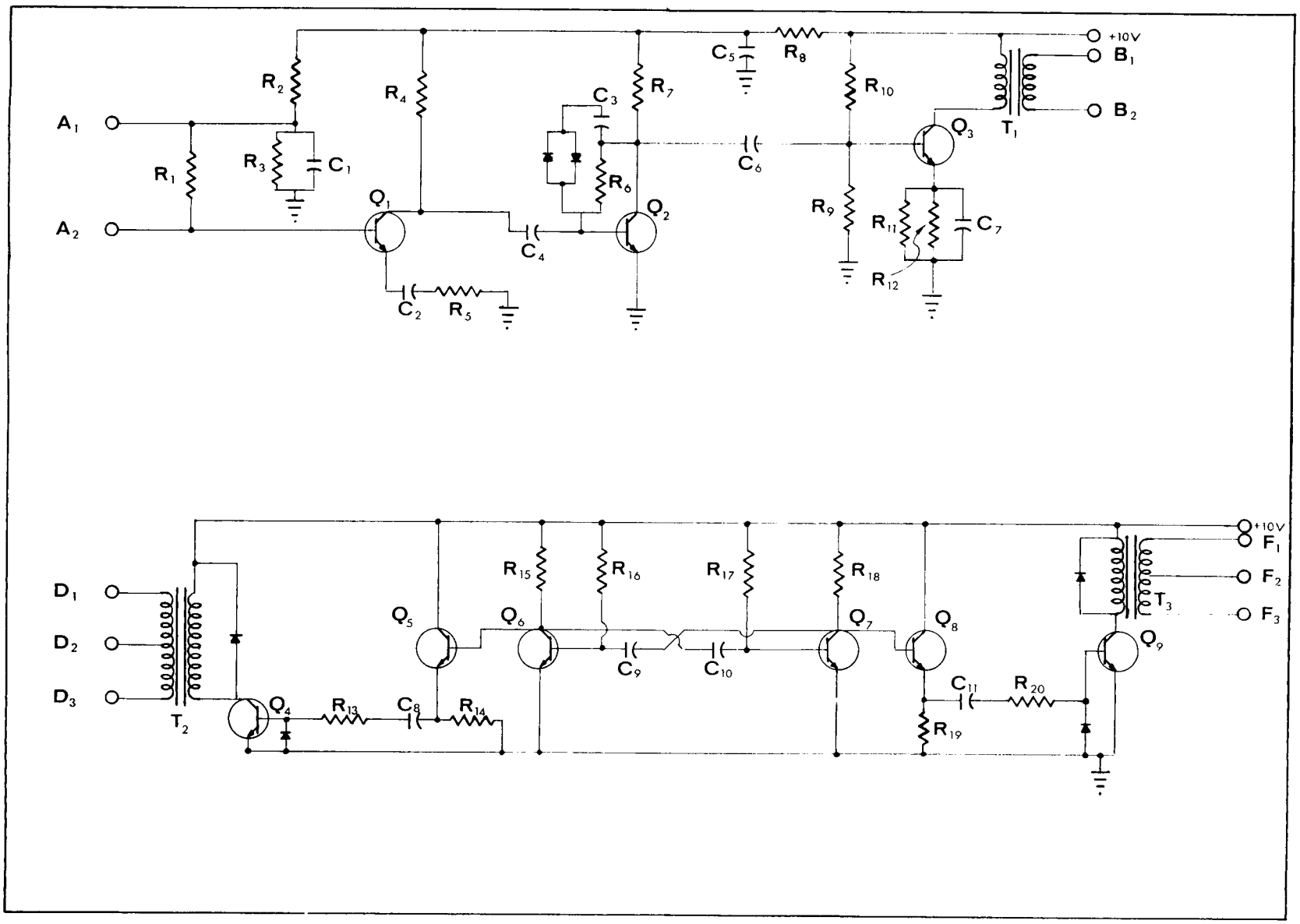
A1
A2
R1
R2
R3
C1
R4
Q1
C2
R5
C3
R6
R7
Q2
C4
C5
R8
C6
R10
R9
Q3
R11
R12
C7
T1
+10V
B1
B2
D1
D2
D3
T2
Q4
R13
C8
R14
Q5
Q6
R15
R16
C9
R17
C10
Q7
R18
Q8
C11
R19
R20
Q9
T3
+10V
F1
F2
F3

#2

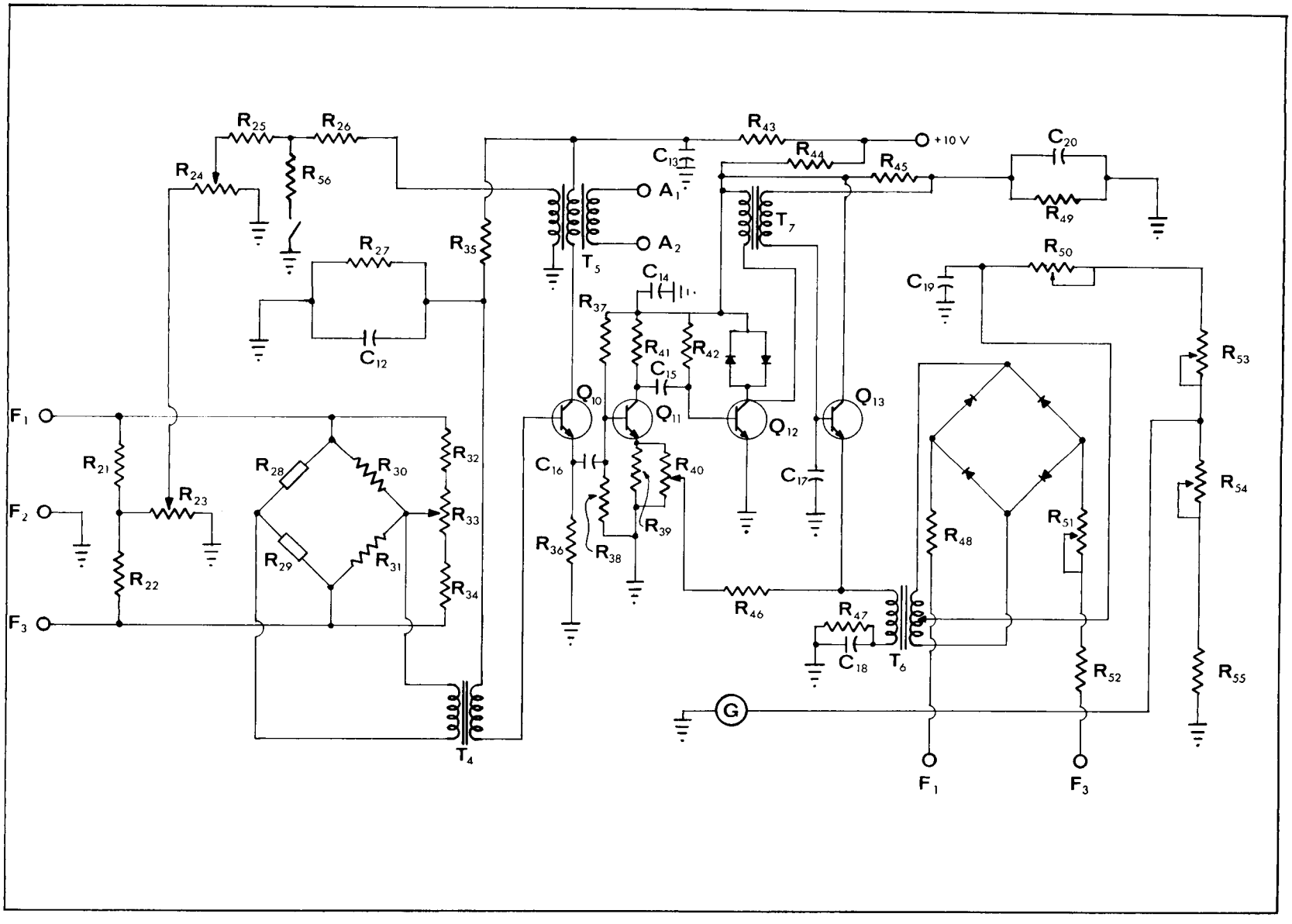
R25
R26
R24
R56
R27
C12
R35
T5
A1
A2
C13
R43
R44
+10 V
R45
C20
R49
T7
R50
C19
C14
R37
R41
R42
C15
Q10
Q11
Q12
Q13
C16
C17
R40
R39
R36
R38
R46
R47
C18
T6
R48
R51
R52
R53
R54
R55
F1
F2
F3
R21
R23
R22
R28
R30
R29
R31
R32
R33
R34
T4
G

#3

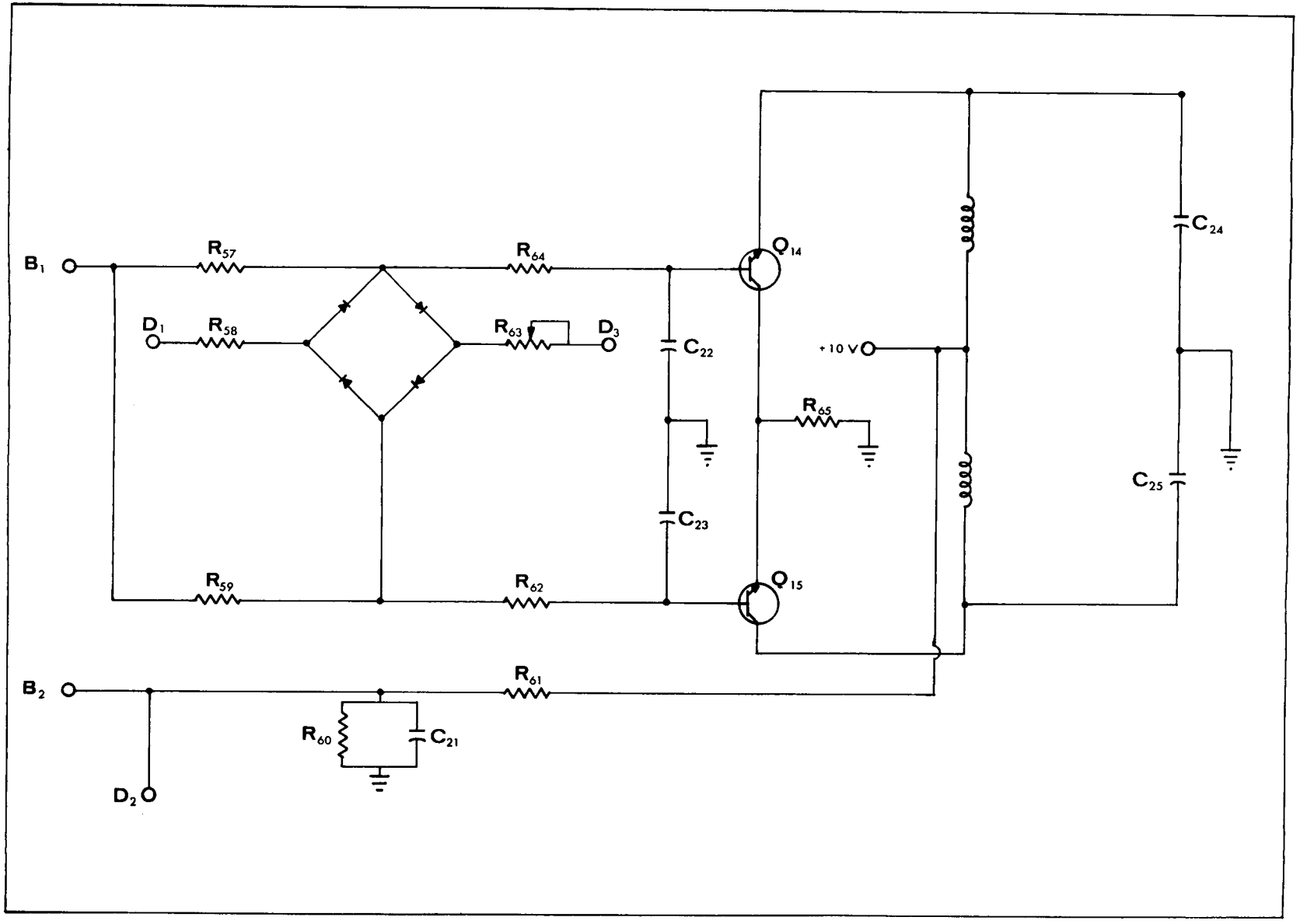
B1
R57
R64
Q14
D1
R58
R63
D3
C22
+10 V
R65
C24
C23
C25
R59
R62
Q15
B2
R61
R60
C21
D2

Appendix D-4

Values of Circuit Elements in the Force Control System Electrical Circuit Diagrams (pp. 201-3)

Resistors

No.	Value	No.	Value	No.	Value
1	560	23	10K	45	47K
2	15K	24	500	46	22K
3	2.2K	25	560	47	470
4	3.3K	26	560	48	560
5	1K	27	10K	49	10K
6	220K	28	120	50	10K
7	4.7K	29	120	51	100
8	1K	30	125	52	510
9	10K	31	125	53	1000
10	47K	32	2.2K	54	100
11	470	33	500	55	56
12	100	34	2.2K	56	500
13	2.2K	35	4.7K	57	560
14	2.2K	36	1K	58	220
15	4.7K	37	68K	59	560
16	67K	38	10K	60	1K
17	67K	39	220	61	2.2K
18	4.7K	40	1K	62	500
19	2.2K	41	4.7K	63	250
20	2.2K	42	470K	64	560
21	2.2K	43	470	65	2.5
22	2.2K	44	100		

Capacitors

No.	Value	No.	Value	No.	Value
1	5	10	.01	19	2500
2	10	11	5	20	10
3	.01	12	10	21	10
4	5	13	100	22	5
5	100	14	250	23	5
6	5	15	10	24	.082
7	250	16	5	25	.082
8	5	17	.05		
9	.01	18	10		

All values in ohms and microfarads, K=1000.

All transformers are Thordason-Meissner model TR-222.
All transistors are 2N2923.
All diodes are 1N626.

NOTE ON BIBLIOGRAPHY

The standard abbreviations have been used for all journal articles cited. Following is a list of abbreviations used for some reports and translations.

Reports

USAEC - United States Atomic Energy Commission.

UKAEA - United Kingdom Atomic Energy Authority.

Translations

RSIC - Redstone Scientific Information Center, Huntsville, Alabama.

DSIR - National Lending Library for Science and Technology, Boston Spa, Yorkshire, England.

SLA - Special Libraries Association: Translation Center, The John Crerar Library, 35 West 33rd St., Chicago, Illinois.

ASLIB - Association of Special Libraries and Information Bureau, 3 Belgrave Square, S.W. 1, London, England.

BIBLIOGRAPHY

1. Aaron, R. L., "A Theoretical Study of the Thermal Conductance of Joints with Varying Ambient Pressures," Southern Methodist University Master's Thesis, April 1963.

2. Aaron, R. L., and Blum, H. A., "Heat Transfer Across Surfaces in Contact: Effects of Ambient Pressure Changes," AIChE Paper 63-B-9, May 1963.

3. Accomazzo, M. A., and Miller, J., "Heat Transfer Across the Fuel-Clad Interface in Shrink Fit Hydride-Stainless Steel Fuel Elements," North American Aviation Memo, NAA-SR-MEMO-9184, Nov. 8, 1963.

4. Adamantiades, A., "Experimental Determination of Contact Conductance for Some Stainless Steel Contacts," USAEC Report No. NYO-9458, July 1962.

5. Ashby, N., "Study of Interfacial Conductivity," Sixth Monthly Progress Report, NASA Contract No. NAS 8-20126, P.L.C. Research Associates, Inc., Boulder, Colorado, June 31, 1966.

6. Airapetyants, S. V., and Ryabinin, M. N., "Reproducible Thermal Pressure Contacts," Thermoelectric Properties of Semiconductors, (edited by V. A. Kutasov, authorized translation from the Russian), Consultants Bureau, New York, pp. 32-33, 1964.

7. Alcock, J. R., "Communications on a Review of Recent Progress in Heat Transfer," Proc. Inst. Mech. Engrs., V. 149, pp. 126-132, 1943.

8. Alekseeva, O. P., and Ivanov, A. V., "Heat Conduction Problem for an Unbounded Double-Layer Rod in the Case of Imperfect Contact Between the Layers," IZV. VYS. UCHEB ZAV. ENERGETIKA, V. 3, No. 1, pp. 122-128, Jan. 1960.

9. Anderson, A. C., Salinger, G. L., and Wheatley, J. C., "Transfer of Heat Below 0.15°K.," Review of Scientific Instruments, V. 32, No. 10, pp. 1110-1113, Oct. 1961.

10. Anderson, R. R., "Interface Thermal Conductance Tests of Riveted Joints in a Vacuum," Douglas Aircraft Company Report TU24871, February 6, 1964.

11. Andrews, I. D. C., "An Investigation of the Thermal Conductance of Bolted Joints," Royal Aircraft Establishment (England), Technical Note WE. 46, Jan. 1964.

12. Armond, G., Lapujoulade, J., and Paigne, J., "A Theoretical and Experimental Relationship Between the Leakage of Gases Through the Interface of Two Metals in Contact and Their Superficial Micro-Geometry," Vacuum, V. 14, No. 2, pp. 53-57, Feb. 1964.

13. Aron, W. K., and Colombo, G., "Controlling Factors of Thermal Conductance Across Bolted Joints in a Vacuum," ASME Paper, 63-W-196, 1963.

14. Ascoli, A., and Cermagnoli, E., "Consideration of the Thermal Contact Resistance Between Facing Flat Metal Surfaces," (Italian), Energia Nucleare, V. 3, No. 2, pp. 113-118, April, 1956. English Translation (USA), DSIR-28790-ct., Oct. 1956.

15. Ascoli, A., and Germagnoli, E., "Measurement of the Thermal Resistance of Uranium and Aluminum Flat Surfaces in Contact," (Italian) Energia Nucleare, V. 3, No. 1, pp. 23-31, 1961. English Translation (USA), RSIC-99, Nov. 6, 1963.

16. Ashmead, F. A. H., "Thermal Resistance of Joints," College of Aeronautics Diploma Thesis, Great Britain, May 1955.

17. Astakhov, O. P., Petrov, V. I., and Fedynskii, O. S., "Note on Contact Thermal Resistance in Heat Transfer to Liquid Metals," Atom. Energ., V. 11, No. 3, pp. 255-257, Sept. 1961.

18. Atkins, H. L., "Bibliography on Thermal Metallic Contact Conductance," NASA TM X-53227, April 15, 1965.

19. Atkins, H. L., and Fried, E., "Thermal Interface Conductance in a Vacuum," AIAA Paper, 64-253, Marshall Space Center, NASA, Huntsville, Alabama, 1964.

20. Austin, J. B., "Relative Influence of Metallic Resistances in Thermal Circuits," The Flow of Heat in

Metals, American Society for Metals, Cleveland, Ohio, p. 82, 1942.

21. Bailie, R. C., and Fan, I. T., "Temperature Transient After Contact Heating," Int. J. of Heat and Mass Transfer, V. 6, No. 10, pp. 926-927, Oct. 1963.

22. Barber, A. D., Weiner, J. H., and Boley, B., "An Analysis of the Effect of Thermal Contact Resistance in a Sheet Stringer Structure," Journal of the Aeronautical Sciences, V. 24, No. 3, pp. 232-234, Mar. 1957.

23. Barnes, L. J., and Dillinger, J. R., "Thermal Boundary Resistance Between Some Superconducting and Normal Metals," Phys. Rev. Letters, V. 10, No. 7, pp. 287-289, April 1, 1963.

24. Barzelay, M. E., Tong, K. N., and Holloway, G. F., "Thermal Conductance of Contacts in Aircraft Joints," NACA TN-3167, Mar. 1954.

25. Barzelay, M. E., Tong, K. N., and Holloway, G. F., "Effect of Pressure on Thermal Conductance of Contact Joints," NACA TN-3295, May 1955.

26. Barzelay, M. E., and Holloway, G. F., "Effect of an Interface on Transient Temperature Distribution in Composite Aircraft Joints," NACA TN-3824, Apr. 1957.

27. Barzelay, M. E., and Holloway, G. F., "Interface Conductances of Twenty-seven Riveted Aircraft Joints," NACA TN-3991, July 1957.

28. Barzelay, M. E., and Schaefer, John W., "Temperature Profiles and Interface Thermal Conductance of Stainless Steel and Titanium Alloy Panels under Combined Loading and Heating," Syracuse University Report ME 406-577F, July 1957.

29. Barzelay, M. E., "Range of Interface Thermal Conductance for Aircraft Joints," NACA TN D-426, May 1960.

30. Batho, C., "The Partition of the Load in Riveted Joints," J. Franklin Inst., V. 182, No. 5, pp. 553-604, Nov. 1916.

31. Behrman, L. A., "Thermal Conductance of Two Stacked Composite Circular Cylinders with Mixed Boundary Conditions," ASME Paper 63-WA-147, Nov. 1963.

32. Berman, R., "Some Experiments on Thermal Contact at Low Temperatures," J. Appl. Phys., V. 27, No. 4, pp. 318-323, April 1956.

33. Berman, R., and Mate, C. F., "Thermal Contact at Low Temperatures," Nature, V. 182, pp. 1661-1663, December 13, 1958.

34. Bernard, J. J., "La Resistance Thermique Des Joints," (French) Groupe Consultatif Pour La Recherche et la Realisation Aeronautiques, AGARD Report No. 212, Oct. 1958, ASTIA Document No. AD221-409.

35. Bloom, Mitchell F., "A Review of the Parameters Influencing Thermal Contact Conductance Between Metal Interfaces," Douglas Aircraft Report SM-42082, August 9, 1962.

36. Bloom, Mitchell F., "Preliminary Results from a New Thermal Contact Conductance Apparatus," Douglas Aircraft Engineering Paper 1672, Aug. 1963.

37. Bloom, Mitchell F., "Thermal Contact Conductance in a Vacuum Environment," Douglas Aircraft Report SM-47700, Dec. 1964. Also presented at 1964 Thermal Conductivity Conference, U. S. Naval Radiological Lab., San Francisco, California, October 13-16, 1964.

38. Blum, H. A., and Moore, C. J., Jr., "Heat Transfer Across Surfaces in Contact: Transient Effects of Ambient Temperatures and Pressures," Progress Report, NASA Contract NsG 711. Also presented at 1964 Thermal Conductivity Conference, U. S. Naval Radiological Lab., San Francisco, California, October 13-16, 1964.

39. Blum, H. A., and Moore, C. J., Jr., "Transient Phenomena in Heat Transfer Across Surfaces in Contact," ASME Paper No. 65-HT-59, Aug. 1965.

40. Boeschoten, F., "On the Possibility to Improve the Heat Transfer of Uranium and Aluminum Surfaces in Contact," Proceedings of the International Conference on the Peaceful Uses of Atomic Energy, V. 9, pp. 208-209, Geneva, Aug. 1955.

41. Boeschoten, F., and Van der Held, E., "The Thermal Conductance of Contacts Between Aluminum and Other Metals," Physica, V. 23, pp. 37-44, 1957.

42. Bory, C., and Cordier, H., "Thermal Contact Resistances," from French Institute of Fuels and Energy, Transmission of Heat Seminar, Feb. 1961.

43. Bowden, F. P., and Tabor, D., "The Area of Contact Between Stationary and Between Moving Surfaces," Proc. Roy. Soc. Lond., A., V. 169, pp. 391-413, 1939.

44. Bowden, F. P., and Tabor, D., The Friction and Lubrication of Solids, Oxford University Press, 1954.

45. Brooks, W. A., Jr., Griffith, G. E., and Strass, H. K., "Two Factors Influencing Temperature Distributions and Thermal Stresses in Structures," NACA TN-4052, June 1957.

46. Browning, J. W., "A Transient Study of Thermal Contact Resistance," a study performed at Southern Methodist University, Dallas, Texas, May 12, 1962.

47. Brunot, A. W., and Buckland, F. F., "Thermal Contact Resistance of Laminated and Machined Joints," Trans. ASME, V. 71, pp. 253-257, 1949.

48. Brutto, E., Casagrande, I., and Perona, G., "Thermal Contact Resistance Between Cylindrical Metallic Surfaces," Energia Nucleare, (Milan), V. 6, No. 8, pp. 532-540, Aug. 1959.

49. Businger, J. A., and Buettner, K. J. K., "Thermal Contact Coefficients," J. Meteorol., V. 18, No. 3, p. 422, June 1961.

50. Butler, S., "The Effect of Joints on the Thermal Stress in Supersonic Flight," British Aircraft Ltd. Report T.O.R. 149, Feb. 1962.

51. Bybee, Jerry L., "The Effect of Pressure on Roughness Characteristics of Metal Surfaces in Contact," a study performed at Southern Methodist University, Dallas, Texas, March 15, 1965.

52. Campbell, W. E., "Use of Statistical Control in Corrosion and Contact Resistance Studies," Trans. Electrochem. Soc., V. 81, pp. 377-390, April 1942.

53. Carroll, T. W., "Statistical Calculation of Geometric Parameters for Semi-Smooth Contiguous Surfaces," M. S. Thesis, M. I. T., Jan. 1962.

54. Cetinkale (Veziroglu), T. N., "Thermal Conductance of Metal Surfaces in Contact," Ph. D. Thesis, London University, London, England, 1951.

55. Cetinkale (Veziroglu), T. N., and Fishenden, M., Thermal Conductance of Metal Surfaces in Contact," General Discussion on Heat Transfer, Proceedings of Inst. of Mech. Engr. and ASME, London, England, pp. 271-275, Sept. 1951.

56. Challis, L. J., and Cheeke, J. D. N., "The Thermal Conductance of Copper-Lead-Copper Sandwiches at Liquid Helium Temperatures," Physics Letters, V. 5, No. 5, pp. 305-307, August 1, 1963.

57. Clark, W. T., and Powell, R. W., "Measurement of Thermal Conduction by the Thermal Comparator," J. Sci. Instr., V. 39, No. 11, pp. 545-551, Nov. 1962.

58. Clausing, A. M., and Chao, B. T., "Thermal Contact Resistance in a Vacuum Environment," University of Illinois Experimental Station Report ME-TN-242-1, August 1963. Also J. Heat Transfer, V. 87, No. 2, p. 243, Feb. 1965.

59. Clausing, A. M., "Some Influences of Macroscopic Constrictions on the Thermal Contact Resistance," University of Illinois Experimental Station Report ME-TN-242-2, April 1965.

60. Cole, R. L., "An Experimental Investigation of the Heat Transfer Mechanism Across an Aircraft Structure Joint," Master's Thesis, Southern Methodist University, Dallas, Texas, January 1961.

61. Cordier, H., "Experimental Study of Contact Thermal Resistance," (French), Annales de Physique, No. 1-2, pp. 5-19, Jan.-Feb. 1961.

62. Cordier, H., and Maimi, R., "Experimental Study of the Influence of Pressure on Thermal Contact Resistance," (French), Comptes Rendus Acad. Des Sc., V. 250, No. 17, pp. 2853-2855, April 25, 1960, English Translation (USA), SLA Translation No. 63-10777.

63. Coulbert, C. D., and Liu, C., "Thermal Resistance of Aircraft Structure Joints," WADC Technical Note 53-50, June 1953.

64. Cunnington, G. R., Jr., "Thermal Conductance of Filled Aluminum and Magnesium Joints in a Vacuum Environment," ASME Paper 64-WA/HT-40.

65. Cunningham, G. W., and Spretnak, J. W., "A Study of the Effect of Applied Pressure on Surface Contact Area," Int. J. Mech. Sci., V. 4, pp. 231-240, 1962.

66. Davies, W., "Thermal Transients in Graphite Copper Contacts," Brit. J. Appl. Phys., V. 10, No. 12, pp. 516-522, Dec. 1959.

67. Dean, R. A., "Thermal Contact Conductance Between UO_2 and Zircaloy 2," USAEC Report CVNA-127, 1962.

68. Douglas Aircraft Company, Inc., "Thermal Resistance of Bolted Aluminum Joints," Technical Memorandum AZ-860-S MECH-63-TM-50, January 28, 1963.

69. Dubovis, M. I., "The Evaluation of Temperature on the Plane of Contact in Systems with Heat Removal into a Semi-Infinite Medium, Soviet J. of Eng. Phys., V. 4, No. 11, pp. 89-93, November 1961, (Faraday Translation, New York).

70. Dugeon, E. H., and Prior, B. W., "The Contact Thermal Conductance of Aluminum-Sheathed Tubes," National Research Council of Canada Report MT-24, Oct. 1954.

71. Dugeon, E. H., and Prior, B. W., "The Contact Thermal Conductance of an Aluminum-Sheathed Nickel or Tin-Plated Uranium Rod," National Research Council of Canada, Report MT-29, September 26, 1955.

72. Dutkiewicz, R. K., "Interfacial Gas Gap for Heat Transfer Between Two Randomly Rough Surfaces," Proceedings of the Third International Heat Transfer Conference, V. 4, p. 118, August 1966.

73. Dyban, E. P., and Kondak, N. M., "Research on Heat Exchange in Course of Contact Between Parts," IZV. AN SSSR OTD. TEKHN. NAUK, V. 9, pp. 62-79, 1955. English Translation ASLIB-GB158.

74. Dyban, E. P., Kondak, N. M., and Shvets, I. T., "Investigation of Contact Heat Exchange Between Machine Parts," (Russian), IZV. AKAD. NAUK. USSR OTD. TEKH. NAUK., V. 9, pp. 63-79, Sept. 1954. English Translation IGRL-T/W.12, issued by United Kingdom Atomic Energy Authority.

75. Dyban, E. P., Kondak, N. M., and Shvets, I. T., "Studies on Contact Heat Exchange Between Heat Engine Parts," (Russian), Trudy Institute Teploenergetika, No. 12, pp. 21-53, 1955. English Translation (USA), RSIC-322.

76. Dyban, E. P., and Shvets, I. T., Air Cooling of Gas Turbine Rotors, Chap. 10, "Contact Heat Exchange in Turbine Parts, pp. 191-233, IZDATEI 'STVO KIEVSKOGO UNIVERSITETA KIEV, 1959, English Translation-Technical Documents Liaison Office. MCL-1406/1+2+3+4, July 18, 1962. ASTIA Document No. AD-281-848.

77. Dyban, E. P., and Shvets, I. T., "Contact Heat Transfer Between Two Flat Metallic Surfaces," Soviet J. Eng. Physics, V. 7, No. 3, pp. 3-9, March 1964, (Faraday Translations, N. Y.).

78. D'yachenko, P. E., Tolkacheva, N. N., Andreev, G. A., and Karpova, T. M., The Actual Contact Area Between Touching Surfaces, (Russian), Institute of Mechanical Engineering, Academy of Science Press, Moscow, 1963, 68 pages. English Translation by Consultants Bureau, N. Y., 1964.

79. Dyson, J., and Hirst, W., "The True Contact Area Between Solids," Proceedings of the Physical Society, Section B., V. 67, pp. 309-312, 1954.

80. Elliott, D. H., "A Study of Thermal Resistance Across Aluminum Joints in a High Vacuum," "Model No. Saturn S-IVB," Douglas Aircraft Company Report SM-46759, December 1964. See also ASME Paper No. 65-HT-53, August 1965.

81. Elliott, D. H., "Thermal Resistance Across Bolted Aluminum Joints and Across Flat Surfaces Pressed Together in a Vacuum," Douglas Aircraft Company, Inc., Technical Memorandum No. 89, Serial No. A3-863-K411-63, April 1964.

82. Fenech, H., "The Thermal Conductance of Metallic Surfaces in Contact," Ph. D. Thesis, M.I.T., May 1959.

83. Fenech, H., and Henry, J. J., "An Analysis of Thermal Contact Resistance," Transactions of the American Nuclear Society, V. 5, No. 2, pp. 476-477, Nov. 1962.

84. Fenech, H., and Rohsenow, W. M., "Thermal Conductance of Metallic Surfaces in Contact," USAEC Report NYO-2136, May 1959.

85. Fenech, H., and Rohsenow, W. M., "Prediction of Thermal Conductance of Metallic Surfaces in Contact," Jour. Heat Transfer, V. 85, No. 1, pp. 15-24, Feb. 1963.

86. Fishenden, M., and Kepinsky, A., "Resistance to Heat Transfer in Gap Between Two Parallel Surfaces in Contact," Proceedings of the Seventh Congress on Applied Mechanics, V. 3, pp. 193-195, 1948.

87. Fisher, J. T., "The Design and Construction of an Apparatus to Determine the Heat Transfer Coefficient of 304 Stainless Steel Joints in Contact in a Vacuum," M. S. Thesis, Dept. of Chemical Engineering, University of Rochester, Rochester, New York, 1964.

88. Flamming, D. C., "The Use and Comparison of Autoradiographical and Statistical Methods for Determining the Number of Contacts Between Two Surfaces Pressed Together," B. S. Thesis, M.I.T., June 1963.

89. Fontenot, J. E., Jr., "Thermal Conductance of Contacts and Joints," The Boeing Company, Aero-Space Division, Saturn Booster Branch, Document No. D5-12206, New Orleans, La., Dec. 1964.

90. Frank, I., "Transient Temperature Distribution in Aircraft Structures," J. Aero. Sci., V. 25, No. 4, pp. 265-267, April 1959.

91. Fried, E., "Study of Thermal Contact Conductance," Final Report NASA (M-RP-T) Contract NAS8-5207, General Electric Document No. 64SD652, May 1, 1964. Also presented at the International Thermal Conductivity Conference National Physical Laboratory, Teddington, Middlesex, England, July 15-17, 1964.

92. Fried, E., "Study of Interface Thermal Contact Conductance," Summary Report, NASA (M-RP-T) Contract NAS8-11247, General Electric Document No. 65SD 4395, March 1965.

93. Fried, E., "The Thermal Conductance of Space Vehicle Interfaces-Experimental Results," General Electric Report No. 61GL65, March 1961.

94. Fried, E., "Thermal Joint Conductance in a Vacuum," ASME Paper No. AHGT-18, Aviation and Space Hydraulic and Gas Turbine Conference, Los Angeles, California, March 1963.

95. Fried, E., "Metallic Interface Thermal Conductance - Measurement Techniques," Paper presented at the Fourth Conference on Thermal Conductivity, U. S. Naval Radiological Defense Laboratory, San Francisco, California, Oct. 13-16, 1964.

96. Fried, E., and Costello, F. A., "Interface Thermal Contact Resistance Problem in Space Vehicles," Presented at American Rocket Society Conference, Palm Springs, California, April 1961, (see also ARS Journal, V. 32, pp. 237-243, 1962).

97. Fried, E., and Kelly, M. J., "Thermal Conductance of Metallic Contacts in a Vacuum," AIAA Paper No. 65-661, September 1965.

98. Fujimoto, T., and Takao, K., "Heat Transfer in the Rarefied Gases," (in two parts) Bulletin of JSME, V. 2, No. 6, pp. 197-209, June 1959.

99. Gardner, K. A., and Carnavos, T. C., "Thermal Contact Resistance in Finned Tubing," J. Heat Transf., C82, No. 4, pp. 279-293, April 1960.

100. Gatewood, B. E., "Effect of Thermal Resistance of Joints Upon Thermal Stresses," Air Force Inst. of Technology Report No. 56-6, May 1956, ASTIA Document No. AD106-014.

101. Gex, R. C., "Thermal Resistance of Metal-to-Metal Contacts," an Annotated Bibliography, Lockheed Special Bibliography Report SB-61-39, July 1961, ASTIA Document 263-181.

102. Gilchrist, E. J., "Experimental Interface Heat Transfer Contact Coefficients in the Minuteman Solid Rocket Nozzle," Aerophysics Dept. Solid Rocket Operations, Aerojet General Corporation (Sacramento, Calif.) Report, July 1964, Air Force Contract AF04(694)-258.

103. Graff, W. J., "Thermal Conductance Across Metal Joints," Machine Design, V. 32, No. 19, pp. 166-172, 1960.

104. Greenwood, J. A., and Tripp, J. H., "Elastic Contact of Rough Spheres," Burndy Research Division, Research Report No. 21, February 1965.

105. Greenwood, J. A., and Williamson, J. B. P., "The Contact of Nominally Flat Surfaces," Burndy Research Division, Research Report No. 15, July 1964.

106. Griffith, G. E., and Miltonberger, G. H., "Some Effects of Joint Conductivity on the Temperatures and Thermal Stresses in Aerodynamically Heated Skin Stiffener Combinations," NACA TN 3699, June 1956.

107. Hain, P. L., "Thermal Conductance of an Interface," Southern Methodist University, Master's Thesis, Dallas, Texas, May 26, 1961.

108. Heasley, J. H., "Transient Heat Flow Between Contacting Solids," Int. J. Heat Mass Transfer, V. 8, No. 1, p. 147, Jan. 1965.

109. Hefley, H. F., "Thermal Conductance of Intersurfaces," Southern Methodist University, Master's Thesis, Dallas, Texas, September 1962.

110. Held, W., "Heat Transfer Between Worked Metal Surfaces," (German) Allgemein Wärmetechnik, V. 8, No. 1, pp. 1-8, 1957, English Translation (USA) RSIC-76.

111. Hencky, H., "Uber einige statisch bestimmte Fälle des Gleichgewichts in plastischen Körpern, Z. Angew. Mech., V. 3, p. 241, 1923.

112. Henry, J. J., "The Thermal Resistance of Metals in Contact," M. S. Thesis, M.I.T., August 1961.

113. Henry, J. J., "Some Methods of Surface Analysis for the Prediction of Thermal Resistance of Metal Contacts," USAEC Report NYO 9457, Nov. 1961.

114. Henry, J. J., "Thermal Conductance of Metallic Surfaces in Contact," USAEC Report NYO-9459, Feb. 1963.

115. Henry, J. J., and Fenech, H., "The Use of Analogue Computers for Determining Surface Parameters Required for Prediction of Thermal Contact Conductance," ASME Paper 63-WA-104, 1963, see also J. of Heat Transf., V. 86, Series C, No. 4, pp. 543-552, Nov. 1964.

116. Hertz, Heinrich, "Study of the Contact of Elastic Solid Bodies," (German), Journal für Die Reine und Angewandte Mathematik, V. 29, pp. 156-171, 1882, English Translation (USA) by Egon Benesi, Translation No. SLA 57-01164, March 15, 1957.

117. Holloway, G. F., "The Effect on an Interface on the Transient Distribution in Composite Aircraft Joints," Syracuse University Thesis, 1954, also NACA TN-3824, April 1957.

118. Holm, R., Electrical Contacts, Handbook, Springer Verlag, Berlin, 3rd ed., 1958.

119. Holm, R., "Calculation of the Temperature in a Contact Heated in the Contact Surface and Application to the Problem of Temperature Rise in a Sliding Contact," J. Appl. Phys., V. 19, No. 4, pp. 361-366, April 1948.

120. Horn, S. S., "Thermal Contact Resistance of Graphite," M. S. Thesis, M.I.T., September 1963.

121. Horton, J. C., "Electrical Contacts in Vacuum," (A) Brushes, Status Report No. 2, Marshall Space Flight Center Report MTP-R&VE-M-63-17, December 28, 1962.

122. Horvay, G., and Edsall, R. H., "The Interface Temperature of Two Media in Poor Thermal Contact," AIME Metallurgical Society Transaction, V. 218, No. 5, pp. 927-933, October 1960.

123. Houtman, W., "Selection and Evaluation of Interstitial Materials for Use Between Cold Plates and Equipment in a Vacuum Environment," McDonnell Aircraft Corporation Report TRO52-068.02.04, April 1963, ASTIA Document No. AD418-941.

124. Hsieh, C. K., "On the Nature of Thermal Contact Conductance," Master of Science Thesis, Purdue University, August 1964.

125. Ittner, W. B., and Magill, P. J., "A Survey of Contact Resistance Theory for Nominally Clean Surfaces," IBM Journal of Research and Development, V. 1, No. 1, pp. 44-48, January 1957.

126. Iwaki, A., and Mori, M., "Distribution of Surface Roughness When Two Surfaces are Pressed Together," Journal of JSME, V. 1, No. 4, pp. 329-337, 1958.

127. Jacobs, R. B., and Starr, C., "Thermal Conductance of Metallic Contacts," Rev. Sci. Instr. V. 10, pp. 140-141, April 1939.

128. Jansson, R. M., "The Heat Transfer Properties of

Structural Elements for Space Instruments," M.I.T. Instrumentation Lab Report E-1173, June 1962.

129. Jelinek, D., "Heat Transfer of Proposed Structural Joints in the Rocket Package for the F-86D Airplane," North American Aviation Lab Report No. NA-49-831, September 30, 1949.

130. Kapinos, V. V., and Il'chenko, O. T., "Thermal Conductivities Due to Protruding Asperities," (Russian) IZVESTIYA VYSSHIKH UCHEBNYAK ZAVEDENIY ENERGETIKA, No. 9, pp. 77-89, 1958, English Translation (USA) RSIC-281.

131. Kapinos, V. M., and Il'chenko, O. T., "Determining the Contact Thermal Resistance of Mixed Pairs," KHARKOV POLITEKHNICHESKII INST. TRUDY, SERIYA METALLURGICHESKAIA, V. 5, pp. 217-223, 1959.

132. Kapinos, V. M., and Il'chenko, O. T., "Thermal Resistance of a Contact Layer," KHARKOV POLITEKHNICHESKII INST. TRUDY, SERIYA METALLURGICHESKAIA, V. 5, pp. 160-181, 1959.

133. Kapinos, V. M., Il'chenko, O. T., "Thermal Resistance of Turbine Blade Base Joints," (Russian) ENERGMOASHINOSTROENIE, V. 5, No. 6, pp. 23-26, June 1959, English Translation (USA) RSIC-261.

134. Karush, W., "Temperature of Two Metals in Contact," USAEC Report AECD-2967, December 22, 1944.

135. Kaspareck, W. E., and Dailey, R. M., "Measurement of Thermal Contact Conductance Between Dissimilar Metals in a Vacuum," ASME Paper No. 64-HT-38, August 1964.

136. Kaszubineki, L. J., "Determination of the Number of Contacts Between Two Surfaces Pressed Together," M. S. Thesis, M.I.T., August 1962.

137. Keller, J. D., "Heat Transmission in Strip Coil Annealing," Iron and Steel Engineers, V. XXV., No. XI, pp. 60-67, November 1948.

138. Kiss, M. von, "Der Wärmeübergang Zwischen Sich Berührenden Metallischen Oberflächen," NEUE TECH. V. 5, pp. 714-724, December 1965.

139. Koh, B., and John, J. E. A., "The Effect of Inter-

facial Metallic Foils on Thermal Contact Resistance, ASME Paper No. 65-HT-44, August 1965.

140. Kouwenhoven, W. B., and Potter, J. H., "Thermal Resistance of Metal Contacts," J. Am. Weld. Soc., (Welding Research Supplement), V. 27, Part 2, pp. 515s-520s, October 1948.

141. Kouwenhoven, W. B., and Tampico, J., "Measurement of Contact Resistance," J. Am. Weld. Soc., (Welding Research Supplement), V. 19, pp. 408s-413s, October 1940.

142. Kouwenhoven, W. B., and Tampico, J., "Surface Polish and Contact Resistance," J. Am. Welding Soc., V. 20, No. 10, pp. 468s-471s, October 1941.

143. Laming, L. C., "Thermal Conductance of Machined Metal Contacts," Proceedings of the International Heat Transfer Conference, Part I, No. 8, pp. 65-76, Boulder, Colorado, September 1961.

144. Laming, L. C., "Thermal and Electrical Conductance of Machined Metal Contacts," University of London, Ph. D. Thesis, 1959, (see also National Engineering Laboratory Heat Paper No. 182, November 1960).

145. Lardner, T. J., "Effect of a Variable Thermal Joint Conductance," Jet Propulsion Laboratory Section Report No. 354-10, January 2, 1964.

146. Lardner, T. J., "Thermal Joint Conductance, Midplane Stress Distribution," Jet Propulsion Laboratory Space Program Summary Report No. 37-19, V. 4, pp. 83-89, February 28, 1963.

147. Lindholm, U. S., and Kirkpatrick, R. C., "Transient Heat Conduction at High Thermal Flux," ASME Paper No. 63-WA-347, November 1963.

148. Ling, F. F., "A Quasi-Iterative Method for Computing Interface Temperature Distribution," Air Force Office of Scientific Research Report AFOSR TN58-1004, ASTIA Document No. AD206-147, October 1958, (see also ZEITSCHRIFT FUR ANGEWANDTE MATHEMATICK UND PHYSIK, V. 10, No. 5, pp. 461-474, September 1959).

149. Ling, F. F., "On Asperity Distribution of Metallic Surfaces," J. Appl. Phys. V. 29, No. 8, pp. 1168-

1174, August 1958.

150. Ling, F. F., and Lucek, R. C., "On Model Studies of Metallic Surface Asperities," Air Force Office of Special Research Report TN58-1134, ASTIA Document No. AD208-083, December 1958.

151. Ling, F. F., and PU, S. L., "Probable Interface Temperatures of Solids in Sliding Contact," Air Force Technical Documentary Report No. RTD-TDR-63-4184, ASTIA Document No. AD433-1587, February 1964.

152. McDonald, T. W., "Thermal Contact Resistance," Transactions of the Engineering Institute of Canada, Paper No. EIC-63-MECH-12, V. 6, No. B-12, July 1963.

153. Maerschalk, J. C., "The Effects of Creep on Thermal Contact Conductance Between Thin Plates in Vacuum," Collins Radio Company, Engineering Report No. 523-0757819-00181M, Cedar Rapids, Iowa, April 15, 1964, see also M. S. Thesis, University of Iowa, April 1965.

154. Massachusetts Institute of Technology, Progress Report, "Description of Method for Determining Geometric Parameters of Surfaces in Contact," USAEC Report NYO-9456, May 1961.

155. Massachusetts Institute of Technology, Progress Report, "Some Methods of Surface Analysis for the Prediction of Thermal Resistance of Metal Contacts," USAEC Report NYO-9457, November 1961.

156. Meerovich, I. G., and Muchnik, G. F., "A Transient Temperature Field in Multi-Layer Systems," Teplofiz. Vysok. Temperature, V. 1, No. 2, p. 291, 1963.

157. Mersman, W. A., "Heat Conduction in an Infinite Composite Solid with an Interface Resistance," Trans. Am. Math. Soc., V. 53, pp. 14-24, January 1943.

158. Meissner, Hans, "Studies of Contacts with Barriers in Between," John Hopkins University Report, ASTIA Document No. AD225-070, September 1959.

159. Mikesell, R. P., and Scott, R. B., "Heat Conduction Through Insulating Supports in Very Low Tempera-

ture Equipment," J. Res. N.B.S., V. 57, No. 6, pp. 371-378, December 1956, (see also NBS Report 3507, November 18, 1954).

160. Miller, V. S., "Effective Method of Reducing Thermal Contact Resistance," (Russian) INZHENERNO-FIZICHESKII ZHURNAL, V. 6, No. 4, pp. 71-74, April 1963. English language translation, Soviet J. Engr. Physics (Faraday Translation).

161. Miller, V. S., "Features of Contact Heat Transfer in Reactor Fuel Elements," IZV. VYSSH. UCHEB. ZAV., ENERGETIKA, pp. 67-70, No. 3, 1962. English Translation (USA) AEC-TR-5410 and NASA Technical Translation F-8849.

162. Miller, V. S., "Thermal Resistances in Contact Areas of Heating Elements," AKADEMIYA NAUK UKRAYNSKOY USSR INSTYUT TEPLOENERGETYKY ZBIRNY PRATS, V. 24, pp. 133-139, 1962. English Translation (USA) NASA Technical Translation F-8839.

163. Miller, V. S., "Results of Experimental Investigation of Contact Heat Exchange Between Flat Metal Surfaces," AKADEMIIA NAUK USSR, KIEV. INSTITUT TEPLOENERGETIKI ZBIRNY PRATS, V. 20, pp. 44-53, 1960, English Translation (USA) RSIC-272.

164. Miller, V. S., "Determining the Thermal Contact Resistance Between Metal-Ceramic Surfaces," AKADEMIIA NAUK USSR KIEV. INSTITUT TEPLONERGETIKI ZBIRNY PRATS, V. 20, pp. 54-59, April 1960. English Translation (USA) RSIC-401.

165. Miller, V. S., "Heat Exchange Between Contacting Metal-Powder Components," DOPOVIDI AKAD. NAUK UKR. RSR, No. 1, pp. 40-43, Jan. 1961. English Translation (USA) HB-5196, Henry Brutcher Technical Translations, Altadena, California.

166. Mizushina, T., Iuchi, S., Sasano, T., and Tamura, H., "Thermal Contact Resistance Between Mercury and a Metal Surface," Int. J. Heat Mass Transfer, V. 1, pp. 139-146, 1960.

167. Moon, J. S., and Keeler, R. N., "A Theoretical Consideration of Directional Effects in Heat Flow at the Interface of Two Dissimilar Metals," Int. J. Heat Mass Transfer, V. 5, No. 10, pp. 967-973, Oct. 1962.

168. Muchnik, G. F., and Meerovich, I. G., "Nonstationary Heat Conductivity of Solids in Contact," Teplofiz. Vysok. Temp., V. 1, No. 3, pp. 404-408, 1963. English Translation, Soviet J. Engr. Physics, Faraday Translation, N. Y.

169. Mueller-Hillebrand, D., "Surface Contacts Under High Load Forces," WISS. VEROEFF. SIEMENSWERKE, V. 20, pp. 85-103, 1941.

170. Neeper, D. A., and Dillinger, J. R., "Thermal Resistance of Indium - Sapphire Boundaries Between 1.1-2.1°K," Phys. Rev., V. 135A, pp. 1028-1033, August 17, 1964.

171. Northrup, E. F., "Some Aspects of Heat Flow," Trans. Amer. Electro-Chem. Soc., V. 24, pp. 85-103, September 1913.

172. Pearson, J. A., "Thermal Resistance of the Joint Between a Nuclear Fuel and its Canning Material," Nuclear Energy (GB), pp. 444-449, December 1962.

173. Petri, F. J., "An Experimental Investigation of Thermal Contact Resistance in a Vacuum," ASME Paper 63-WA-156, November 1963.

174. Podstrigach, Ya. S., "Temperature Distribution in a System of Solid Bodies in Contact Via a Thin Intermediate Layer," INZHENERNO-FIZICHESKII ZHURNAL, V. 6, No. 10, pp. 129-136, Oct. 1963, English Translation (USA), RSIC-148.

175. Pohle, F., Lardner, T., and French, F., "Temperature Distributions and Thermal Stresses in Structures with Contact Resistances," Polytechnic Institute of Brooklyn Report, PIBA 1557, Air Force Report AFOSR TN 60-504, ASTIA Document No. AD237-149.

176. Potter, J. H., "Thermal Resistance of Metallic Contacts," Ph. D. Dissertation, John Jopkins University, 1948.

177. Powell, R. W., "The Place of Heat Conduction in the Theory, Practice, and Testing of Bonds," Applied Materials Research, V. 1, No. 3, pp. 166-169, October 1962.

178. Powell, R. W., "Experiments Using a Simple Thermal Comparator for Measurements of Thermal Conductivity, Surface Roughness and Thickness of Foils or of

Surface Deposits," J. Sci. Instr., V. 34, pp. 485-492, Great Britain, 1957.

179. Powell, R. W., Tye, R. P., and Jolliffe, B. W., "Heat Transfer at the Interface of Dissimilar Materials: Evidence of Thermal Comparator Experiments," Int. J. Heat Mass Transfer, V. 5, pp. 897-902, October 1962.

180. Putnaerglis, R. A., "A Review of Literature on Heat Transfer Between Metals in Contact and by Means of Liquid Metals," Report No. R.34, Department of Mechanical Engineering, McGill University, Montreal, 1953.

181. Quinville, J. A., Sneyd, J. M., "Methods of Calculating Heat Conduction for Aerodynamic Heating of Supersonic Wing Structures," Appendix VII, "Temperature Distributions in Two Insulated Rods with Contact Resistance at the Plane of Contact," Northrop Aircraft Report NAI-54, ASTIA Document No. AD78265, June 1954.

182. Rapier, A. C., Jones, T. M., and McIntosh, J. E., "The Thermal Conductance of Uranium Dioxide/Stainless Steel Interfaces," Int. J. Heat Mass Transfer, V. 6, pp. 397-416, May 1963.

183. Robertson, A. L., Ross, A. M., Notley, M. J. F., and Macewan, J.R., "Temperature Distribution in UO_2 Fuel Elements," J. Nucl. Mat., V. 7, No. 3, pp. 225-262, 1962.

184. Roess, L. C., "Theory of Spreading Conductance," Appendix A of an unpublished report of the Beacon Laboratories of Texas Company, Beacon, N. Y.

185. Rogers, G. F. C., "Heat Transfer at the Interface of Dissimilar Metals," Int. J. Heat Mass Transfer, V. 2, pp. 150-154, 1961.

186. Rosenfeld, S. J., "Analytical and Experimental Investigation of Bolted Joints," NACA TN1458, October 1947.

187. Ross, A. M., and Stoute, R. L., "Heat Transfer Coefficients Between UO_2 and Zircoloy 2," Atomic Energy Commission of Canada, Ltd., Report, AECL-1552, 1962.

188. Sanderson, P. D., "Heat Transfer From the Uranium Rods

to the Magnox in a Gas Cooled Reactor," ASME, International Developments in Heat Transfer, Part I, No. 8, Boulder, Colorado, Sept. 1961.

189. Schaaf, S. A., "On the Superposition of a Heat Source and Contact Resistance," Quart. Appl. Math., V. 5, pp. 107-111, April 1947.

190. Schauer, D. A., and Giedt, W. H., "Contact Conductance Measurements During Transient Heating," Proceedings of the Third International Heat Transfer Conference, V. 4, p. 100, August 1966.

191. Schmidt, E. H. W., and Jung, E., "Measurement of the Thermal Contact Resistance from Stainless Steel to Liquid Sodium," Modern Developments in Heat Transfer, pp. 251-263, Academic Press, New York, 1963.

192. Seide,P., "On One Dimensional Temperature Distribution in Two-Layered Slabs with Contact Resistances at the Plane of Contact," J. Aero/Space Sci., V. 25 No. 8, pp. 523-524, August 1958.

193. Shetsova, E. M., "Determination of Actual Contact Areas of Surfaces by Means of Transparent Models," (Russian) AKADEMIA NAUK SSSR, INSTITUT MASAINOVEDENIA, SBORNIK IZNOS V. MASHINAKH, V. 7, pp. 12-33, 1953, English Translation (USA) RSIC-192.

194. Shlykov, Yu. P., Ganin, E. A., "Thermal Contact Resistance," Atom. Energ., V. 9, No. 6, pp. 496-498, Dec. 1960, Faraday Translation, N. Y.

195. Shlykov, Yu. P., Ganin, E. A., "Experimental Study of Contact Heat Exchange," TEPLOENERGETIKA, V. 8, No. 7, pp. 73-76, July 1961, English Translation (USA) RSIC-128.

196. Shlykov, Yu. P., Ganin, E. A., "Thermal Resistance of Metallic Contacts," Int. Journal Heat Mass Transfer, V. 7, No. 8, pp. 921-929, 1964.

197. Shlykov, Yu. P., Ganin, E. A., and Demkin, N. B., "Investigation of Contact Heat Exchange," (Russian with Summary in English), TEPLOENERGETIKA, V. 7, No. 6, pp. 72-76, June 1960, English Translation (USA), RSIC-117, and United Kingdom Atomic Energy Authority Translation TRG-IS-280.

198. Shteinberg, V. M., "New Method for Calculating a Non-Steady State Temperature Field for a Semi-Infinite

Inhomogeneous Complex of Bodies in Mutual Thermal Contact," Int. Conference on Heat and Mass Transfer," MINSK, January 23-27, 1961.

199. Shvets, I. T., and Dyban, E. P., "Contact Heat Transfer Between Plane Metal Surfaces," International Chemical Engineering, V. 4, No. 4, pp. 621-624, October 1964.

200. Shvets, I. T., Dyban, E. P., and Kondak, N. M., "Studies on Contact Heat Exchange Between Heat Engine Parts," English Translation (USA) RSIC-322, 1964.

201. Simmons, C. V., "The Effect of Thermal Contact Resistance on Structural Temperatures Within Three Regions of the Saturn - IB, S - IB Lower Tail Assembly," Structures and Mechanics Engineering Department, Chrysler Corp., Space Division, Huntsville Operations.

202. Sonokama, Konomo, "Thermal Contact Resistance," (Survey), Journal of JSME, V. 64, No. 505, pp. 240-250, 1961. See also Translation No. RSIC-215.

203. Skipper, R. S. G., and Wooton, K. J., "Thermal Resistance Between Uranium and Can," International Conference on Peaceful Uses of Atomic Energy, Proceedings, V. 7, pp. 684-690, 1958.

204. Smith, C. F., "Apparatus for Measuring Temperature Drop Across an Interface," NASA TMX-53091, July 17, 1964.

205. Stoyukhin, B. P., "Instantaneous Temperature at Contact Surfaces Caused by Friction," NAUCH. DOKL. VYS. SHKOLY: MASH. i. PRIB., No. 4, pp. 73-81, 1958, English Translation (USA) RSIC-142.

206. Stubstad, W. R., "Thermal Contact Resistance Between Thin Plates in a Vacuum," Collins Radio Company, (Cedar Rapids, Iowa) Report 52-0756961-00181M, July 1964. See also M.S. Thesis, State University of Iowa, and ASME Paper No. 65-14-16, August 1965.

207. Stubstad, W. R., "Measurements of Thermal Contact Conductance in Vacuum," ASME Paper 63-WA-150, December 1963.

208. Sud Aviation, "Thermal Conductance of Lap Joints Between AU4G1 Sheets," (French) Test Report No. C.R. 72-003-50, December 1957, English Translation (Great Britain) by G. W. Wickens, Royal Aircraft Establishment (Farnsborough) Translation No. 949, June 1961, ASTIA Document No. AD-262-578.

209. Sud Aviation, "Thermal Conductance of Cemented-Lap Joints Between AU4G1 Sheets," (French) Test Report C.R. 72-003-51, March 1959, English Translation (Great Britain) by G. W. Wickens, Royal Aircraft Establishment (Farnsborough) Translation 952, July 1961, ASTIA Document No. 262-823.

210. Sud Aviation, "Thermal Conductance of Steel Joints," (French) Test Report C.R. 72-013-50, March 1960, English Translation (Great Britain) by M. H. S. Brown, Royal Aircraft Establishment (Farnsborough) Library Translation No. 950, July 1961, ASTIA Document No. 262-820.

211. Swann, W. F. G., "Concerning Thermal Junction Resistances in the A. F. Jaffe Method for Measurement of Thermal Conductivity," J. Franklin Inst., V. 268, No. 4, pp. 294-296, October 1959.

212. Swann, W. F. G., "Theory of the A. J. Jaffe Method for Rapid Measurement of the Thermal Conductivity of Solids," J. Franklin Inst., V. 267, No. 5, pp. 363-380, May 1959.

213. Tachibana, F., "Study on Thermal Resistance of Contact Surface," (Japanese) Nihon Kikai Gakukai Shi, V. 55, No. 397, pp. 102-107, 1952, English Translation RSIC-29, June 1963.

214. Tampico, J., "Measurement of Contact Resistance," Dissertation at Johns Hopkins University, 1941.

215. Tarasov, L. P., "Relation of Surface Roughness Readings to Actual Surface Profile," Trans. ASME, V. 67, No. 3, pp. 189-196, April 1945.

216. Tate, M. B., and Rosenfeld, S. J., "Preliminary Investigation of the Loads Carried by Individual Bolts in Bolted Joints, NACA TN 1051, May 1946.

217. Taylor, T. A., "The Thermal Conductivity of Insulating and Other Materials," Trans. ASME, V. 41, p. 605, 1919.

218. Thomas, T. R., Probert, S. D., "Variation of Thermal Conductance of Multilayered Stacks Under Load," presented at International Thermal Conductivity Conference, National Physical Laboratory, Teddington, Middlesex, England, July 15-17, 1964. See also UKAEA-TRG Report 1013(R/X)."

219. Thomas, T. R., and Probert, S. D., "Improved Thermal Insulation Using Thermoelectric Phenomena," Brit. J. Appl. Phys., V. 15, pp. 1120-1123, May 1964.

220. Thomas, T. R., Probert, S. D., and Warman, D., "Cryostat for Measurement of Heat Conduction Under Mechanical Loads," J. Sci. Instru., V. 41, pp. 88-91, 1964.

221. Testerman, M. K., "Method of Determining Surface Roughness," WADC Technical Report 58-230, ASTIA Document No. AD 155-828.

222. Tittle, C. W., "Boundary Value Problems in Composite Media: Quasi-Orthogonal Functions," J. Appl. Physics, V. 38, pp. 486-488, April 1965.

223. Urakawa, K., "Graphical Solution of Contact Heat Transfer," Trans. J. Soc. Mech. Engrs., V. 29, No. 204, p. 1416, 1963.

224. Usov, A. L., "A Study of Contact Heat Exchange on the Surface of a Three-Layered Slab of Flooring," (Russian), INZ. FIZ. ZHURNAL, V. 6, No. 11, pp. 119-122, 1963, English Translation by Faraday Translation, N. Y.

225. Van Dusen, M. S., "A Simple Apparatus for Comparing the Thermal Conductivity of Metals and Very Thin Specimens of Poor Conductors," J. Opt. Soc. Am., V. 6, pp. 739-743, September 1922.

226. Velissaropoulos, P. D., "Apparatus for Measuring Contact Conductance," M.S. Thesis, M.I.T., August 1963.

227. Vernotte, P., "Le Partage d'un Flux de Chateur Nuissant a l'intersurface de Deaux Milieux Limites, en Contact Imparfait, Paradoxe Sur La Propagation de la Chaleur," Comptes Rendus Acad. Sci., V. 207, pp. 124-126, July 1938.

228. Vernotte, P., "Proprietes de la Solution de Fourier dans les Systemes Complexes; Application au Partage d'un Flux Entre Corps au Contact," Comptes Rendus Acad. Sci., V. 206, pp. 1286-1288, May 2, 1938.

229. Vernotte, P., "Extension of Fourier's Method to Composite Systems with Resistances to Heat Flow Between Certain Regions," Comptes Rendus Acad. Sci., V. 224, pp. 1416-1418, May 19, 1947.

230. Voigt, F., "The Load Distribution in Bolted or Riveted Joints in Light Alloy Structures," NACA TN 1135, April 1947.

231. Walther, J. D., "A Study of Transient Thermal Contact Conductance," Master's Thesis, Southern Methodist University, School of Engineering, Dallas, Texas, DDC No. AD 297-995.

232. Ward, A. L., "Dependence of Metal-To-Semiconductor Contact Resistance Upon Control Loading," Diamond Ordnance Fuze Laboratory Report TR-731, ASTIA Document AD228-744, July 30, 1959.

233. Weills, N. D., and Ryder, E. A., "Thermal Resistance Measurements of Joints Formed Between Stationary Metal Surfaces," Trans. ASME, V. 71, pp. 259-267, 1949.

234. Wheeler, R. G., "Thermal Conductance of Fuel Element Materials," USAEC Report No. HW-60343, April 1959.

235. Wheeler, R. G., "Thermal Contact Conductance," USAEC Report No. HW-53598, November 1957.

236. Williams, A., "Comment on Rogers Paper 'Heat Transfer at the Interface of Dissimilar Metals'" Int. J. Heat Mass Transfer, V. 3, p. 159, 1961.

237. Williams, A., "Heat Transfer at the Interface of Dissimilar Metals, A Further Consideration," University of Manchester (England) Report ARC. 23, 498 STRUT. 2409, February 1962.

238. Williams, A., "Heat Transfer Through Metal to Metal Joints," Proceedings of the Third International Heat Transfer Conference, V. 4, p. 109, August 1966.

239. Wong, H. Y., "Thermal Conductance of Metallic Contacts - A Survey," presented at the International Conference on Thermal Conductivity, National Physical Laboratory, Teddington, Middlesex, England, July 15-17, 1964.

240. Wright-Patterson Air Force Base Report, "Thermo-Mechanical Analysis of Structural Joint Study," Report WADD TR61-5, January 1962.

241. Yamauchi, K., "Graphical Solution of Contact Heat Conduction," (Japanese), Transactions of Japan Society of Mechanical Engineers, V. 29, No. 201, pp. 1001-1004, 1963.

242. Yovanovich, M. M., "Thermal Contact Conductance in a Vacuum," Mech. Eng. Thesis, M.I.T., February 1966. See also M.I.T. Reports on NASA Contract No. NGR-22-009-065.

243. Yovanovich, M. M., and Fenech, A., "Thermal Contact Conductance of Nominally Flat, Rough Surfaces in a Vacuum Environment," Third Aerospace Sciences Meeting, AIAA Paper No. 66-42, January 1966.

244. Zavaritskii, N. V., "Thermal Resistance of Metal Surfaces in Contact at Helium Temperatures," (Russian) Zhurnal Tekhnicheskoi Fiziki, V. 21, pp. 453-457, 1951, English Translation (USA), RSIC-406, April 1965.

OTHER REFERENCES

245. Gebhart, B., Heat Transfer, McGraw-Hill Book Company, Inc., New York, 1961.

246. Jakob, M., Heat Transfer, John Wiley and Sons, Inc., New York, 1957.

247. Kennard, E. H., Kinetic Theory of Gases, McGraw-Hill Book Company, Inc., New York, 1938.

248. Carslaw, H. S., and Jaeger, J. C., Conduction of Heat in Solids, Oxford University Press, London, 1959.

249. Beck, J. V., personal communication, February 21, 1966.

250. Williams, D. R., "The Thermal Conductivity of Several Metals: An Evaluation of a Method Employed by the National Bureau of Standards," Southern Methodist University Master's Thesis, November, 1966.

251. Schneider, P. J., Temperature Response Charts, John Wiley and Sons, Inc., New York, 1963.

252. Watson, T. W. and Robinson, H. E., "Thermal Conductivity of Some Commercial Iron-Nickel Alloys," J. Heat Transfer, C83, No. 4, pp. 403-408, November, 1961.

253. Tittle, C. W., personal communication, April 17, 1965.